UCSF
UC San Francisco Electronic Theses and Dissertations

Title
Cytoskeletal signaling and the regulation of attraction and repulsive axon guidance in C. elegans

Permalink
https://escholarship.org/uc/item/8m94x6vv

Author
Yu, Timothy W.

Publication Date
2001

Peer reviewed|Thesis/dissertation

eScholarship.org Powered by the California Digital Library
University of California

Cytoskeletal signaling and the regulation of attractive and

repulsive axon guidance in *C. elegans*

by

Timothy W. Yu

DISSERTATION

Submitted in partial satisfaction of the requirements for the degree of

DOCTOR OF PHILOSOPHY

in

Neuroscience

in the

GRADUATE DIVISION

of the

UNIVERSITY OF CALIFORNIA, SAN FRANCISCO

Copyright 2002

by

Timothy W. Yu

Acknowledgemnts

I would like to thank my advisor, Cori Bargmann, to whom I am greatly indebted for the guidance, graciousness, and enthusiasm she has shown me over the years. Her insight and passion for science have set an example that will be difficult to match.

I would like to express my gratitude to my thesis committee members, Marc Tessier-Lavigne, Wendell Lim and Ulrike Heberlein, for their encouragement and generosity over the course of my studies. I would like to acknowledge Wendell especially for early discussions that laid a groundwork for much of the studies presented here.

Thanks to the members of the Bargmann lab, who have been the most intelligent, eclectic, and creative group of colleagues I could hope for. I have borne my Bargmann lab nametags at meetings with pride. I would also like to thank our neighbors in the Martin and Tessier-Lavigne labs for their comments and advice. Their perspectives contributed as much to my graduate school experience as any benchwork.

Thanks to my mother and father, Alice and John, and my sister Elaine, who have whole-heartedly supported me throughout my educational pursuits.

I would not have made it without my friends who have provided me sustenance throughout graduate school through food, books, music, squash, and badminton. In particular I would like to thank Tracy Saxton, who has added much joy to my last years of graduate school.

Cytoskeletal signaling and the regulation of attractive and repulsive axon guidance in *C. elegans*

by

Timothy W. Yu

Thesis advisor: Cori Bargmann, Ph.D.

Professor, HHMI, Department of Anatomy

University of California, San Francisco

Abstract

Developing axons in the nervous system must often take long and complicated routes to reach their targets. To do so they rely upon growth cones, actin-rich expansions at the tips of migrating axons that sense and respond to a remarkable variety of attractive and repulsive guidance cues. How do guidance cues signal to the growth cone cytoskeleton, and how is information from different cues integrated?

These studies focused initially on the *C. elegans* axon guidance receptor SAX-3/Robo, a member of a conserved family of axon guidance receptors that responds to the repulsive cue Slit. Mutations in *sax-3* disrupt a variety of guidance events including nerve ring formation, midline axon crossing and migrations of the CAN cell. *sax-3* and its ligand *slt-1* also work in parallel with the *unc-6/Netrin-unc-40/DCC* guidance system to direct ventral guidance of AVM.

Chapters 2 and 3 show that SAX-3/Robo signaling involves direct associations with cytoskeletal modulators. A screen for molecules that interact with the SAX-3 cytoplasmic domain led to the identification of two candidate molecules involved in SAX-3 signaling:

UNC-34/ENA, a homolog of cytoskeletal regulator Enabled, and c-NCK, a homolog of the cytoskeletal adapter protein Nck/Dock. Comparison of *unc-34/ena* and *sax-3* phenotypes reveals similar roles in the regulation of midline crossing, AVM ventral guidance and CAN cell migration. Genetic interactions between *sax-3* and *unc-34* also indicate an important role for *unc-34* in *sax-3* signaling.

Chapter 3 also describes a novel example of crosstalk between attractive and repulsive receptors in axon guidance. Genetic interactions with activating and inactivating mutations provide evidence that signaling by SAX-3 also involves an unexpected, UNC-6-independent function of the Netrin receptor UNC-40/DCC. UNC-40 binds SAX-3 directly, supporting a model in which interactions between UNC-40 and SAX-3 potentiates SAX-3 signaling.

In Chapter 4, I present a genetic analysis of attractive and repulsive guidance of the AVM neuron. Results of a screen of twenty candidate axon guidance genes suggest the existence of considerable specificity in axon guidance signaling pathways in the AVM growth cone. Mutations in eleven genes (*ced-2, ced-5, ced-10, unc-115, ephexin, unc-33, unc-53, max-1, mig-17, unc-129,* and *unc-130*) are shown to affect Netrin- but not Slit-dependent guidance. Mutations in one gene (*unc-34*) selectively affect Slit-dependent guidance, and mutations in four genes, (*abl-1, mig-2, unc-73,* and *unc-71*) affect both Netrin and Slit pathways. These results reveal an underlying organization of growth cone signaling pathways, and provide a foundation for the comprehensive analysis of genetic pathways underlying Slit and Netrin guidance.

Cori Bargmann

Table of contents

Title page i

Copyright ii

Dedication iii

Preface iv

Abstract v

Chapter 1: Dynamic regulation of axon guidance 1

1.1 Summary 2

1.2 Introduction 3

1.3 Transcriptional regulation of axon guidance molecules 4

1.4 Post-transcriptional regulation of axon guidance molecules 6

1.5 Cytoskeletal signal transduction pathways mediating guidance responses 9

1.6 Formation of multimeric complexes by guidance receptors 11

1.7 Diversification of guidance responses by combinatorial assembly 12

1.8 Mechanistic implications 17

1.9 Conclusions 18

Figures 20

1.10 References 26

Chapter 2: *C. elegans* Enabled and Nck are candidate SAX-3 signaling molecules 41

2.1 Summary 42

2.2 Introduction 43

2.3 Results 46

2.4 Discussion....53
2.5 Materials and Methods....55
Tables....59
Figures....61
2.6 References....81

Chapter 3: SAX-3/Robo signaling mediated by UNC-34/Enabled and a Netrin-independent function of UNC-40/DCC....86

3.1 Summary....87
3.2 Introduction....88
3.3 Results....90
3.4 Discussion....97
3.5 Materials and Methods....100
Tables....104
Figures....106
3.6 References....118

Chapter 4: Untangling attractive and repulsive pathways in the guidance of the AVM axon....125

4.1 Summary....126
4.2 Introduction....127
4.3 Results....129
4.4 Discussion....138
4.5 Conclusions....146
4.6 Materials and Methods....147

Tables..... 149

Figures..... 157

4.7 References..... 177

List of Tables

Table 2-1 Conserved proline-rich motifs in SAX-3/Robo receptors..... 59

Table 2-2 Yeast two-hybrid results with the SAX-3 cytoplasmic domain..... 60

Table 3-1 Neuronal guidance in wild-type, *sax-3* mutants and *unc-34* mutants..... 104

Table 3-2 Suppression of *SLT-1* gain-of-function phenotype by *sax*-3, *unc-34* , and *unc-40*..... 105

Table 4-1 Genes analyzed for effects on AVM axon guidance.....149

Table 4-2 Parent strains used for analysis of AVM axon guidance..... 152

Table 4-3 Strains constructed for analysis of AVM ventral guidance..... 153

Table 4-4 Classification of genes into UNC-6/Netrin or Slit pathways..... 156

List of Figures

Figure 1-1 The four major families of instructive guidance cues and receptors..... 20

Figure 1-2 Transcriptional regulation of axon guidance cues and their receptors..... 22

Figure 1-3 Combinatorial regulation of axon guidance receptor signaling..... 24

Figure 2-1 Isolation of c-NCK in a two-hybrid screen with SAX-3 61

Figure 2-2 *c-nck* cDNA sequence..... 63

Figure 2-3 Relationship of cNCK to other Nck/Dock family members..... 65

Figure 2-4 cNCK binds to SAX-3 motif B via its second SH3 domain..... 67

Figure 2-5 Expression pattern of *c-nck* in adult hermaphrodites..... 69

Figure 2-6 SAX-3 motif C binds the Mena EVH1 domain..... 71

Figure 2-7 Identification of a *C. elegans* Enabled homolog..... 73

Figure 2-8 *c-ena* cDNA coding sequence..... 75

Figure 2-9 RNAi-mediated disruption of *c-ena* causes cell migration defects..... 77

Figure 2-10 Structure-function analysis of the SAX-3 cytoplasmic domain supports a role for motifs B and C in SAX-3 guidance..... 79

Figure 3-1 *unc-34* and *sax-3* mutants share axon guidance phenotypes at the ventral midline and in ventral guidance..... 106

Figure 3-2 *unc-34* double mutant analysis in AVM ventral guidance..... 108

Figure 3-3 Suppression of Slit gain-of-function phenotypes by *unc-34* and *unc-40*... 110

Figure 3-4 Genetic interactions between *sax-3* and *unc-34* in the nerve ring.....112

Figure 3-5 Genetic interactions between *sax-3* and *unc-40* in the nerve ring.....114

Figure 3-6 SAX-3, UNC-34 and UNC-40 proteins can associate.....116

Figure 4-1 The AVM axon is guided by dorsal SLT-1/Slit and ventral UNC-6/Netrin..... 157

Figure 4-2 Strategy for identifying components of Slit and Netrin signaling pathways..... 159

Figure 4-3 Involvement of *unc-34/ena* and *abl-1* in Slit and Netrin signaling..... 161

Figure 4-4 Involvement of the cell engulfment genes *ced-2, ced-5, and ced-10* in Slit and Netrin signaling..... 163

Figure 4-5 Involvement of the Rac genes *ced-10* and *mig-2* in Slit and Netrin signaling..... 165

Figure 4-6 Involvement of the Rac-associated genes *unc-115, unc-73* and *ephexin* in Slit and Netrin signaling..... 167

Figure 4-7 Involvement of the axonal outgrowth genes *unc-14, unc-33, unc-51* and *unc-53* in Slit and Netrin signaling.....168

Figure 4-8 Involvement of the ADAM metalloprotease genes *unc-71* and *mig-17* in Slit and Netrin signaling..... 170

Figure 4-9 Involvement of motor axon guidance genes *max-1, unc-69, unc-129,* and *unc-130* in Slit and Netrin signaling..... 172

Figure 4-10 Summary of results of AVM analysis..... 174

Chapter 1

Dynamic regulation of axon guidance

Chapter 1 is a modified version of the following manuscript:

Yu, T. W. and Bargmann, C. I. (2001).

Dynamic regulation of axon guidance.

Nat Neurosci **4 Suppl**, 1169-1176.

1.1 Summary

To reach their proper targets, axons rely upon the actions of highly conserved families of attractive and repulsive guidance molecules, including the Netrins, Slits, Semaphorins, and Ephrins. These guidance systems are used to generate an astonishingly varied set of neuronal circuits. This chapter considers the mechanisms by which a few guidance systems can be used to generate diverse outcomes. Studies have revealed extensive transcriptional and post-transcriptional regulation of guidance cues and their receptors, as well as combinatorial mechanisms that integrate information from different families of guidance cues.

1.2 Introduction

Neurons rely upon a variety of attractive and repulsive guidance cues to navigate to their targets (Tessier-Lavigne and Goodman, 1996). Genetic, biochemical, and molecular approaches have identified four conserved families of guidance cues with prominent developmental effects: the Netrins, Slits, Semaphorins, and Ephrins (Figure 1-1). Netrins, Slits, and some Semaphorins are secreted molecules that associate with cells or extracellular matrix, whereas Ephrins and other Semaphorins are expressed at the cell surface. Netrins can act as attractants or repellents; Slit, Semaphorins, and Ephrins act primarily as repellents but can be attractive or adhesive in some contexts. For each of these cues, one or more transmembrane receptors have been identified: UNC-40/DCC and UNC-5 receptors for Netrins (Culotti and Merz, 1998), Robo receptors for Slits (Guthrie, 1999; Van Vactor and Flanagan, 1999), Neuropilin and Plexin receptors for Semaphorins (Raper, 2000; Tamagnone and Comoglio, 2000), and Eph receptors for Ephrins (Flanagan and Vanderhaeghen, 1998; Wilkinson, 2001). In the case of Netrin and Slit, a small number of ligands interact with a small number of receptors; in the case of Semaphorins and Ephrins, large families of related ligands interact with corresponding families of receptor proteins. These are not the only guidance factors — neurotrophins, HGF/scatter factor, and TGF-beta family members can guide axons, and additional candidate receptors include the protocadherin family, odorant receptors, Ig-CAMs, and Neurexins. Nonetheless, the number of guidance cues and receptors seems small relative to the immense complexity of the nervous system.

The conserved Netrin, Slit, Semaphorin and Ephrin pathways are remarkably versatile. Each of the guidance cues has been implicated in numerous axon guidance or targeting events. Moreover, the functions of the guidance molecules are not restricted to

axon migrations. Netrin and Slit affect neuronal and mesodermal cell migrations (Ackerman *et al.*, 1997; Hedgecock *et al.*, 1990; Kramer *et al.*, 2001; Zallen *et al.*, 1999); Semaphorins mediate bone and heart morphogenesis (Behar *et al.*, 1996); Ephrins direct neural crest migration and angiogenesis (Wilkinson, 2001). How are a few guidance molecules used to generate a variety of structures in the nervous system (and elsewhere)? Recent work has revealed extensive regulation of guidance cues and their receptors, and uncovered mechanisms that integrate information from different families of guidance cues. Here we will consider three general mechanisms that regulate guidance molecules to yield diverse outcomes. First, the expression of guidance cues and their receptors can be regulated in specific patterns. Second, the signal transduction pathways downstream of receptors can be intrinsically different between cells, or extrinsically regulated by other pathways. Third, the activity of receptors can be regulated by the assembly of receptor complexes with novel signaling properties.

1.3 Transcriptional regulation of axon guidance molecules

Any particular guidance cue and its receptor are expressed at numerous times in development, and often in the adult brain (Giger *et al.*, 1998; Itoh *et al.*, 1998; Luo *et al.*, 1995; Wadsworth *et al.*, 1996; Yuan *et al.*, 1999). Transcriptional regulation of guidance cues and receptors confers both spatial and temporal controls for axon guidance.

The expression of guidance cues is often dynamic and precisely tuned to the decisions that occur at a particular time and place. For example, the developing *Xenopus* tadpole has laterally-placed eyes, and axon guidance at the optic chiasm initially drives all axons to the contralateral brain (Figure 1-2A). Later in development, both eyes migrate medially so that left and right visual fields overlap. Corresponding ipsilateral axon

projections from the eye to the brain form to accommodate the overlapping visual fields. The appearance of ipsilateral axons during frog development correlates with the appearance of repulsive ephrin-B cues at the midline of the optic chiasm (Nakagawa *et al.*, 2000). The late appearance of ephrin-B directs the axons of later-born EphB-expressing retinal neurons to the ipsilateral brain, creating visual projections that represent the modified eye location in the frog.

Both gene activation and gene repression by transcriptional regulators have roles in shaping guidance decisions. The UNC-130 forkhead transcription factor is required in *C. elegans* to repress expression of a secreted UNC-129 axon guidance cue by ventral muscles (Nash *et al.*, 2000) (Figure 1-2B). The ventral-only expression of the transcription factor UNC-130, followed by dorsal-only expression of the UNC-129 guidance cue, are essential for a normal D/V guidance axis.

The transcription of guidance receptors as well as guidance cues can be regulated in development. In *C. elegans*, certain cells that migrate away from Netrin sources are exposed to Netrin throughout their development, but they turn on the expression of the repulsive Netrin receptor UNC-5 at the exact time that they make the guidance decision. For these cells, the timing of *unc-5* transcription is the central regulatory event: precocious *unc-5* expression is sufficient to induce precocious repulsion from Netrin (Su *et al.*, 2000).

Complex guidance decisions may be directed by complex expression patterns, as seen in the retinotopic map of the visual system in the vertebrate brain. The expression of ephrin-A ligands in the tectum occurs in an anterior-to-posterior gradient, and the expression of EphA receptors in retinal ganglion cells follows a complementary nasal-to-temporal gradient (Flanagan and Vanderhaeghen, 1998) (Figure 1-2C). Axons expressing high levels of EphA receptor are repelled from low levels of ephrin-A ligand, whereas axons with lower EphA receptor levels can tolerate higher ephrin-A levels. A competition between axons, rather than

the absolute level of receptor, drives their relative positions in the tectum (Brown *et al.*, 2000). The opposing ligand and receptor gradients are largely specified by transcriptional mechanisms (Retaux and Harris, 1996; Rhinn *et al.*, 1999; Schulte and Cepko, 2000) and they are essential for orderly targeting and creation of the visual map.

Many axon pathfinding mutants identified in fly, worm, or mouse genetic screens correspond to mutations in specific transcription factors (Baran *et al.*, 1999; Erkman *et al.*, 2000; Hartmann *et al.*, 2000; Kania *et al.*, 2000; Landgraf *et al.*, 1999; Lundgren *et al.*, 1995; Much *et al.*, 2000; Thor *et al.*, 1999; Thor and Thomas, 1997). Transcription factors often have tissue-specific effects on guidance, but in most cases the genes they regulate are unknown. We suggest that these transcription factors are the tissue-specific regulators that define local expression of general guidance molecules.

1.4 Post-transcriptional regulation of guidance cues and receptors

The activity of guidance pathways is regulated not only by transcriptional mechanisms, but also by post-transcriptional mechanisms that regulate the levels or availability of receptors and ligands. Regulatory strategies include receptor down-regulation, ligand inactivation of receptor, alternative splicing, regulated proteolysis, and ligand presentation.

Receptor down-regulation. Regulation of the guidance receptor Robo plays a key role in the patterning of the *Drosophila* nervous system. Most axons in the fly CNS cross the midline once, but do not recross because of Robo-mediated repulsion from the midline repellent Slit. *robo* RNA is present in neurons when they initially cross the midline, but the Robo protein is transiently inactivated by the *commissureless*(*comm*) gene until after midline crossing. When *comm* is absent, Robo function is de-repressed, and axons never cross the midline (Kidd *et al.*, 1998b; Seeger *et al.*, 1993). *comm* encodes a transmembrane protein

that decreases the surface expression of Robo in commissural axons, rendering them insensitive to Slit until after midline crossing (Kidd *et al.*, 1998b; Tear *et al.*, 1996). In wild-type animals, Robo protein is sequestered in internal vesicles in axons that cross the midline (Kidd *et al.*, 1998a). This result suggests that Robo stability, delivery to the cell surface, or internalization is regulated during axon guidance.

Ligand inactivation of receptor. Guidance receptors can also be regulated by their own ligands. Temporal retinal axons express high levels of EphA3 receptors, and are repelled by target tissues expressing high levels of ephrin-A ligands (Figure 1-2C). Interestingly, however, overexpression of ephrin-A2 or ephrin-A5 in temporal axons abolishes their repulsive response to ephrin-A proteins on other tissues (Dutting *et al.*, 1999; Hornberger *et al.*, 1999). This result suggests that the expression of ephrin-A can desensitize or inactivate Eph receptors on the same cell. Nasal axons express ephrin-A2 and ephrin-A5 as well as a moderate level of Eph receptors, and they are not repelled by tissues expressing ephrin-A. Enzymatic removal of ephrin-A ligands from nasal retinal axons, or genetic inactivation of ephrin-A2 and ephrin-A5, increases the sensitivity of nasal axons to repulsive target tissues (Feldheim *et al.*, 2000; Hornberger *et al.*, 1999). These results indicate that endogenous ephrin-A proteins reduce Eph function on nasal axons. ephrin-A2 and ephrin-A5 are expressed in high-nasal-to-low-temporal gradients in retinal neurons, suggesting that inhibition of Eph receptor function by retinal Ephrins contributes to the proper formation of the topographic projection.

Alternative splicing. Eph receptor signaling can also be regulated by alternative splicing of the Eph receptor. ephrin-A5 and EphA7 mediate closing of the neural folds and formation of the neural tube by an adhesive interaction, unlike the repulsive interactions characteristic of Eph signaling (Holmberg *et al.*, 2000). The adhesive response is generated by an alternative splice form of EphA7 that lacks the tyrosine kinase domain and suppresses

tyrosine phosphorylation of full-length EphA7. Loss of EphA7 catalytic activity shifts the cellular response from repulsion to adhesion. It will be interesting to see whether this mechanism contributes to attractive functions of ephrins in axon guidance (Castellani *et al.*, 1998).

Regulated proteolysis. Regulated proteolytic cleavage of guidance receptors and their ligands can either inhibit or facilitate signaling. Many cell surface proteins undergo metalloprotease-mediated ectodomain shedding, including the Netrin receptor DCC. Proteolytic activity appears to downregulate the Netrin response: inhibition of metalloprotease function stabilizes full-length DCC, and potentiates Netrin-stimulated axon outgrowth (Galko and Tessier-Lavigne, 2000).

Proteases can also play facilitatory roles in guidance responses. Guidance cues elicit rapid neurite retraction after interactions with repulsive ligands like Semaphorins or Ephrins. However, the signaling between guidance receptors and ligands involves multivalent, high affinity receptor-ligand interactions, generating adhesive forces that must be overcome for axon repulsion or retraction to occur. Proteolytic cleavage of Ephrin plays a key role in this disadhesion step (Hattori *et al.*, 2000). Mouse hippocampal growth cones contacting the repulsive cue ephrin-A2 respond by collapsing and rapidly retracting. ephrin-A2 forms a stable complex with the metalloprotease Kuzbanian, which triggers cleavage of ephrin-A2 upon Eph receptor binding. When cleavage is blocked by mutations in ephrin-A2, disadhesion does not occur and axon withdrawal is delayed.

Ligand presentation. For secreted guidance ligands, the final pattern of expression can be regulated by interactions with other cell-associated proteins or extracellular matrix proteins. In *Drosophila,* Netrin can be concentrated at particular choicepoints through binding to cell-associated DCC (Hiramoto *et al.*, 2000). In this context, DCC acts to

present Netrin to other cells. Slit binds to Netrin and laminin, suggesting that binding interactions between guidance ligands could affect their localization (Brose *et al.*, 1999).

1.5 Cytoskeletal signal transduction pathways mediating guidance responses

Axon guidance receptors can act both by conferring selective adhesion to substrates and by transducing signals to the growth cone. Simple adhesion of the growth cone to substrate may be sufficient for some forms of axon guidance, since the growth of neurites *in vitro* can be controlled by gradients or sharp boundaries of fibronectin or laminin (Lander, 1990). Although navigation through corridors of extracellular matrix may require only adhesion and traction, the guidance cues listed in Figure 1-1 function by activating specific signaling pathways and not purely by adhesion and disadhesion.

Guidance receptors can initiate signaling cascades that instruct the growth cone to turn towards or away from a source of ligand, change speed, expand or collapse. The signaling pathways used in axon guidance are not fully understood, but it is likely that they act locally on the growth cone, and not by long-range signaling to the cell body. Signaling is converted into local changes in the actin cytoskeleton of the growth cone, which modulate the stability of the growth cone and its conversion to a microtubule-rich axon shaft (Tanaka and Sabry, 1995). The Rho family of GTPases, which direct the formation of a wide range of cytoskeletal structures (Nobes and Hall, 1995), are strongly implicated in axon guidance (Luo, 2000; Luo *et al.*, 1994; Steven *et al.*, 1998; Zipkin *et al.*, 1997). Local activation of Rho family GTPases is likely to be a central component of growth cone turning responses, although the pathways that link specific GTPases to specific guidance receptors are not fully understood (Shamah *et al.*, 2001). Cytoskeletal effectors are discussed in more detail elsewhere (Mueller, 1999; Song and Poo, 2001).

In this discussion of regulation of guidance pathways, three general aspects of intracellular signal transduction are particularly interesting. First, the intrinsic properties of a cell's cytoskeleton dictate its response to guidance information. Netrin or Slit can direct either cell migration or axon migration depending upon the intrinsic properties of the cell that senses Netrin or Slit (am I migrating, or is my axon migrating?) (Ackerman *et al.*, 1997; Hedgecock *et al.*, 1990; Kramer *et al.*, 2001; Zallen *et al.*, 1999). The intracellular mechanisms that direct that decision are unknown.

Second, the regulated expression of specific intracellular signaling components can be a source of guidance information. The cytoplasmic VAB-8 protein is required mostly for posterior axon guidance in normal *C. elegans* development (Wightman *et al.*, 1996). Ectopic expression of VAB-8 is sufficient to specify a posterior direction of axon outgrowth to the *C. elegans* ALM neuron, which normally sends its axon anteriorly (Wolf *et al.*, 1998). At a more subtle level, the ratios of activity of a cytoplasmic tyrosine kinase, ABL, and several other regulators (the ENA protein, which is phosphorylated by ABL, and the tyrosine phosphatases, which antagonize its activity) can determine the outcome of Robo-mediated guidance decisions, particularly in sensitized genetic backgrounds (Bashaw *et al.*, 2000; Sun *et al.*, 2000).

Third, there is evidence from *in vitro* studies that the activity of second messenger pathways within the cell can specify the outcome of guidance decisions. Netrin is normally attractive to *Xenopus* spinal cord neurons, but this attraction is converted to repulsion when cAMP levels are low. Similar effects have been reported with manipulations of calcium (Hong *et al.*, 2000; Zheng, 2000). Conversely, Semaphorin is normally repulsive to spinal neurons but becomes attractive in high cGMP levels (Ming *et al.*, 1997; Song *et al.*, 1998). Cortical neurons in slice preparations exhibit paradoxical opposite responses to Semaphorin: their axons are repelled from Semaphorin, but their dendrites are attracted to Semaphorin

(Polleux *et al.*, 1998; Polleux *et al.*, 2000). Attraction of cortical dendrites to Semaphorin is associated with guanylyl cyclase activity that is localized to dendrites, suggesting that cGMP levels act as an endogenous regulator of Semaphorin signaling that distinguishes axons from dendrites. Although their mechanisms of action remain mysterious, these results suggest that calcium and cyclic nucleotides modulate the cytoskeletal components underlying attraction and repulsion.

1.6 Formation of multimeric complexes by guidance receptors

Dimerization or multimerization is an essential step in activation of many classes of receptors, and this principle appears to apply in axon guidance as well. The mechanisms of multimerization are best defined for the Eph transmembrane tyrosine kinase receptors (Bruckner and Klein, 1998; Davis *et al.*, 1994). The exact valency of the physiological Eph signaling complex is not clear: it is dimeric at least, but may have more than two subunits. The cytoplasmic SAM (sterile-alpha) motif, a conserved motif within Eph receptors is involved in formation of tetrameric and possibly higher order oligomers (Smalla *et al.*, 1999; Stapleton *et al.*, 1999; Thanos *et al.*, 1999), but mice bearing EphA4 receptors lacking the SAM domain have no detectable defects in EphA4 function (Kullander *et al.*, 2001). In all likelihood, the multimerization function provided by the SAM domain is redundant with other clustering mechanisms used by Eph receptors. The ligand itself may have this function, since activation of Eph receptors by GPI-anchored and/or transmembrane Ephrin ligands requires that the ligand be presented in multimeric form (Davis *et al.*, 1994). Ligand clustering may be a common motif that contributes to complex formation and signaling. Crystal structures of receptors bound to their ligands demonstrate that in addition to

receptor-receptor interactions, dimerization can be facilitated by ligand-ligand, ligand-extracellular matrix, or ligand-receptor contacts (Schlessinger, 2000).

Netrin also induces multimerization of its receptor DCC via the P3 domain, a short motif within the DCC cytoplasmic region (Stein *et al.*, 2001). The essential role of the P3 domain in Netrin signaling can be supplied by replacing P3 with the SAM multimerization domain from Eph receptors. This result suggests that axon guidance receptors have a modular organization, with discrete domains that confer functions like dimerization.

1.7 Diversification of guidance responses by combinatorial assembly

Eph and DCC signaling can create homomultimeric receptor complexes; further complexity can arise from the formation of heteromultimer complexes between different receptor molecules. Heteromeric interactions between receptors create the possibility for specificity by a combinatorial logic, in which individual subunits can act in several complexes with distinct properties. Combinatorial assembly of receptor complexes can expand the repertoire of ligands to which growth cones respond, as exemplified by the Semaphorin receptors. Semaphorins are a large family of secreted, GPI-linked, or transmembrane proteins that share an extracellular Sema domain. In three examples, their receptors have been shown to be members of the transmembrane Plexin receptor family: Sema3 proteins signal through PlexinA1 or PlexinA2 (PlexinA), transmembrane Sema4D binds to Plexin B1, and GPI-anchored Sema7A binds to PlexinC1 (Takahashi *et al.*, 1999; Tamagnone *et al.*, 1999). Interestingly, Plexins also contain a Sema domain with an autoinhibitory function; relief of Plexin autoinhibition by Sema domain displacement appears to be a component of receptor activation (Takahashi and Strittmatter, 2001).

The Sema3 family of Semaphorins contains different members with distinct biological activities. Specificity is generated because their functional receptors are not PlexinA alone, but heteromultimers containing both a Neuropilin and a PlexinA molecule (Figure 1-3A). Neuropilins are transmembrane molecules that bind Semaphorins and Plexins; they appear to modulate Sema-Plexin binding and are probably not directly involved in signaling (Nakamura *et al.*, 1998; Takahashi *et al.*, 1999). The combination of Neuropilin-1 and PlexinA confers sensitivity to the ligand Sema3A (He and Tessier-Lavigne, 1997; Kitsukawa *et al.*, 1997; Kolodkin *et al.*, 1997; Takahashi *et al.*, 1999), whereas the combination of Neuropilin-2 and PlexinA confers sensitivity to Sema3F (Chen *et al.*, 1997) (Figure 1-3A). The functions of Neuropilins are not limited to Semaphorin signaling. When co-expressed with the receptor tyrosine kinase VEGF-R2, Neuropilin-1 confers enhanced sensitivity to an entirely different peptide, the angiogenic VEGF-165 protein (Soker *et al.*, 1998; Whitaker *et al.*, 2001).

In addition to the core receptor complex that contains Neuropilin and Plexin, a modulatory role for a third molecule, the transmembrane cell adhesion protein L1-CAM, has been inferred from studies of mice lacking L1 activity (Castellani *et al.*, 2000). Axons from cortical explants or DRG neurons from wild-type mice are efficiently repelled by COS cells expressing Sema3A, but explants from L1-deficient animals are not. These results suggest that L1 contributes to the Sema3A repulsive response. Bath application of an L1 fragment to cortical slices blocked Sema3A-induced collapse and had the surprising effect of converting Sema3A-induced repulsion into attraction. The mechanism of L1 action is unknown, and it may be an indirect effect mediated through cGMP levels or another process like axon fasciculation (bundling). Nonetheless, its activity is of interest as a potential modifier of Semaphorin receptors.

Graded responses. Combinatorial receptor function has implications for signaling as well as ligand binding, and can underlie the generation of graded responses to a single ligand. This idea is exemplified by the action of *Drosophila* Robo proteins. *Drosophila* Robo was first characterized for its role preventing inappropriate midline crossing by axons, but Robo proteins also act in positioning of longitudinal tracts around the midline. This role was first discovered through characterization of Slit, the Robo ligand (Kidd *et al.*, 1999). In addition to disruption of midline crossing, *slit* mutants exhibit a striking defect in which all of the longitudinal tracts coalesce into a single midline bundle. Conversely, overexpression of Slit leads to lateral displacement of longitudinals away from the midline. Thus Slit can define the distance between axons and the midline. Different axon bundles occupy medial, intermediate, or lateral positions with respect to the midline. The position of a given tract is determined largely by its particular complement of three different Robo receptors, Robo, Robo2, and Robo3 (Figure 1-3B) (Rajagopalan *et al.*, 2000a; Rajagopalan *et al.*, 2000b; Simpson *et al.*, 2000a; Simpson *et al.*, 2000b). Robo, Robo2, and Robo3 are expressed in partially overlapping subsets of medial, intermediate, and lateral tracts (Figure 1-3B). Robo is expressed on all axons, and it acts primarily to keep the medial axons from crossing the midline. Disruption of intermediate and laterally-expressed Robo2 and Robo3 shifts the corresponding axon tracts to a medial position. Ectopic expression of laterally-expressed Robo2 or Robo3 in medial axons drives them to a lateral position. Thus the different Robos have different biological activities, which may reflect different affinities for Slit or the formation of heteromeric complexes with different signaling potencies. These findings demonstrate that the expression of particular Robos can confer graded responsiveness to a single Slit guidance cue.

Drosophila midline guidance is modulated by another set of transmembrane proteins, the receptor tyrosine phosphatases (RPTPs) (Sun *et al.*, 2000). It is possible that these act as

part of the combinatorial Robo receptor complex. A conserved tyrosine residue in Robo has significant effects on Robo signaling and has been proposed as a site of PTP regulation (Bashaw *et al.*, 2000). However, the PTPs act in many guidance decisions, so as mentioned above for L1-CAM and Semaphorin signaling, their action at the midline could be an indirect effect mediated through axon fasciculation or other mechanisms, not only through Robo.

Response conversion. Interactions between different receptors in a signaling complex can lead to the dramatic conversion of a guidance response from attraction to repulsion. Netrin is a bifunctional axon guidance signal that can mediate either attraction or repulsion. The transmembrane receptor DCC is the major conserved receptor involved in attraction to Netrin (Hedgecock *et al.*, 1990). DCC binds Netrin directly (Stein *et al.*, 2001), although DCC expression is not always sufficient for a response to Netrin (Chan *et al.*, 1996). A second proposed Netrin receptor, the A2B adenosine receptor, appears to bind Netrin but it is not essential for the Netrin response (Corset *et al.*, 2000; Stein *et al.*, 2001).

Repulsion from Netrin primarily depends on the action of the UNC-5 transmembrane receptor, which is structurally unrelated to DCC (Hedgecock *et al.*, 1990; Leung-Hagesteijn *et al.*, 1992). UNC-5 also binds directly to Netrin (Leonardo *et al.*, 1997). Ectopic expression of UNC-5 can drive repulsion not only in cells that were formerly Netrin-insensitive (Hamelin *et al.*, 1993), but also in cells that were formerly attracted to Netrin via DCC (Hamelin *et al.*, 1993; Hong *et al.*, 1999) (Figure 1-3C). This conversion to repulsion is the result of direct interactions between DCC and UNC-5 cytoplasmic domains that are induced by binding to Netrin. In the new UNC-5/DCC receptor complex, the attractive function of DCC is silenced. Instead, the DCC protein potentiates the UNC-5 repulsive response (Colavita and Culotti, 1998; Hedgecock *et al.*, 1990; Hong *et al.*, 1999), although DCC is not as important as UNC-5 for repulsion (Hedgecock *et al.*,

1990). These results demonstrate that inclusion of different receptor subunits in a complex can not only modulate the strength of the guidance response, but the polarity as well.

Conversion from attraction to repulsion is observed in several other Netrin signaling paradigms. Lowering calcium or cAMP levels or adding laminin-1 fragments to the bath can switch *Xenopus* neurons from attraction to repulsion by Netrin (Hong *et al.*, 2000; Hopker *et al.*, 1999; Ming *et al.*, 1997). However, the molecular targets of calcium, cAMP and laminin are unknown. The UNC-5/DCC example is the first to demonstrate a direct interaction between guidance receptors that changes their signaling properties.

Signal integration. Multiple guidance cues can be arranged in opposing or complementary patterns, and a growth cone must prioritize its responses to these cues. Heteromeric receptor complexes also provide the possibility of integration, where information from several guidance cues can be sorted out in a single decision. Several recent observations suggest that interactions between receptors can dictate the response to guidance cues. Experiments in *Xenopus* neurons provide evidence of hierarchical integration of guidance information. Stage 22 *Xenopus* spinal neurons grow toward Netrin-1, but when Slit is applied, the growth cones lose their ability to turn towards Netrin (Stein and Tessier-Lavigne, 2001). This silencing of Netrin responses occurs through direct binding of Robo to DCC that is induced by Slit (Figure 1-3D). Interestingly, the Robo-DCC complex has properties that are not predictable based on the individual responses of DCC and Robo. First of all, Stage 22 *Xenopus* neurons are not repelled by Slit, so for these neurons Slit-Robo function is only manifested as a modification of the Netrin response. Second, Slit silences only the turning response to Netrin: Netrin stimulates outgrowth of Stage 22 neurons whether Slit is present or not. The signaling complex has a set of properties that are related to its components, but more than just the sum of the parts.

Later in development, Stage 28 *Xenopus* neurons respond to Slit, but not Netrin . Unlike Stage 22 neurons, they are repelled by Slit. This observation suggests that the interactions between guidance receptors are themselves regulated by other factors. A third situation has been observed in *C. elegans,* where genetic analysis suggests that DCC binds to Robo and potentiates Robo signaling in a Netrin-independent fashion (Figure 1-3D) (see Chapter 3). Receptor interactions can thus lead to cooperative guidance functions that depend on either of the normal ligands of the receptors.

A different kind of silencing has been described in the cerebellum, where the G protein-coupled receptor CXCR4 mediates attractive guidance towards the chemokine SDF-1 during granule cell migration (Lu *et al.*, 2001). The activity of the chemokine receptor is inhibited by "reverse" Ephrin signaling, in which EphB receptors signal back to the transmembrane ephrin-B protein. ephrin-B binds to a regulator of G protein signaling (RGS) protein and silences chemokine receptor signaling, presumably by inactivating G proteins through the RGS protein (Figure 1-3D). In this case, silencing involves an interaction between two downstream signaling molecules, not a direct interaction between receptors.

1.8 Mechanistic implications

Guidance receptors signal as multimeric complexes, and the composition of guidance complexes can define ligand interactions and the nature of guidance responses. Some receptors appear be relatively specific for a particular function: for example, UNC-5 is only known to act in Netrin repulsion. Other receptors appear to be more promiscuous, interacting with multiple partners in a variety of signaling events: DCC has roles in Netrin

attraction, Netrin repulsion, Netrin presentation, and Robo signaling, and Neuropilins act in Semaphorin signaling and VEGF signaling.

The existence of combinatorial signaling mechanisms is a fascinating aspect of axon guidance, but it should not be taken to mean that everything signals through everything. Both genetic and biochemical evidence strongly implicate DCC in attractive Netrin signaling, but its roles in other guidance processes are usually more subtle — suggestions rather than demands. Communication between guidance molecules is valuable because it modulates their function in a context, not because it supplants their specificity.

Why should neurons use multifunctional receptor proteins like DCC and Neuropilin during axon guidance? First, as mentioned above, they provide the opportunity to link responses to different ligands in a combinatorial fashion. Second, they could provide biochemical activities that potentiate the functions of other proteins. One receptor subunit might stabilize the expression, subcellular localization, or ligand binding properties of other receptor subunits. Neuropilins may be a candidate for this sort of activity. Alternatively, one receptor could provide specific intracellular signaling motifs that are useful in many guidance decisions. For example, DCC stimulates neurite outgrowth, and might add an outgrowth-stimulatory activity to several different complexes by activating a signaling module.

1.9 Conclusions

The regulation of guidance receptors and ligands allows a single guidance system to generate a variety of different responses. Some regulatory mechanisms, like transcriptional regulation, are characteristic of all guidance systems. Others, like regulated ligand cleavage, have only been described in a single case but may be more widespread. The identification of these

Figure 1-1

The four major families of instructive guidance cues and receptors. Major families are indicated by column headings, with species-specific names underneath. Typical guidance responses, alternate responses (in parentheses), and known modifiers of each pathway are shown. Abbreviations: *ALPS*, Agrin-Laminin-Perlecan-Slit domain. *C*, Netrin C-terminus. *CUB*, C1/Uegf/BMP-1 domain. *EGF*, epidermal growth factor. *FNIII*, fibronectin type III domain. *GPI*, glycosylphosphatidyl-inositol anchor. *Ig*, immunoglobulin domain. *LRR*, leucine-rich repeat. *MAM*, meprin/A5 antigen motif. *MRS*, Met tyrosine kinase-related sequence. *RK*, arginine/lysine-rich basic domain. *SAM*, sterile alpha motif. *SP*, "Sex and Plexins" domain. *TK*, tyrosine kinase domain. *TSP*, thrombospondin domain. *VI*, *V*, homology to laminin domain VI and V, respectively.

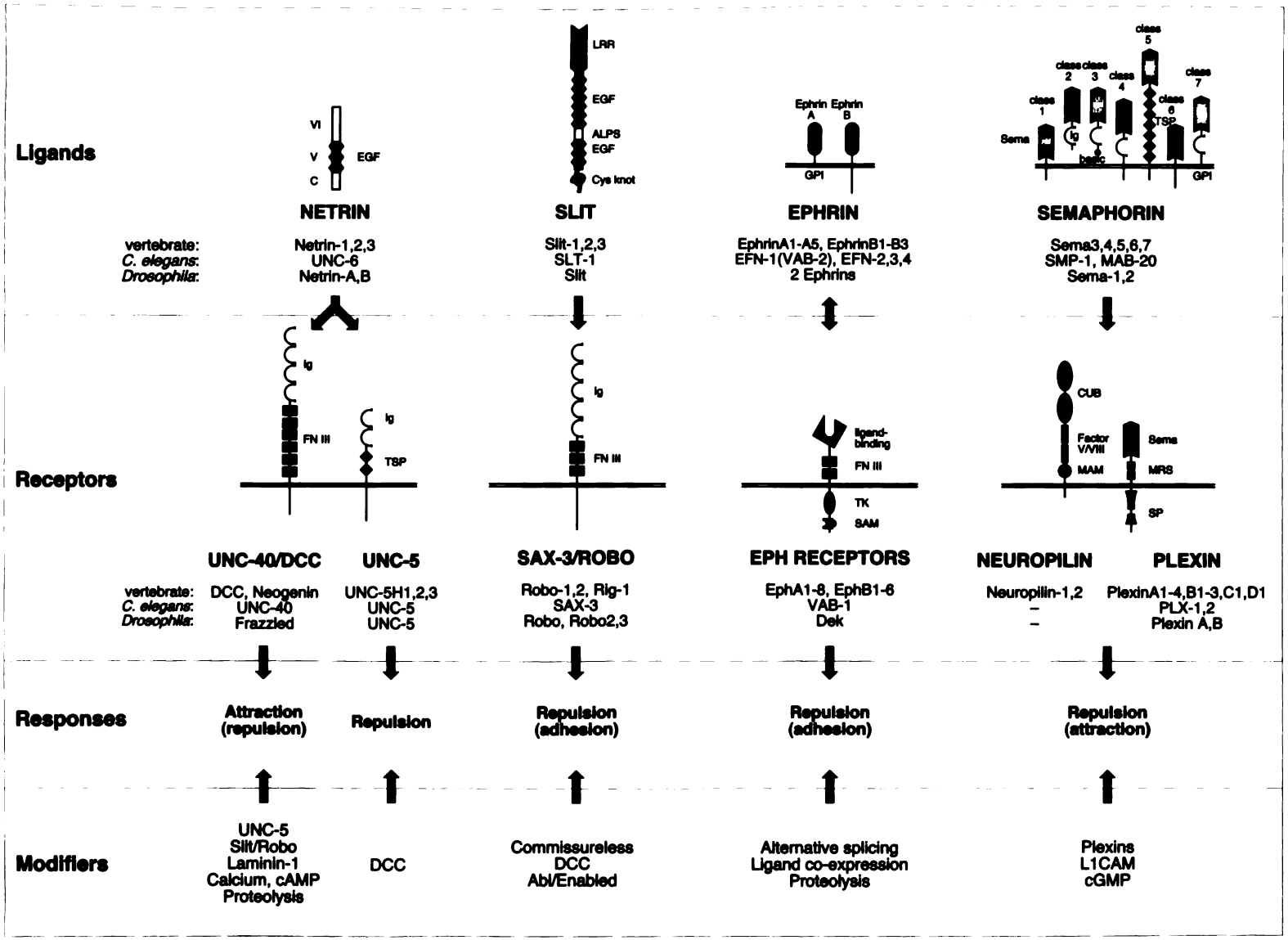
Ligands
VI
V
C
EGF
LRR
EGF
ALPS
EGF
Cys knot
Ephrin A
Ephrin B
GPI
class 1
class 2
class 3
class 4
class 5
class 6
class 7
Sema
Ig
TSP
basic
GPI
NETRIN
SLIT
EPHRIN
SEMAPHORIN
vertebrate:
C. elegans:
Drosophila:
Netrin-1,2,3
UNC-6
Netrin-A,B
Slit-1,2,3
SLT-1
Slit
EphrinA1-A5, EphrinB1-B3
EFN-1(VAB-2), EFN-2,3,4
2 Ephrins
Sema3,4,5,6,7
SMP-1, MAB-20
Sema-1,2
Receptors
Ig
FN III
Ig
TSP
Ig
FN III
ligand-binding
FN III
TK
SAM
CUB
Factor V/VIII
MAM
Sema
MRS
SP
UNC-40/DCC
UNC-5
SAX-3/ROBO
EPH RECEPTORS
NEUROPILIN
PLEXIN
vertebrate:
C. elegans:
Drosophila:
DCC, Neogenin
UNC-40
Frazzled
UNC-5H1,2,3
UNC-5
UNC-5
Robo-1,2, Rig-1
SAX-3
Robo, Robo2,3
EphA1-8, EphB1-6
VAB-1
Dek
Neuropilin-1,2
–
–
PlexinA1-4,B1-3,C1,D1
PLX-1,2
Plexin A,B
Responses
Attraction (repulsion)
Repulsion
Repulsion (adhesion)
Repulsion (adhesion)
Repulsion (attraction)
Modifiers
UNC-5
Slit/Robo
Laminin-1
Calcium, cAMP
Proteolysis
DCC
Commissureless
DCC
Abl/Enabled
Alternative splicing
Ligand co-expression
Proteolysis
Plexins
L1CAM
cGMP

Figure 1-2

Transcriptional regulation of axon guidance cues and their receptors. (**A**) Induction of EphrinB at the Xenopus optic chiasm induces ipsilateral projections. (**B**) Transcriptional repression of the *C. elegans* guidance cue *unc-129* controls dorsal axon guidance. (**C**) EphrinA and EphA gradients specify topography of chick retinotectal projections.

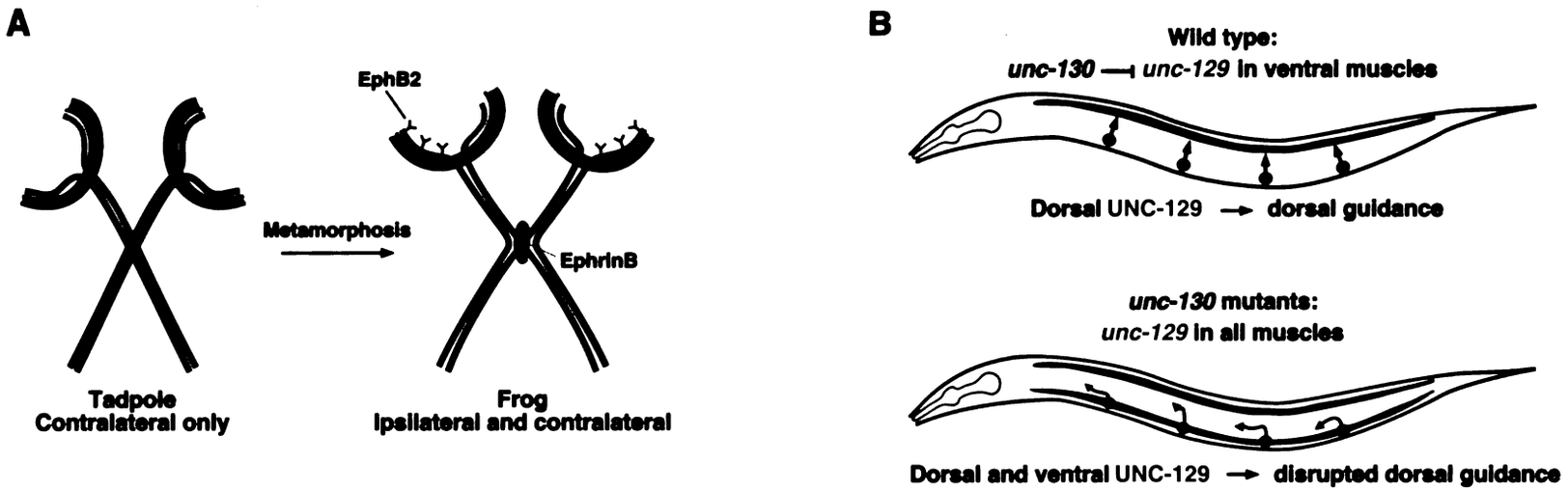
A
EphB2
Metamorphosis
EphrinB
Tadpole
Contralateral only
Frog
Ipsilateral and contralateral
B
Wild type:
unc-130 ⊣ unc-129 in ventral muscles
Dorsal UNC-129 → dorsal guidance
unc-130 mutants:
unc-129 in all muscles
Dorsal and ventral UNC-129 → disrupted dorsal guidance
C
N
T
A
P
Retina
Tectum
EphA3
EphA4,A5
EphrinA2
EphrinA5
EphrinA2
EphrinA5

Figure 1-3

Combinatorial regulation of axon guidance receptor signaling. (**A**) Combinatorial assembly of Semaphorin receptors increases the diversity of ligands to which a family of guidance receptors can respond. (**B**) Combinatorial codes of Robo receptors confer different, graded responses to a single Slit guidance cue. (C) Addition of subunits to a DCC receptor complex can convert the nature of the guidance response from attractive to repulsive. (**D**) Interactions between receptors allow combinatorial integration of different guidance pathways. *DCC*, deleted in colorectal cancer (netrin receptor). *SDF-1*, stromal cell-derived factor (chemokine). *CXCR4*, chemokine receptor. *PDZ-RGS*, PDZ domain-containing regulator of G-protein signaling.

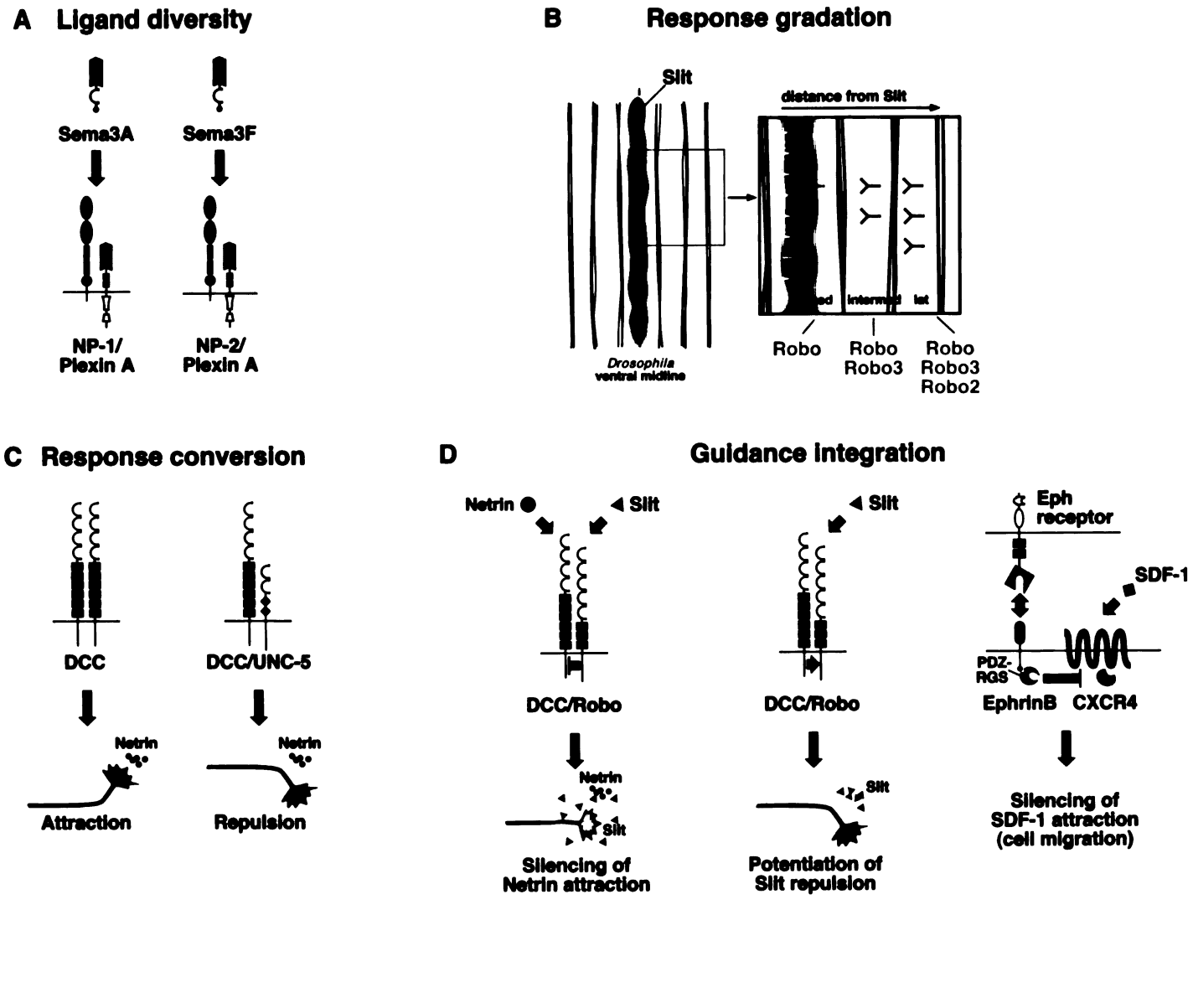
A Ligand diversity
Sema3A
Sema3F
NP-1/
Plexin A
NP-2/
Plexin A
B Response gradation
Slit
distance from Slit
Drosophila
ventral midline
Robo
Robo
Robo3
Robo
Robo3
Robo2
C Response conversion
DCC
DCC/UNC-5
Netrin
Netrin
Attraction
Repulsion
D Guidance integration
Netrin
Slit
Slit
Eph
receptor
SDF-1
PDZ-
RGS
DCC/Robo
DCC/Robo
EphrinB
CXCR4
Netrin
Slit
Slit
Silencing of
Netrin attraction
Potentiation of
Slit repulsion
Silencing of
SDF-1 attraction
(cell migration)

1.10 References

Ackerman, S. L., Kozak, L. P., Przyborski, S. A., Rund, L. A., Boyer, B. B., and Knowles, B. B. (1997). The mouse *rostral cerebellar malformation* gene encodes an UNC-5-like protein. *Nature* **386**, 838-842.

Baran, R., Aronoff, R., and Garriga, G. (1999). The *C. elegans* homeodomain gene *unc-42* regulates chemosensory and glutamate receptor expression. *Development* **126**, 2241-2251.

Bashaw, G. J., Kidd, T., Murray, D., Pawson, T., and Goodman, C. S. (2000). Repulsive axon guidance: Abelson and Enabled play opposing roles downstream of the roundabout receptor. *Cell* **101**, 703-715.

Behar, O., Golden, J. A., Mashimo, H., Schoen, F. J., and Fishman, M. C. (1996). Semaphorin III is needed for normal patterning and growth of nerves, bones and heart. *Nature* **383**, 525-528.

Brose, K., Bland, K. S., Wang, K. H., Arnott, D., Henzel, W., Goodman, C. S., Tessier-Lavigne, M., and Kidd, T. (1999). Slit proteins bind Robo receptors and have an evolutionarily conserved role in repulsive axon guidance. *Cell* **96**, 795-806.

Brown, A., Yates, P. A., Burrola, P., Ortuno, D., Vaidya, A., Jessell, T. M., Pfaff, S. L., O'Leary, D. D., and Lemke, G. (2000). Topographic mapping from the retina to the midbrain is controlled by relative but not absolute levels of EphA receptor signaling. *Cell* **102**, 77-88.

Bruckner, K., and Klein, R. (1998). Signaling by Eph receptors and their ephrin ligands. *Curr Opin Neurobiol* **8**, 375-382.

Castellani, V., Chedotal, A., Schachner, M., Faivre-Sarrailh, C., and Rougon, G. (2000). Analysis of the L1-deficient mouse phenotype reveals cross-talk between Sema3A and L1 signaling pathways in axonal guidance. *Neuron* **27**, 237-249.

Castellani, V., Yue, Y., Gao, P. P., Zhou, R., and Bolz, J. (1998). Dual action of a ligand for Eph receptor tyrosine kinases on specific populations of axons during the development of cortical circuits. *J Neurosci* **18**, 4663-4672.

Chan, S. S., Zheng, H., Su, M. W., Wilk, R., Killeen, M. T., Hedgecock, E. M., and Culotti, J. G. (1996). UNC-40, a *C. elegans* homolog of DCC (Deleted in Colorectal Cancer), is required in motile cells responding to UNC-6 netrin cues. *Cell* **87**, 187-195.

Chen, H., Chedotal, A., He, Z., Goodman, C. S., and Tessier-Lavigne, M. (1997). Neuropilin-2, a novel member of the neuropilin family, is a high affinity receptor for the semaphorins Sema E and Sema IV but not Sema III. *Neuron* **19**, 547-559.

Colavita, A., and Culotti, J. G. (1998). Suppressors of ectopic UNC-5 growth cone steering identify eight genes involved in axon guidance in *Caenorhabditis elegans. Developmental Biology* **194**, 72-85.

Corset, V., Nguyen-Ba-Charvet, K. T., Forcet, C., Moyse, E., Chedotal, A., and Mehlen, P. (2000). Netrin-1-mediated axon outgrowth and cAMP production requires interaction with adenosine A2b receptor. *Nature* **407**, 747-750.

Culotti, J. G., and Merz, D. C. (1998). DCC and netrins. *Curr Opin Cell Biol* **10**, 609-613.

Davis, S., Gale, N. W., Aldrich, T. H., Maisonpierre, P. C., Lhotak, V., Pawson, T., Goldfarb, M., and Yancopoulos, G. D. (1994). Ligands for EPH-related receptor tyrosine kinases that require membrane attachment or clustering for activity. *Science* **266**, 816-819.

Dutting, D., Handwerker, C., and Drescher, U. (1999). Topographic targeting and pathfinding errors of retinal axons following overexpression of ephrinA ligands on retinal ganglion cell axons. *Dev Biol* **216**, 297-311.

Erkman, L., Yates, P. A., McLaughlin, T., McEvilly, R. J., Whisenhunt, T., O'Connell, S. M., Krones, A. I., Kirby, M. A., Rapaport, D. H., Bermingham, J. R., *et al.* (2000). A POU domain transcription factor-dependent program regulates axon pathfinding in the vertebrate visual system. *Neuron* **28**, 779-792.

Feldheim, D. A., Kim, Y. I., Bergemann, A. D., Frisen, J., Barbacid, M., and Flanagan, J. G. (2000). Genetic analysis of ephrin-A2 and ephrin-A5 shows their requirement in multiple aspects of retinocollicular mapping. *Neuron* **25**, 563-574.

Flanagan, J. G., and Vanderhaeghen, P. (1998). The ephrins and Eph receptors in neural development. *Annu Rev Neurosci* **21**, 309-345.

Galko, M. J., and Tessier-Lavigne, M. (2000). Function of an axonal chemoattractant modulated by metalloprotease activity. *Science* **289**, 1365-1367.

Giger, R. J., Pasterkamp, R. J., Heijnen, S., Holtmaat, A. J., and Verhaagen, J. (1998). Anatomical distribution of the chemorepellent semaphorin III/collapsin-1 in the adult rat and human brain: predominant expression in structures of the olfactory-hippocampal pathway and the motor system. *J Neurosci Res* **52**, 27-42.

Guthrie, S. (1999). Axon guidance: starting and stopping with slit. *Current Biology* **9**, R432-435.

Hamelin, M., Zhou, Y., Su, M. W., Scott, I. M., and Culotti, J. G. (1993). Expression of the UNC-5 guidance receptor in the touch neurons of *C. elegans* steers their axons dorsally. *Nature* **364**, 327-330.

Hartmann, B., Hirth, F., Walldorf, U., and Reichert, H. (2000). Expression, regulation and function of the homeobox gene *empty spiracles* in brain and ventral nerve cord development of *Drosophila*. *Mech Dev* **90**, 143-153.

Hattori, M., Osterfield, M., and Flanagan, J. G. (2000). Regulated cleavage of a contact-mediated axon repellent. *Science* **289**, 1360-1365.

He, Z., and Tessier-Lavigne, M. (1997). Neuropilin is a receptor for the axonal chemorepellent Semaphorin III. *Cell* **90**, 739-751.

Hedgecock, E. M., Culotti, J. G., and Hall, D. H. (1990). The *unc-5*, *unc-6*, and *unc-40* genes guide circumferential migrations of pioneer axons and mesodermal cells on the epidermis in *C. elegans*. *Neuron* **4**, 61-85.

Hiramoto, M., Hiromi, Y., Giniger, E., and Hotta, Y. (2000). The *Drosophila* Netrin receptor Frazzled guides axons by controlling Netrin distribution. *Nature* **406**, 886-889.

Holmberg, J., Clarke, D. L., and Frisen, J. (2000). Regulation of repulsion versus adhesion by different splice forms of an Eph receptor. *Nature* **408**, 203-206.

Hong, K., Hinck, L., Nishiyama, M., Poo, M. M., Tessier-Lavigne, M., and Stein, E. (1999). A ligand-gated association between cytoplasmic domains of UNC5 and DCC family receptors converts netrin-induced growth cone attraction to repulsion. *Cell* **97**, 927-941.

Hong, K., Nishiyama, M., Henley, J., Tessier-Lavigne, M., and Poo, M. (2000). Calcium signaling in the guidance of nerve growth by netrin-1. *Nature* **403**, 93-98.

Hopker, V. H., Shewan, D., Tessier-Lavigne, M., Poo, M., and Holt, C. (1999). Growth-cone attraction to netrin-1 is converted to repulsion by laminin-1. *Nature* **401**, 69-73.

Hornberger, M. R., Dutting, D., Ciossek, T., Yamada, T., Handwerker, C., Lang, S., Weth, F., Huf, J., Wessel, R., Logan, C., *et al.* (1999). Modulation of EphA receptor function by coexpressed ephrinA ligands on retinal ganglion cell axons. *Neuron* **22**, 731-742.

Itoh, A., Miyabayashi, T., Ohno, M., and Sakano, S. (1998). Cloning and expressions of three mammalian homologues of *Drosophila slit* suggest possible roles for Slit in the formation and maintenance of the nervous system. *Brain Res Mol Brain Res* **62**, 175-186.

Kania, A., Johnson, R. L., and Jessell, T. M. (2000). Coordinate roles for LIM homeobox genes in directing the dorsoventral trajectory of motor axons in the vertebrate limb. *Cell* **102**, 161-173.

Kidd, T., Bland, K. S., and Goodman, C. S. (1999). Slit is the midline repellent for the robo receptor in *Drosophila*. *Cell* **96**, 785-794.

Kidd, T., Brose, K., Mitchell, K. J., Fetter, R. D., Tessier-Lavigne, M., Goodman, C. S., and Tear, G. (1998a). Roundabout controls axon crossing of the CNS midline and defines a novel subfamily of evolutionarily conserved guidance receptors. *Cell* **92**, 205-215.

Kidd, T., Russell, C., Goodman, C. S., and Tear, G. (1998b). Dosage-sensitive and complementary functions of *roundabout* and *commissureless* control axon crossing of the CNS midline. *Neuron* **20**, 25-33.

Kitsukawa, T., Shimizu, M., Sanbo, M., Hirata, T., Taniguchi, M., Bekku, Y., Yagi, T., and Fujisawa, H. (1997). Neuropilin-semaphorin III/D-mediated chemorepulsive signals play a crucial role in peripheral nerve projection in mice. *Neuron* **19**, 995-1005.

Kolodkin, A. L., Levengood, D. V., Rowe, E. G., Tai, Y. T., Giger, R. J., and Ginty, D. D. (1997). Neuropilin is a semaphorin III receptor. *Cell* **90**, 753-762.

Kramer, S. G., Kidd, T., Simpson, J. H., and Goodman, C. S. (2001). Switching repulsion to attraction: changing responses to slit during transition in mesoderm migration. *Science* **292**, 737-740.

Kullander, K., Mather, N. K., Diella, F., Dottori, M., Boyd, A. W., and Klein, R. (2001). Kinase-dependent and kinase-independent functions of EphA4 receptors in major axon tract formation in vivo. *Neuron* **29**, 73-84.

Lander, A. D. (1990). Mechanisms by which molecules guide axons. *Curr Opin Cell Biol* **2**, 907-913.

Landgraf, M., Roy, S., Prokop, A., VijayRaghavan, K., and Bate, M. (1999). *even-skipped* determines the dorsal growth of motor axons in *Drosophila*. *Neuron* **22**, 43-52.

Leonardo, E. D., Hinck, L., Masu, M., Keino-Masu, K., Ackerman, S. L., and Tessier-Lavigne, M. (1997). Vertebrate homologues of *C. elegans* UNC-5 are candidate netrin receptors. *Nature* **386**, 833-838.

Leung-Hagesteijn, C., Spence, A. M., Stern, B. D., Zhou, Y., Su, M. W., Hedgecock, E. M., and Culotti, J. G. (1992). UNC-5, a transmembrane protein with immunoglobulin and thrombospondin type 1 domains, guides cell and pioneer axon migrations in *C. elegans*. *Cell* **71**, 289-299.

Lu, Q., Sun, E. E., Klein, R. S., and Flanagan, J. G. (2001). Ephrin-B reverse signaling is mediated by a novel PDZ-RGS protein and selectively inhibits G protein-coupled chemoattraction. *Cell* **105**, 69-79.

Lundgren, S. E., Callahan, C. A., Thor, S., and Thomas, J. B. (1995). Control of neuronal pathway selection by the *Drosophila* LIM homeodomain gene *apterous*. *Development* **121**, 1769-1773.

Luo, L. (2000). Trio quartet in *D.* (*melanogaster*). *Neuron* **26**, 1-2.

Luo, L., Liao, Y. J., Jan, L. Y., and Jan, Y. N. (1994). Distinct morphogenetic functions of similar small GTPases: *Drosophila Drac1* is involved in axonal outgrowth and myoblast fusion. *Genes Dev* **8**, 1787-1802.

Luo, Y., Shepherd, I., Li, J., Renzi, M. J., Chang, S., and Raper, J. A. (1995). A family of molecules related to collapsin in the embryonic chick nervous system. *Neuron* **14**, 1131-1140.

Ming, G. L., Song, H. J., Berninger, B., Holt, C. E., Tessier-Lavigne, M., and Poo, M. M. (1997). cAMP-dependent growth cone guidance by netrin-1. *Neuron* **19**, 1225-1235.

Much, J. W., Slade, D. J., Klampert, K., Garriga, G., and Wightman, B. (2000). The *fax-1* nuclear hormone receptor regulates axon pathfinding and neurotransmitter expression. *Development* **127**, 703-712.

Mueller, B. K. (1999). Growth cone guidance: first steps towards a deeper understanding. *Annu Rev Neurosci* **22**, 351-388.

Nakagawa, S., Brennan, C., Johnson, K. G., Shewan, D., Harris, W. A., and Holt, C. E. (2000). Ephrin-B regulates the ipsilateral routing of retinal axons at the optic chiasm. *Neuron* **25**, 599-610.

Nakamura, F., Tanaka, M., Takahashi, T., Kalb, R. G., and Strittmatter, S. M. (1998). Neuropilin-1 extracellular domains mediate semaphorin D/III-induced growth cone collapse. *Neuron* **21**, 1093-1100.

Nash, B., Colavita, A., Zheng, H., Roy, P. J., and Culotti, J. G. (2000). The forkhead transcription factor UNC-130 is required for the graded spatial expression of the UNC-129 TGF-beta guidance factor in *C. elegans*. *Genes Dev* **14**, 2486-2500.

Nobes, C. D., and Hall, A. (1995). Rho, rac, and cdc42 GTPases regulate the assembly of multimolecular focal complexes associated with actin stress fibers, lamellipodia, and filopodia. *Cell* **81**, 53-62.

Polleux, F., Giger, R. J., Ginty, D. D., Kolodkin, A. L., and Ghosh, A. (1998). Patterning of cortical efferent projections by semaphorin-neuropilin interactions. *Science* **282**, 1904-1906.

Polleux, F., Morrow, T., and Ghosh, A. (2000). Semaphorin 3A is a chemoattractant for cortical apical dendrites. *Nature* **404**, 567-573.

Rajagopalan, S., Nicolas, E., Vivancos, V., Berger, J., and Dickson, B. J. (2000a). Crossing the midline: roles and regulation of Robo receptors. *Neuron* **28**, 767-777.

Rajagopalan, S., Vivancos, V., Nicolas, E., and Dickson, B. J. (2000b). Selecting a longitudinal pathway: Robo receptors specify the lateral position of axons in the *Drosophila* CNS. *Cell* **103**, 1033-1045.

Raper, J. A. (2000). Semaphorins and their receptors in vertebrates and invertebrates. *Curr Opin Neurobiol* **10**, 88-94.

Retaux, S., and Harris, W. A. (1996). Engrailed and retinotectal topography. *Trends Neurosci* **19**, 542-546.

Rhinn, M., Dierich, A., Le Meur, M., and Ang, S. (1999). Cell autonomous and non-cell autonomous functions of *Otx2* in patterning the rostral brain. *Development* **126**, 4295-4304.

Schlessinger, J. (2000). Cell signaling by receptor tyrosine kinases. *Cell* **103**, 211-225.

Schulte, D., and Cepko, C. L. (2000). Two homeobox genes define the domain of EphA3 expression in the developing chick retina. *Development* **127**, 5033-5045.

Seeger, M., Tear, G., Ferres-Marco, D., and Goodman, C. S. (1993). Mutations affecting growth cone guidance in *Drosophila*: genes necessary for guidance toward or away from the midline. *Neuron* **10**, 409-426.

Shamah, S. M., Lin, M. Z., Goldberg, J. L., Estrach, S., Sahin, M., Hu, L., Bazalakova, M., Neve, R. L., Corfas, G., Debant, A., and Greenberg, M. E. (2001). EphA receptors regulate growth cone dynamics through the novel guanine nucleotide exchange factor ephexin. *Cell* **105**, 233-244.

Simpson, J. H., Bland, K. S., Fetter, R. D., and Goodman, C. S. (2000a). Short-range and long-range guidance by Slit and its Robo receptors: a combinatorial code of Robo receptors controls lateral position. *Cell* **103**, 1019-1032.

Simpson, J. H., Kidd, T., Bland, K. S., and Goodman, C. S. (2000b). Short-range and long-range guidance by slit and its Robo receptors. Robo and Robo2 play distinct roles in midline guidance. *Neuron* **28**, 753-766.

Smalla, M., Schmieder, P., Kelly, M., Ter Laak, A., Krause, G., Ball, L., Wahl, M., Bork, P., and Oschkinat, H. (1999). Solution structure of the receptor tyrosine kinase EphB2 SAM domain and identification of two distinct homotypic interaction sites. *Protein Sci* **8**, 1954-1961.

Soker, S., Takashima, S., Miao, H. Q., Neufeld, G., and Klagsbrun, M. (1998). Neuropilin-1 is expressed by endothelial and tumor cells as an isoform- specific receptor for vascular endothelial growth factor. *Cell* **92**, 735-745.

Song, H., Ming, G., He, Z., Lehmann, M., McKerracher, L., Tessier-Lavigne, M., and Poo, M. (1998). Conversion of neuronal growth cone responses from repulsion to attraction by cyclic nucleotides. *Science* **281**, 1515-1518.

Song, H., and Poo, M. (2001). The cell biology of neuronal navigation. *Nat Cell Biol* **3**, E81-88.

Stapleton, D., Balan, I., Pawson, T., and Sicheri, F. (1999). The crystal structure of an Eph receptor SAM domain reveals a mechanism for modular dimerization. *Nat Struct Biol* **6**, 44-49.

Stein, E., and Tessier-Lavigne, M. (2001). Hierarchical organization of guidance receptors: silencing of netrin attraction by slit through a Robo/DCC receptor complex. *Science* **291**, 1928-1938.

Stein, E., Zou, Y., Poo, M., and Tessier-Lavigne, M. (2001). Binding of DCC by netrin-1 to mediate axon guidance independent of adenosine A2B receptor activation. *Science* **291**, 1976-1982.

Steven, R., Kubiseski, T. J., Zheng, H., Kulkarni, S., Mancillas, J., Ruiz Morales, A., Hogue, C. W., Pawson, T., and Culotti, J. (1998). UNC-73 activates the Rac GTPase and is required for cell and growth cone migrations in *C. elegans*. *Cell* **92**, 785-795.

Su, M., Merz, D. C., Killeen, M. T., Zhou, Y., Zheng, H., Kramer, J. M., Hedgecock, E. M., and Culotti, J. G. (2000). Regulation of the UNC-5 netrin receptor initiates the first reorientation of migrating distal tip cells in *Caenorhabditis elegans*. *Development* **127**, 585-594.

Sun, Q., Bahri, S., Schmid, A., Chia, W., and Zinn, K. (2000). Receptor tyrosine phosphatases regulate axon guidance across the midline of the *Drosophila* embryo. *Development* **127**, 801-812.

Takahashi, T., Fournier, A., Nakamura, F., Wang, L. H., Murakami, Y., Kalb, R. G., Fujisawa, H., and Strittmatter, S. M. (1999). Plexin-neuropilin-1 complexes form functional semaphorin-3A receptors. *Cell* **99**, 59-69.

Takahashi, T., and Strittmatter, S. M. (2001). Plexin-A1 autoinhibition by the plexin sema domain. *Neuron* **29**, 429-439.

Tamagnone, L., Artigiani, S., Chen, H., He, Z., Ming, G. I., Song, H., Chedotal, A., Winberg, M. L., Goodman, C. S., Poo, M., *et al.* (1999). Plexins are a large family of receptors for transmembrane, secreted, and GPI-anchored semaphorins in vertebrates. *Cell* **99**, 71-80.

Tamagnone, L., and Comoglio, P. M. (2000). Signaling by semaphorin receptors: cell guidance and beyond. *Trends Cell Biol* **10**, 377-383.

Tanaka, E., and Sabry, J. (1995). Making the connection: cytoskeletal rearrangements during growth cone guidance. *Cell* **83**, 171-176.

Tear, G., Harris, R., Sutaria, S., Kilomanski, K., Goodman, C. S., and Seeger, M. A. (1996). *commissureless* controls growth cone guidance across the CNS midline in *Drosophila* and encodes a novel membrane protein. *Neuron* **16**, 501-514.

Tessier-Lavigne, M., and Goodman, C. S. (1996). The molecular biology of axon guidance. *Science* **274**, 1123-1133.

Thanos, C. D., Goodwill, K. E., and Bowie, J. U. (1999). Oligomeric structure of the human EphB2 receptor SAM domain. *Science* **283**, 833-836.

Thor, S., Andersson, S. G., Tomlinson, A., and Thomas, J. B. (1999). A LIM-homeodomain combinatorial code for motor-neuron pathway selection. *Nature* **397**, 76-80.

Thor, S., and Thomas, J. B. (1997). The *Drosophila islet* gene governs axon pathfinding and neurotransmitter identity. *Neuron* **18**, 397-409.

Van Vactor, D., and Flanagan, J. G. (1999). The middle and the end: slit brings guidance and branching together in axon pathway selection. *Neuron* **22**, 649-652.

Wadsworth, W. G., Bhatt, H., and Hedgecock, E. M. (1996). Neuroglia and pioneer neurons express UNC-6 to provide global and local netrin cues for guiding migrations in *C. elegans*. *Neuron* **16**, 35-46.

Whitaker, G. B., Limberg, B. J., and Rosenbaum, J. S. (2001). Vascular endothelial growth factor receptor-2 and neuropilin-1 form a receptor complex that is responsible for the differential signaling potency of vegf165 and vegf121. *J Biol Chem* **276**, 25520-25531.

Wightman, B., Clark, S. G., Taskar, A. M., Forrester, W. C., Maricq, A. V., Bargmann, C. I., and Garriga, G. (1996). The *C. elegans* gene *vab-8* guides posteriorly directed axon outgrowth and cell migration. *Development* **122**, 671-682.

Wilkinson, D. G. (2001). Multiple roles of EPH receptors and ephrins in neural development. *Nat Rev Neurosci* **2**, 155-164.

Wolf, F. W., Hung, M. S., Wightman, B., Way, J., and Garriga, G. (1998). *vab-8* is a key regulator of posteriorly directed migrations in *C. elegans* and encodes a novel protein with kinesin motor similarity. *Neuron* **20**, 655-666.

Yuan, W., Zhou, L., Chen, J. H., Wu, J. Y., Rao, Y., and Ornitz, D. M. (1999). The mouse SLIT family: secreted ligands for ROBO expressed in patterns that suggest a role in morphogenesis and axon guidance. *Developmental Biology* **212**, 290-306.

Zallen, J. A., Kirch, S. A., and Bargmann, C. I. (1999). Genes required for axon pathfinding and extension in the *C. elegans* nerve ring. *Development* **126**, 3679-3692.

Zheng, J. Q. (2000). Turning of nerve growth cones induced by localized increases in intracellular calcium ions. *Nature* **403**, 89-93.

Zipkin, I. D., Kindt, R. M., and Kenyon, C. J. (1997). Role of a new Rho family member in cell migration and axon guidance in *C. elegans*. *Cell* **90**, 883-894.

Chapter 2

C. elegans Enabled and Nck are candidate SAX-3 signaling molecules

2.1 Summary

Axon guidance receptors convey directional information from extracellular cues to the growth cone cytoskeleton. To understand how this signaling occurs, we sought to identify proteins that act downstream of the Slit receptor SAX-3/Robo. The cytoplasmic domain of SAX-3 encodes a number of conserved, proline-rich motifs. We find that one of these motifs binds to Enabled, a cytoskeletal protein implicated in the control of microfilament dynamics. We identify a *C. elegans* homolog of Enabled, and show that RNA-mediated disruption of *c-ena* results in neuronal migration defects similar to those seen in *sax-3* mutants. In addition, using a yeast two-hybrid screen we identify a second SAX-3-interacting protein, c-NCK. c-NCK is a SH2/SH3 adapter protein that is closely related to the cytoskeletal-associated adapter proteins Nck (42% identity) and Dreadlocks (40% identity). c-NCK binds to SAX-3 via a distinct proline-rich motif, separate from the c-ENA binding site, in an interaction involving its second SH3 domain. Deletions of putative Enabled and Nck binding sites within a rescuing SAX-3 transgene impair rescue of *sax-3* axon guidance defects, supporting a functional role for these interactions. These results implicate Enabled and Nck in linking SAX-3 to cytoskeletal responses in the growth cone.

2.2 Introduction

Guidance cues elicit a wide variety of growth cone responses during development, ranging from expansion or retraction of the entire growth cone to more localized behaviors such as turning. While many of the guidance receptors that mediate these responses have been cloned, the mechanisms by which they work remain incompletely understood. In particular, little is known about how activation of guidance receptors leads to changes in the cytoskeleton. The identification of molecules that link guidance receptors to the cytoskeleton remains an important goal in the field.

Molecular and biochemical approaches have led to the identification of several molecules that are candidate components of axon guidance signaling systems. Members of the Ena/VASP family of proteins were first identified as cellular components that promoted the actin-based motility of the intracellular pathogen *Listeria monocytogenes* (Bear *et al.*, 2001; Machesky, 1997). *Listeria* moves within infected cells through polymerization of an actin "comet" tail, formation of which requires the Arp2/3 complex, cofilin, and capping protein (Loisel *et al.*, 1999). Addition of VASP, profilin and alpha-actinin enhances the formation of actin comet tails (Loisel *et al.*, 1999), suggesting a role for these proteins in actin polymerization and motility. An actin polymerization function for these proteins is also suggested by the ability of a neural-enriched isoform of Mena (mammalian Enabled) to induce actin microspikes in cultured fibroblasts (Gertler *et al.*, 1996). However, mouse fibroblasts lacking VASP and Mena function move more rapidly than wild-type fibroblasts, suggesting that VASP and Mena might inhibit as well as stimulating motility (Bear *et al.*, 2000).

Another protein likely to play a central role in cytoskeletal signaling is Nck. Nck and its close relative Nck2/Grb4 are mammalian homologs of *Drosophila* Dreadlocks (Dock).

Mutations in *Dock* disrupt photoreceptor axon guidance in the *Drosophila* visual system (Garrity *et al.*, 1996). Considerable biochemical evidence implicates Nck in cytoskeletal signaling pathways. The Nck family of molecules encode adapter proteins with three SH3 domains for binding to proline-rich sequences and one SH2 domain for binding phosphotyrosine residues (McCarty, 1998; Pawson and Scott, 1997). Nck associates through these domains with a host of cytoskeletal proteins including Pak1 (Lu *et al.*, 1997) Wiskott-Aldrich Syndrome Protein (WASP) (Rivero-Lezcano *et al.*, 1995; She *et al.*, 1997) and WASP-interacting protein (WIP) (Anton *et al.*, 1998). Nck and WASP are also recruited to sites of actin assembly in the actin-based motility of vaccinia virus, supporting a role in actin polymerization (Frischknecht *et al.*, 1999). Another Nck family member, Nck2/Grb4, has been shown to bind Cbl-associated protein (CAP/ponsin), the Abl-interacting protein-1 (Abi-1), dynamin, heterogenous nuclear ribonucleoprotein K (hnRNPK) and axin (Cowan and Henkemeyer, 2001).

We are studying axon guidance mediated by the receptor SAX-3/Robo in *C. elegans*. The SAX-3/Robo family of receptors has been implicated in short- and long-range chemorepulsion from its secreted ligand Slit in *C. elegans*, *Drosophila* and vertebrates (Hao *et al.*, 2001) (Kidd *et al.*, 1999) (Brose *et al.*, 1999) (Li *et al.*, 1999). In *C. elegans*, *sax-3* mutants exhibit a variety of errors in axon guidance, including anterior misrouting of axons in the nerve ring, abnormal midline crossing in the ventral cord, and defects in ventrally-directed guidance of the AVM neuron (Zallen *et al.*, 1999; Zallen *et al.*, 1998). *sax-3* mutants also have defects in neuronal cell migrations, including posterior migration of the CAN (canal-associated) neuron (Zallen *et al.*, 1999). As expected for an axon guidance receptor, *sax-3* can act cell-autonomously, since expression of *sax-3* in AVM under the *mec-7* promoter rescues guidance defects of a strong *sax-3(ky123)* mutant (Zallen *et al.*, 1999).

SAX-3/Robo proteins share a common structure consisting of five immunoglobulin domains, three fibronectin type III repeats, a transmembrane domain, and a cytoplasmic tail (Kidd *et al.*, 1998; Zallen *et al.*, 1998). The cytoplasmic domain of *C. elegans* SAX-3 is notable for three proline-rich motifs that are conserved between nematodes, flies, and vertebrates (Kidd *et al.*, 1998) (Table 2-1). The first of these (SAX-3 motif A) may be a site for tyrosine phosphorylation (Bashaw *et al.*, 2000; Kidd *et al.*, 1998). A second (SAX-3 motif B) contains multiple PxxP motifs, binding targets for SH3 domains (Feller *et al.*, 1994), while a third (SAX-3 motif C) resembles sequences found in proteins known to bind EVH1 domains of Enabled/VASP family members (Kidd *et al.*, 1998).

In this chapter we report the identification of c-NCK, a *C. elegans* adapter protein, in a yeast two-hybrid screen for proteins that bind to the SAX-3 cytoplasmic domain. c-NCK is highly related to vertebrate Nck and fly Dock and binds to SAX-3 motif B in an interaction involving its second SH3 domain. We also demonstrate that SAX-3 motif C is a binding target for Ena/VASP family proteins, and describe the identification of c-ENA, a novel *C. elegans* homolog of Enabled. RNA-mediated interference experiments with c-ENA disrupt normal movement and CAN cell migrations, consistent with a role in *sax-3* signaling. Finally, in transgenic SAX-3 rescue experiments, deletions of putative Nck and Enabled binding sites are shown to impair rescue of *sax-3* axon guidance defects, supporting a functional role for these interactions.

Further genetic and biochemical evidence that Enabled contributes to axon guidance by SAX-3/Robo is discussed in Chapter 3. Also described in Chapter 3 is independent evidence from *Drosophila* for a role for Enabled in Robo signaling (Bashaw *et al.*, 2000).

2.3 Results

Identification of *C. elegans Nck* as a SAX-3-interacting protein

To identify proteins that bind to SAX-3, we conducted a yeast two-hybrid screen with the SAX-3 cytoplasmic domain. A fragment of the SAX-3 cytoplasmic domain was fused to the DNA binding domain of GAL4 (GAL4D) and used to screen 1-2 million clones from a yeast two-hybrid cDNA library. Two clones (1-1 and 2-1) were identified that strongly transactivated the GAL4D::SAX-3 bait: cotransfection of either with GAL4D::SAX-3 allowed robust growth on His-deficient, 3AT-positive plates with robust activation of a lacZ reporter gene (Figure 2-1A). Sequencing revealed that both clones encoded *C. elegans* ZK470.5, a predicted SH2/SH3 adapter protein that is highly related to *Drosophila* dreadlocks (Dock) and vertebrate Nck (Figure 2-1B). We therefore refer to ZK470.5 as *c-nck*.

The full-length *c-nck* cDNA was obtained from clones 1-1, 2-1 and additional seequences from the *C. elegans* EST database (gift of Y. Kohara). Analysis of the full-length cDNA revealed a 1.6 kB transcript encoding a full-length protein of 425 amino acids (Figure 2-2). c-NCK contains three SH3 domains and one C-terminal SH2 domain (Figure 2-2). Sequence comparisons of existing cDNAs indicated the existence of at least two additional splice forms: a 423 amino acid variant that deletes a isovaline-valine dipeptide at the beginning of the third SH3 domain, and a 424 amino acid variant that deletes a single valine residue after the third SH3 domain (Figure 2-2).

c-NCK is highly related to other Nck family members, with 36% overall identity/51% similarity to fly Dock and 37% identity/51% similarity to vertebrate Nck and Nck2/Nck-beta/Grb4 (Figure 2-3). A comparison of individual SH3 and SH2 domains between family members reveals an even higher degree of similarity, with %identity and

%similarity between c-NCK and Dock ranging from 43-65% and 71-75%, respectively (Figure 2-1B). Based on these observations we conclude c-NCK is a likely to be a true Nck/Dock homolog.

c-NCK binds to SAX-3 motif B via its second SH3 domain

To confirm the observed yeast two-hybrid results and identify domains of c-NCK and SAX-3 involved in this interaction, we performed *in vitro* binding experiments with bacterially expressed SAX-3 and c-NCK.

In coprecipitation experiments, a full-length biotinylated c-NCK probe associated with bacterially expressed GST::SAX-3 protein, but not with GST alone (Figure 2-4). Full-length c-NCK also associated with a GST fusion protein containing only SAX-3 motif B (GST::SAX-3 B), but not to GST fusions to SAX-3 motifs A or C (Figure 2-4). These results confirm the interaction observed in the yeast two-hybrid assay, and identify SAX-3 motif B as a c-NCK binding site.

Previous experiments examining interactions between SAX-3 and a panel of candidate cytoskeletal molecules indicated that motif B was capable of binding SH3 domains (T. Yu, D. Lee, K. Prehoda, and W. Lim, data not shown). To identify domains of c-NCK responsible for binding motif B, we performed a series of Far Western experiments in collaboration with the laboratory of Wendell Lim.

A c-NCK probe containing only the SH3 domains bound to GST::SAX-3 B, but not GST::SAX-3 A, C, or GST alone (Figure 2-4, middle). These results indicated that the c-NCK SH2 domain is dispensible for this interaction. To further narrow down the SAX-3-binding region, individual c-NCK SH3 domains were expressed and assayed for binding. A probe consisting of the first SH3 domain failed to express in bacteria, but the second c-NCK SH3 domain alone expressed well and was sufficient to bind to SAX-3 motif B (Figure 2-4,

bottom). The third SH3 domain was also expressed and bound to positive controls but did not associate with GST::SAX-3 A, B, or C (data not shown). These results show that the observed SAX-3/c-NCK interaction involves the second SH3 domain and not the third SH3 domain. Additional roles for the first SH3 domain and the SH2 domain in promoting this interaction cannot be excluded at this time.

C. elegans c-nck is expressed in neuronal and non-neuronal tissues

To ask whether *c-nck* is expressed in neuronal tissues, we undertook an analysis of the *c-nck* expression pattern using GFP reporter fusions. A construct consisting of 2.6 kB upstream sequence and the first seven amino acids of c-NCK fused to GFP was generated (Figure 2-5A). This transgene does not include all of *c-nck*, so it may not fully reflect the complete *c-nck* expression pattern. Transgenic lines bearing this construct drove GFP expression in a wide variety of neurons (Figure 2-5). Examination of adult worms revealed numerous GFP-expressing motorneurons in the ventral cord (Figure 2-5C). Commissural axons were observed to emanate directly from the cell bodies of these motorneurons (Figure 2-5C), suggesting they are of the AS/DA/DB class (White *et al.*, 1986). Strong GFP expression was also detected in the H-shaped excretory cell (Figure 2-5A,B) as well as head sensory neurons (Figure 2-5D). Additional sites of expression included the CAN neuron, VC motor neurons, a pair of neurons in the phasmid, and cells in the somatic gonad (data not shown). While characterization of *c-nck* expression earlier in development awaits future studies, the observation of *c-nck* expression in neuronal tissues is consistent with an intracellular role in regulating neuronal migrations.

A second proline-rich motif in SAX-3 specifically interacts with EVH1 domains

To identify additional players in SAX-3-mediated guidance, we sought to identify molecules that bound other conserved motifs in the SAX-3 cytoplasmic domain. In collaboration with the laboratory of Wendell Lim, SAX-3 cytoplasmic sequences were expressed as bacterial GST fusion proteins, immobilized on nylon filters and probed for interactions with a variety of candidate molecules.

Ena/VASP family proteins contain EVH1 domains, protein-protein interaction modules that bind the proline-rich sequence D/EFPPPPXD/E (Niebuhr *et al.*, 1997). SAX-3 motif C contains a proline-rich core that resembles the EVH1 binding consensus (Table 2-1). We therefore tested Ena/VASP proteins for their ability to bind to SAX-3.

A biotinylated probe consisting of the EVH1 domain of Mena associated with GST::SAX-3 motif C, but not GST::SAX-3 A, GST::SAX-3 B, or GST alone (Figure 2-6A). Mena also bound to a *Listeria* ActA positive control (Figure 2-6A). Increasing the number of copies by including tandem repeats of motif C (GST::SAX-3 Cx2 and Cx3) enhanced Mena binding, while mutation of a phenylalanine residue predicted to be important for EVH1 domain interactions (GST::SAX-3 C–, F>AIPPPPSNPPP) abolished binding (Fig. 2-6A). Similar results were observed when GST::SAX-3 fusions were tested for their ability to bind EVH1 domains of a related Enabled family member, EVL (Enabled/VASP Like). Like Mena, EVL bound GST::ActA as well as GST::SAX-3 C, Cx2, and Cx3, but failed to bind GST::SAX-3 A, B, C– or GST alone (data not shown).

To test whether the observed Mena binding to SAX-3 motif C was specific, Far Western binding experiments were performed in the presence of ActA competitor peptide. Coincubation with ActA blocked Mena binding to GST::SAX-3 C (Fig. 2-6B). Together, these results demonstrate that SAX-3 cytoplasmic motif C is a ligand for EVH1 domains of Enabled family proteins.

Identification of *C. elegans* Enabled

The discovery that Enabled bound to SAX-3 motif C suggested that guidance by SAX-3 may involve interactions with cytoskeletal proteins of the Enabled/VASP family. At the time of this study, however, no *C. elegans* Enabled family members had been reported. To identify *C. elegans* Enabled homologs, we searched for EVH1 domain-containing proteins in the *C. elegans* genome.

BLAST searches with known EVH1-containing proteins revealed three *C. elegans* proteins containing EVH1 domains: B0280.2 and C07G1.4, two proteins predicted by the *C. elegans* sequencing consortium, and a previously unidentified ORF on the left arm of chromosome V that we named *c-ena*. Phylogenetic analysis of the EVH1 domains indicated that B0280.2 and C07G1.4 are most related to Bee1p and WASP, respectively, while *c-ena* is the closest *C. elegans* relative of Enabled (Figure 2-7). The c-ENA EVH1 domain shares 36%/57% and 38%/62% identity/similarity with *Drosophila* Ena and Mena, respectively (Figure 2-7B). Independently, Frank Gertler and colleagues also identified *c-ena* in searches for nematode homologs of Enabled (F. Gertler, personal communication).

To further characterize this putative *C. elegans* Enabled homolog, we isolated a full-length cDNA. Primers were designed to the *C. elegans* trans-spliced SL1 leader sequence and to sequences internal to predicted *c-ena* coding sequences. RT-PCR reactions amplified two overlapping cDNA fragments, which yielded a single 1.4 kB cDNA (Figure 2-8).

The predicted full-length c-ENA protein is 468 amino acids in length (Figure 2-8). Enabled/VASP family members contain an EVH 1 domain, a central proline-rich domain that interacts with profilin/actin, SH3 domains, and WW domains, and a EVH2 domain thought to be involved in multimerization and F-actin binding (Reinhard *et al.*, 2001). c-ENA shares this overall structure with a N-terminal EVH1 domain, a central proline-rich

domain and C-terminal EVH2 domain (Figure 2-8). c-ENA also contains four potential phosphorylation sites for cAMP- and cGMP-dependent kinases ([RK]- [RK]-X- [ST]). Based on these results we identify c-ENA as the *C. elegans* homolog of Enabled.

Disruption of *C. elegans* Enabled causes CAN cell migration defects

To ask whether Enabled plays a role in neuronal guidance in *C. elegans*, we disrupted *c-ena* using RNA-mediated interference (RNAi) (Fire *et al.*, 1998). Double-stranded RNAs corresponding to *c-ena* coding sequences were synthesized and injected into wild-type *C. elegans* hermaphrodites bearing the *ceh-23::GFP(kyIs4)* marker. *ceh-23::GFP* is expressed in amphid, phasmid, and CAN neurons (Zallen *et al.*, 1999). RNAi of *c-ena* resulted in uncoordinated (Unc) and withered tail (Wit) phenotypes (data not shown). No defects were observed in cell body or axon positioning of the amphid or phasmid neurons (data not shown); however, *c-ena* RNAi-injected adults exhibited CAN cell migration defects (Figure 2-9) in which the CAN cell was displaced anteriorly. Withered tail and CAN migration defects are observed in *sax-3* mutants as well (Figure 2-9). These results were therefore consistent with *c-ena* playing a role in guidance mediated by SAX-3.

The phenotype of *c-ena*-RNAi-injected animals was strikingly similar to that of *unc-34* mutants, which are Unc, Wit, and exhibit CAN cell migration defects. We also noted that *unc-34* mapped to a small interval containing *c-ena*, further suggesting that *unc-34* encodes *c-ena*. In fact, Megan Dell and Gian Garriga made similar, independent observations and demonstrated that *c-ena* corresponds to *unc-34* (Gian Garriga, personal communication). Further experiments exploring the role of *unc-34* in SAX-3 mediated guidance are presented in Chapter 3.

Deletion of SAX-3 motifs B and C disrupt SAX-3 rescue of ventral guidance

To determine the relevance of these binding interactions, we performed structure-function analyses of SAX-3 to determine domains required for SAX-3 activity. In wild-type animals, the AVM axon migrates ventrally (Figure 2-10A). In *sax-3* mutants, AVM often fails to migrate ventrally and extends laterally instead (Figure 2-10A). This defect is 38% penetrant in the strong *sax-3(ky123)* allele. Expression of wild-type *sax-3* under the *mec-7* promoter in *sax-3(ky123)* animals is capable of rescuing the AVM defect (Zallen *et al.*, 1999). As shown in Figure 2-10, expression of *mec-7*::SAX-3 reduced the penetrance of axon guidance defects to <=5% in 2/4 lines tested, with an average 5% defect over the four lines.

If binding of c-NCK and c-ENA is required for SAX-3 guidance, deletion of the domains required for binding might be expected to diminish SAX-3 activity. Mutations disrupting motif A, B, or C were engineered into the rescuing *mec-7*::SAX-3 transgene. The resulting mutants were assayed for their ability to rescue ventral guidance of the AVM neuron. Removal of motif A from the rescuing SAX-3 construct had relatively little effect on rescue, with 3 of 10 *mec-7*::SAX-3ΔA lines rescuing to <=5% and an average defect of 6% across all lines. In contrast, deletion of the c-NCK and c-ENA binding sites resulted in more significant disruption of SAX-3 function. Expression of a *mec-7*::SAX-3ΔB construct yielded 0/5 lines rescuing to <=5%, with an average of 11% defects across all lines (Figure 2-10B, C). Deletion of the c-ENA binding site also diminished rescue: 0 of 8 *mec-7*::SAX-3ΔC lines rescued to <=5%, with an average defect of 15% across all lines (Figure 2-10B, C). Deletion of both c-ENA and c-NCK binding sites (*mec-7*::SAX-3ΔBC) further diminished rescue (0/5 lines <=5%, average defect 21%). These results thus provide evidence that c-NCK and c-ENA binding sites within SAX-3 are required for wild-type SAX-3 activity.

2.4 Discussion

In summary, our results implicate *C. elegans* homologs of Nck and Enabled proteins, two molecules with known roles in regulating actin dynamics, in axon guidance by SAX-3/Robo receptors. *C. elegans* homologs of these genes have not been previously described in the literature. c-NCK and Enabled bind directly to distinct, conserved sites within the SAX-3 cytoplasmic domain. A functional requirement for these sites is shown for SAX-3-mediated rescue of AVM ventral guidance, and inactivation of *c-ena* by RNAi results in CAN cell migration defects reminiscent of *sax-3*. While similar functional data is not yet available for *c-nck*, the observation that *c-nck* is expressed in a wide variety of neuronal tissues is consistent with a role for c-NCK in SAX-3 signaling as well.

A role for Ena/VASP proteins in signaling by SAX-3/Robo receptors

SAX-3 motif C (CC2 in *Drosophila*) was previously noted to contain similarity to known targets of EVH1 domains, despite being an imperfect match to the canonical D/EFPPPPXD/E consensus (Kidd *et al.*, 1998). The observation that motif C binds EVH1 domains of Mena and EVL demonstrates that motif C is indeed an EVH1 binding site. Interestingly, in *Drosophila*, Enabled binds to both CC2 and CC3 (corresponding to SAX-3 motif B) (Bashaw *et al.*, 2000). This may be explained by the fact that CC3 contains a central core region of four prolines (PPPP), while SAX-3 motif B lacks these core prolines (Table 2-1).

c-ena is encoded by the *unc-34* gene (Dell and Garriga, personal communication). Further evidence supporting a role for Enabled in guidance by SAX-3/Robo proteins is treated in Chapter 3 and will not be discussed here.

In addition to c-ENA, the *C. elegans* genome encodes two additional EVH1 domain containing proteins, B0280.2 (related to Bee1p) and C07G1.4 (related to WASP). It will be of interest to determine whether SAX-3 binds the EVH1 domains of these proteins as well.

Functional implications of c-NCK binding to SAX-3/Robo receptors

SAX-3 motif B contains several PxxP motifs and binds to c-NCK in a variety of *in vitro* assays. This interaction is demonstrated to involve at least the second SH3 domain of c-NCK, although roles for the first SH3 domain and the C-terminal SH2 domain cannot be excluded. Given the many documented interactions between Nck family members and additional cytoskeletal components, these results suggest that Nck is a mediator of SAX-3 cytoskeletal responses. In this respect Nck could even facilitate the binding of Ena/VASP proteins to SAX-3. For example, Nck binding to SAX-3 could recruit WASP, which binds to Nck via the third SH3 domain of Nck (She *et al.*, 1997). The observation that Bee1p binds a yeast homolog of WASP-interacting protein WIP (Naqvi *et al.*, 1998) raises the potential of additional complexity.

Another intriguing possibility is that the role of SAX-3 is to modulate Nck function. It has been suggested that Nck primarily interacts with guidance receptors via its SH2 domain, while its SH3 domains link Nck to downstream effector proteins (Lu *et al.*, 1997). Of note, in *Drosophila* Dock has been shown to bind to Dscam via both its SH2 and SH3 domains. Nonetheless, the Cdc42 effector kinase PAK binds to the second SH3 domain of Nck, and membrane localization of a construct containing only the second SH3 domain of Nck results in membrane localization and activation of PAK (Lu *et al.*, 1997). Nck also binds WASP-interacting protein (WIP) via its second SH3 domain. In this light, is possible that instead of signaling through Nck, SAX-3 may be a negative regulator of Nck signaling, by blocking access to downstream effectors such as PAK and WIP.

2.5 Materials and Methods

Strains

Wild-type animals were *C. elegans* variety Bristol, strain N2. The following strains were utilized for these studies: CX3198 [*sax-3(ky123) X*], ZB163 [*mec-4::GFP*], and CX2627 [*kyIs4(ceh-23::GFP) X*]. *sax-3(ky123)* deletes the start ATG and signal sequence of SAX-3. Strains were maintained using standard methods. Animals were grown at 20°C.

Yeast two-hybrid screen for SAX-3-interacting proteins

The yeast strain Y190 (MATa, gal4 gal80 his3 trp2-901 ade2-101 ura3-52 leu2-3,-112 + URA3::GLA>lacZ, LYS2::GAL>HIS3 cyhr) was transformed with a yeast two-hybrid library prepared from mixed stage *C. elegans* cDNA (RB2, random-primed, R. Barstead) with a pAS1CYH2 SAX-3(1024-1273) bait and selected for growth and beta-galactosidase activity on -HisTrpLeu +25mM 3AT +XGal plates. 54 initial positives were picked and winnowed to nine candidates after retesting. Two clones encoded c-NCK (clones 1-1 and 2-1, containing residues 1-380). Additional clones are listed in Table 2-2. In general, stronger positives were assigned lower isolate numbers.

Isolation of *c-nck* cDNA

The sequence of the *c-nck* cDNA was inferred from sequencing of Y2H clones 1-1 and 2-1 and additional sequences from the *C. elegans* EST database, listed below: yk789d09, yk725h6, yk520c11, yk79d3, yk586g10, yk472d2, yk490b7, yk267f12, yk454a8, yk203e11, yk712e5, yk450c5, yk677b1, yk242c8, yk148c10, yk169f10, cm21b3, yk393a5, and yk58f11 (gift of Yuji Kohara).

Sequence analysis

Protein-protein lineups were constructed and analyzed using the ClustalW algorithm in MacVector 6.0 or PILEUP from the GCG software package. Phylogenetic relationships were inferred using GCG and PHYLIP. Further protein sequence analyses were conducted using PFAM and Prosite provided by the Sanger Center (http://genomic.sanger.ac.uk).

***In vitro* protein binding assays**

SAX-3 cytoplasmic sequences were expressed as GST fusions in bacteria using the pGEX 4T-1 expression system (Pharmacia). The following GST fusions were created: GST::SAX-3 A (HDDPSPYATTTLVLSNQ), GST::SAX-3 B (RAPAMPTNPVPPEPPARY), GST::SAX-3 C (MDFIPPPPSNPPPP), GST::SAX-3C– (MDAIPPPPSNPPPP), GST::SAX-3Cx2 (MDFIPPPPSNPPPPgggrsDFIPPPPSNPPPP), GST::SAX-3Cx3 (MDFIPPPPSNPPPPgggrsDFIPPPPSNPPPPgggrsDFIPPPPSNPPPP). GST fusions to the entire SAX-3 cytoplasmic domain (GST::SAX-3cyto) and to a fragment containing motifs A, B and C (GST::SAX-3 ABC long, 978-1224) were also generated. Biotinylated probes for Mena EVH1, EVL EVH1, and c-NCK were generated using the Pinpoint Xa system (Promega). For GST co-precipitation experiments, 2 µg of purified GST fusion protein attached to agarose beads was mixed with 50 µl of bacterial extract containing biotinylated probe in 10 mM Tris 7.5, 150 mM NaCl, 0.1% Triton, 0.05% BSA. Samples were incubated for six hours at 4°C, then spun down and washed three times in buffer. BSA was omitted from the last wash. Bound proteins were separated by SDS-PAGE, transferred to nylon membranes where biotinylated proteins were visualized by ECL. For Far Western experiments, bacterial lysates containing GST::SAX-3 fusion proteins were separated by SDS-PAGE and blotted to nylon membranes. Membranes were incubated with biotinylated probes in TBST, washed extensively and developed for ECL.

Analysis of *c-nck*::GFP expression

2.6 kB of upstream *c-nck* sequence inclusive of the first seven amino acids were amplified with the primers TY132 (5' GGATCCGACCACATAGTCCTCCGACAT 3') and TY133 (5' GGAACATATCTAAACTGACTGGG 3') and cloned into SpeI/BamHI sites of pPD95.77 GFP expression vector (Andy Fire). This expression construct was injected into *lin-15* mutant hermaphrodites with a *lin-15* coinjection marker. Rescued lines were analyzed by fluorescence microscopy.

Double-stranded RNA interference of *c-ena*

Two primer pairs, TY85/86 and TY87/88, were used to amplify 300bp and 317 bp of sequence, respectively, corresponding to bp 4-303 and bp 576-893 of the *c-ena* cDNA (Figure 2-8). Primers included T3 and T7 polymerase sites that were used for *in vitro* transcription reactions to generate sense and antisense *c-ena* RNA. Complementary RNAs were annealed and injected into *ceh-23::GFP* hermaphrodites. RNAi phenotypes were scored in the F1 generation.

Characterization of cell and axon migration phenotypes

Neurons visualized with GFP transgenes were scored in live adult animals. CAN cells were visualized with an integrated *ceh-23::GFP* transgene (*kyIs4 X*). CAN cell positions were scored as a % of the distance between the posterior bulb of the pharnyx and the vulva. AVM axons were scored using the *mec-4::GFP* transgene (strain ZB163). The initial projection of AVM axons were scored as mutant if they failed to project to the ventral cord (anterior or posterior deviations less than 5 cell bodies were scored as wild-type). Images were photographed on a Zeiss Axiocam cooled CCD or visualized by confocal microscopy.

Structure/function analysis of SAX-3

Deletions of motifs A, B, and C were engineered into a rescuing *mec-7*::SAX-3 construct by replacing motifs with restriction sites. Mutated SAX-3 constructs were injected into ZB163 worms which express the *mec-4::GFP* marker in AVM as well as other touch neurons. *str-1*::GFP was used as a coinjection marker. *str-1*::GFP+ lines were identified and scored for ventral axon guidance defects as described.

Table 2-1 Conserved proline-rich motifs in SAX-3/Robo receptors

Motif	Sequence
SAX-3 A	HDDPSPYATTTLVLSNQ
fly Robo CC1	PDNPTPYATTMIIGTSS
human Robo1 CC1	SGQPTPYATTQLIQSNL
human Robo2 CC1	TQATPYATTQILHSNS
SAX-3 B	RA**P**AM**P**TN**P**V**PP**E**PP**ARY
fly Robo CC3	PSPMQPPPPVPV-PEGWY
human Robo1 CC3	YTDDLPPPPVPP-PAIKSP
SAX-3 C	KTLMD**F**-**IPPPP**SNPPPPG-GHVY
fly Robo CC2	INWSEF-LPPPPEHPPPSS-TYGY
human Robo1 CC2	MNWADL-LPPPPAHPPPHSNSEEY
human Robo2 CC2	STWANVPLPPPPVQPLPGTELEHY

Table 2-2 Yeast two hybrid results with the SAX-3 cytoplasmic domain

Protein	isolate name(s)	Notes
ZK470.5	1-1 and 2-1	*C. elegans* NCK
ZC123.2	3-1	Homology to homeobox/Zn finger transcription factors
F52E4.1	8-1 and 22-1	similar to propionyl-CoA carboxylase beta
F58A3.1	20-1	Homology to Ldb/NLI, proteins known to interact with LIM domain transcription factors.
C26B9.5	27-1	Homology to human lysosomal Pro-X carboxypeptidase
T05C12.6	45-1	Homology to dishevelled
T04C10.1	54-1	Homology to *Drosophila minibrain* and yeast protein kinase 1 (YAK-1)

Figure 2-1

Isolation of c-NCK in a two-hybrid screen with SAX-3. (**A**) A yeast two-hybrid bait was constructed by fusing the GAL4 DNA binding domain to amino acids 1024-1273 of SAX-3. This construct contains the conserved proline-rich motifs B and C but truncates motif A. Yeast were cotransformed with the SAX-3 bait and a yeast two-hybrid library prepared from mixed stage *C. elegans* cDNA. Transformants were screened for growth and beta-galactosidase activity on -HisTrpLeu +25mM 3AT +XGal plates. A screen of 1-2 x 10^6 clones led to the identification of two strong positives, Y2H1-1 and 2-1 (boxed). (**B**) 1-1 and 2-1 encode ZK470.5, an SH3/SH2 adapter protein highly related to Dock/Nck. %Identity/similarity to Dock is shown for individual SH2 and SH3 domains. 1-1 and 2-1 differ in the use of an alternative splice site that results in the insertion of an isovaline-glutamine dipeptide at the beginning of the third SH3 domain of 2-1. (C) The deduced *c-nck* genomic locus. Open boxes indicate exons, striped box indicates the location of the IQ alternative splice site, sizes of two large 5' introns indicated below the line.

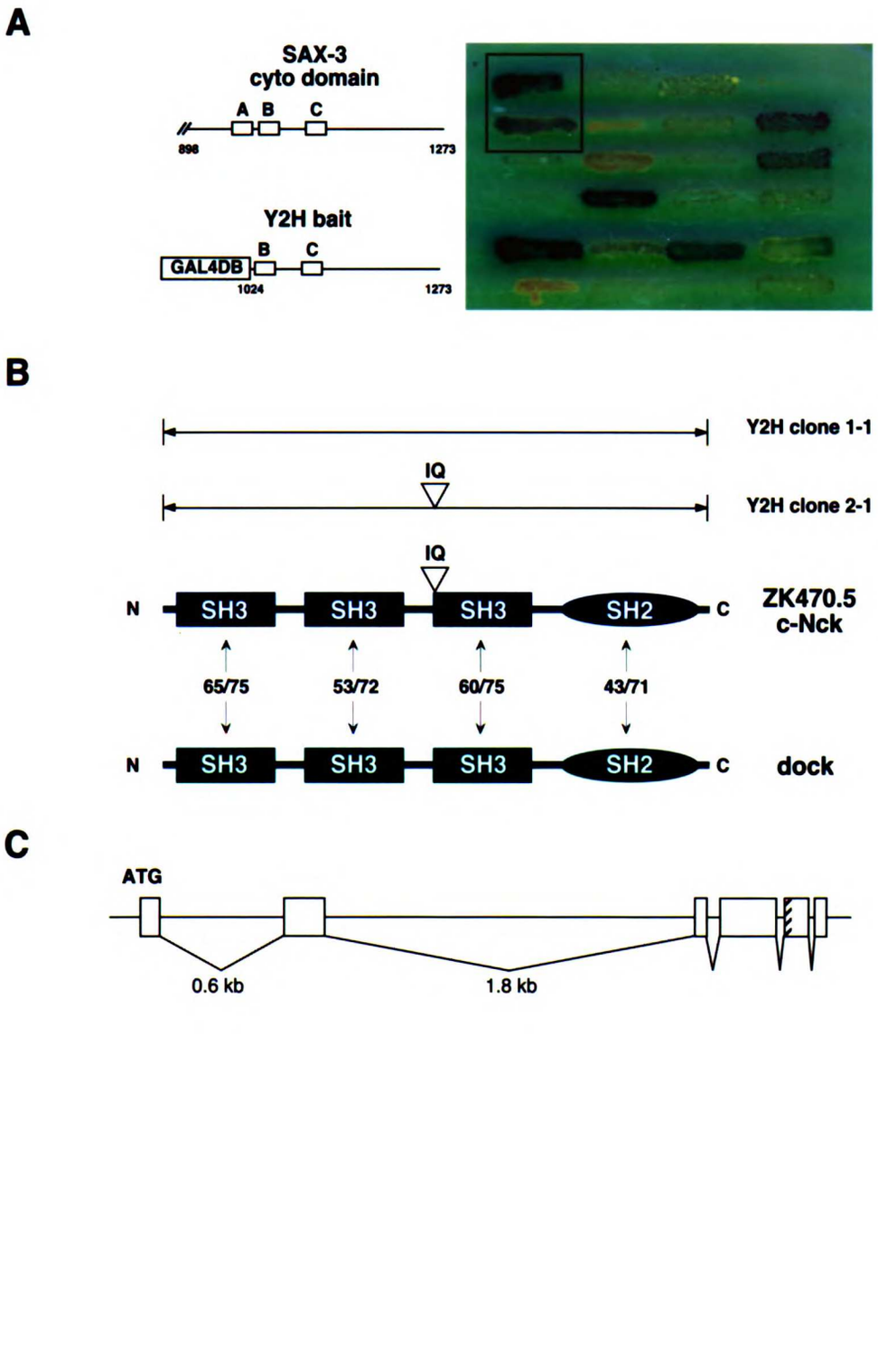
A
SAX-3
cyto domain
A B C
898
1273
Y2H bait
GAL4DB
B C
1024
1273
B
Y2H clone 1-1
IQ
Y2H clone 2-1
IQ
N
SH3
SH3
SH3
SH2
C
ZK470.5
c-Nck
65/75
53/72
60/75
43/71
N
SH3
SH3
SH3
SH2
C
dock
C
ATG
0.6 kb
1.8 kb

Figure 2-2

c-nck cDNA sequence. The *c-nck* cDNA is 1580 bp in length and encodes a protein with three SH3 and one SH2 domain. 5' UTR and 3'UTR are lowercase, coding sequences are uppercase with single amino acid code below. Boundaries of individual SH2 and SH3 domains are bracketed and labeled. Also labeled are two alternative splice sites that result in 1-2 amino acid differences at the beginning and at the end of the third SH3 domain. The boundaries of the yeast two-hybrid clones 1-1 and 2-1 are indicated by the arrows. The 3'UTR contains no clear polyadenylation site and may extend beyond the sequence shown.

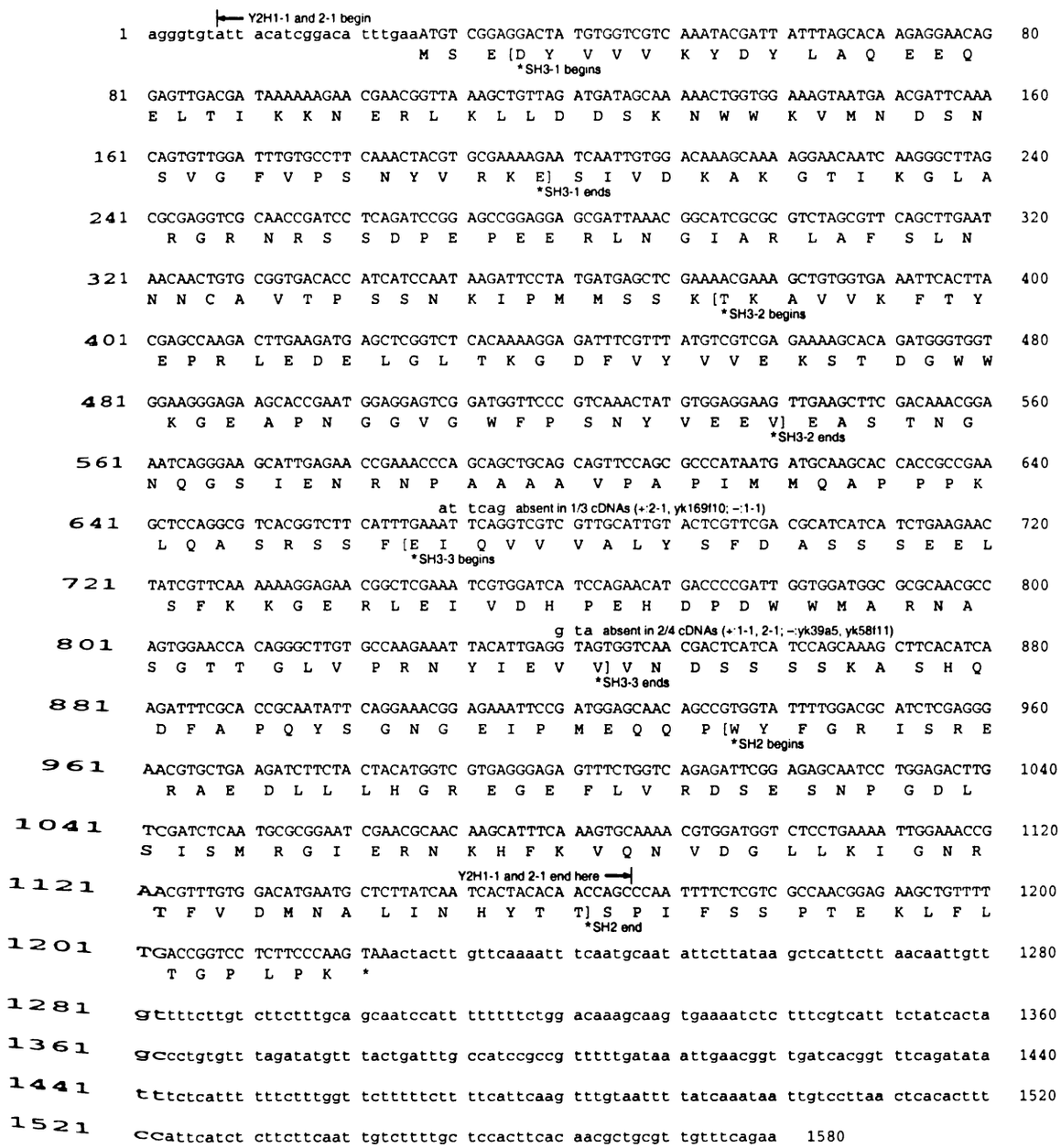
Y2H1-1 and 2-1 begin
*SH3-1 begins
*SH3-1 ends
*SH3-2 begins
*SH3-2 ends
at tcag absent in 1/3 cDNAs (+:2-1, yk169f10; −:1-1)
*SH3-3 begins
g ta absent in 2/4 cDNAs (+:1-1, 2-1; −:yk39a5, yk58f11)
*SH3-3 ends
*SH2 begins
Y2H1-1 and 2-1 end here
*SH2 end

Figure 2-3

Relationship of cNCK to other Nck/Dock family members. (A) Lineup comparisons of *cNCK*, dock, Nck and Nck2/Grb4. Identical residues are shaded, similar residues are boxed. *(B) Phylogenetic* relationships and %identity/similarity between cNCK and other family *members*.

A

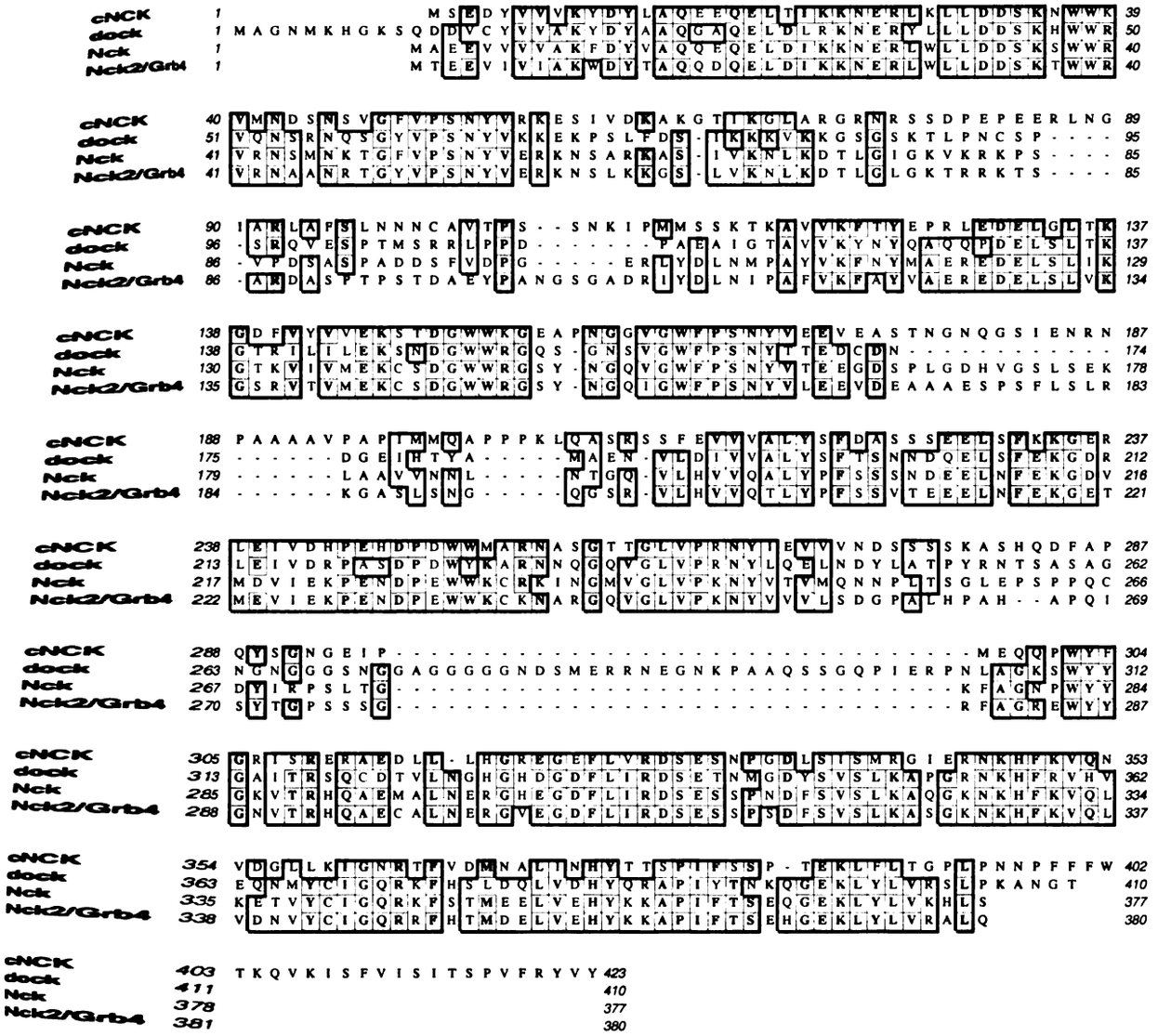

B

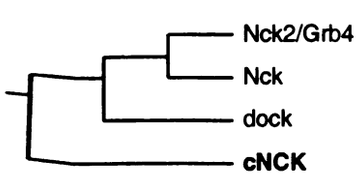

%identity/similarity

	cNCK	dock	Nck	Nck2/Grb4
cNCK		36/51	37/51	37/51
dock			41/58	41/58
Nck				68/79
Nck2/Grb4				

Figure 2-4

cNCK binds to SAX-3 motif B via its second SH3 domain. *Top*, full-length cNCK co-precipitates with the SAX-3 cytoplasmic domain in a GST pulldown assay. SAX-3 motif B is sufficient for this binding interaction. *Middle*, Far Western showing that the SH2 domain of cNCK is dispensable for SAX-3 binding. *Bottom*, Far Western showing that the second SH3 domain of cNCK is sufficient to bind to SAX-3 motif B. Labels: +, positive control; *GST*, GST alone; *SAX-3 cyto*, GST fused to full-length SAX-3 cytoplasmic domain; *SAX-3 ABC*, GST fused to a minimal fragment of the cytoplasmic domain containing motifs A, B, and C (see methods). *A*, GST::SAX-3 motif A; *B*, GST::SAX-3 motif B; *C*, GST::SAX-3 motif C. *Cx2*, *Cx3*, fusion of GST to two or three copies of motif C.

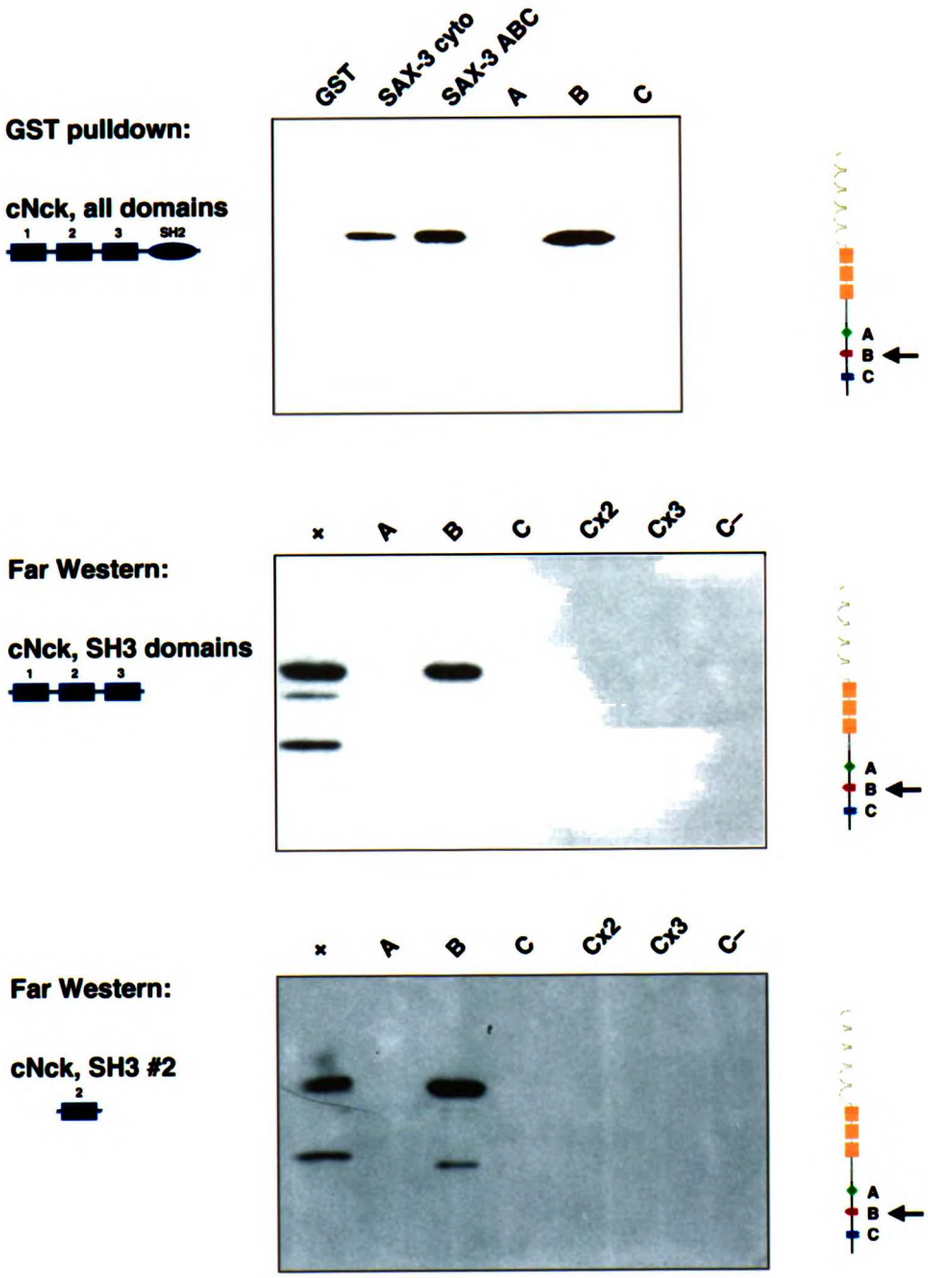
GST pulldown:
cNck, all domains
1
2
3
SH2
GST
SAX-3 cyto
SAX-3 ABC
A
B
C
A
B
C
Far Western:
cNck, SH3 domains
1
2
3
×
A
B
C
Cx2
Cx3
C
A
B
C
Far Western:
cNck, SH3 #2
2
×
A
B
C
Cx2
Cx3
C
A
B
C

***Figure* 2-5**

Expression pattern of *c-nck* in adult hermaphrodites. (**A**) A reporter construct was generated by fusing 2.6 kB of sequence + the first 7 amino acids of *c-nck* to GFP. (**B**) *c-nck*::GFP expression in the H-shaped excretory cell (*asterisk*). (**C**) *c-nck*::GFP expression in the excretory canal (*e*) and motorneurons in the ventral cord (*arrows*). Axonal commissures can be seen leaving some of the motorneuron cell bodies. (**D**) *c-nck*::GFP expression in unidentified head neurons.

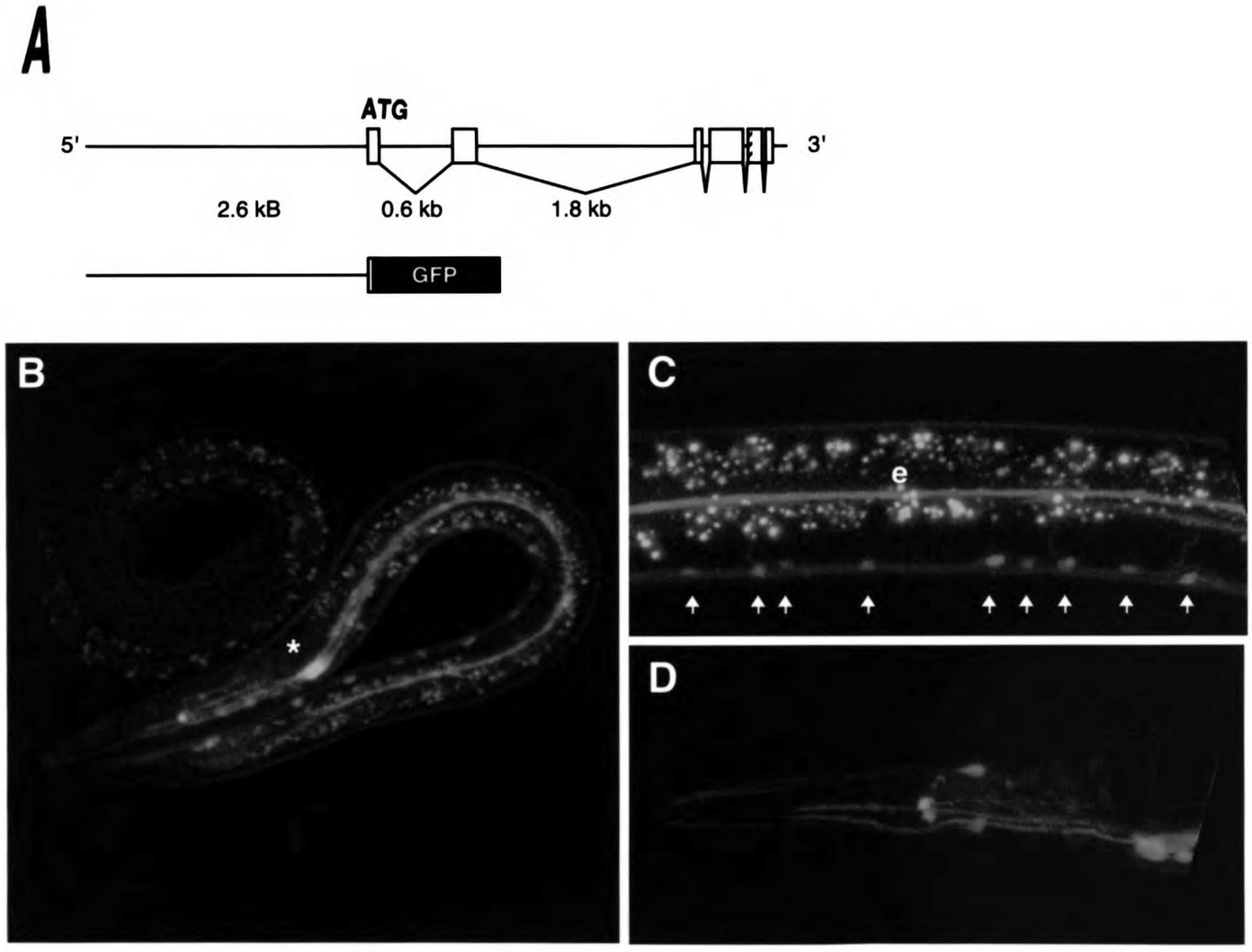
A
ATG
5'
3'
2.6 kB
0.6 kb
1.8 kb
GFP
B
*
C
e
D

Figure 2-6

SAX-3 motif C binds the Mena EVH1 domain. (**A**) Far Westerns demonstrating Mena EVH1 binding to GST::SAX-3 motif C. GST::SAX-3 fusions were separated by SDS-PAGE, blotted and probed with biotinylated Mena EVH1. Mena binds motif C but not A or B. *ActA-1x* and *-4x*, positive controls; *A*, GST::SAX-3 motif A; *B*, GST::SAX-3 motif B; *C*, GST::SAX-3 motif C. *C–*, GST fusion to motif C with F>A mutation; *Cx2*, *Cx3*, fusion of GST to a two or three copies of motif C. (**B**) ActA competes with motif C for Mena binding. Far Westerns were performed in the presence of increasing amounts of ActA competitor peptide. Addition of ActA is seen to block binding to motif C, arguing that ActA and motif C bind to similar sites.

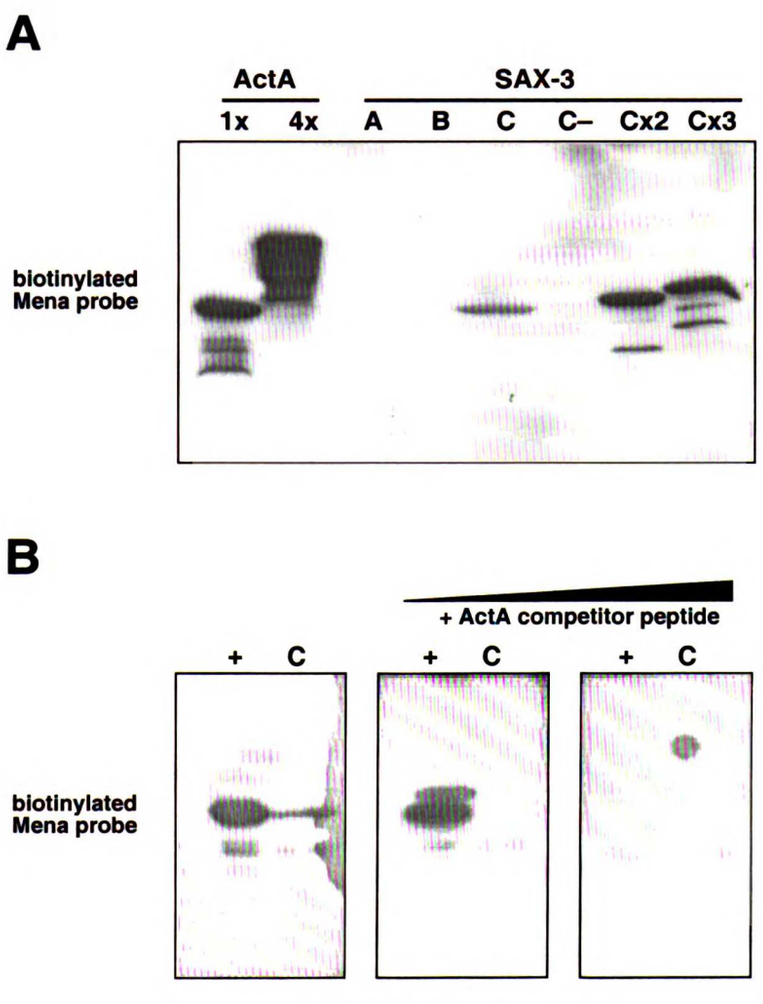
A
ActA
SAX-3
1x
4x
A
B
C
C–
Cx2
Cx3
biotinylated
Mena probe
B
+ ActA competitor peptide
+
C
+
C
+
C
biotinylated
Mena probe

Figure 2-7

Identification of a *C. elegans* Enabled homolog. (**A**) Lineups of the predicted cENA EVH1 domain with EVH1 domains of Ena/VASP, WASP and Homer proteins. Identical residues are shaded, similar residues are boxed. (**B**) *Left*, phylogenetic analysis of three EVH1-containing proteins in *C. elegans* (cENA, B0280.2, C07C1.4) and known EVH1-containing proteins. cENA is the closest homolog of Enabled, C07C1.4 is most related to WASP, and B0280.2 is most related to Bee1p. Comparisons were carried out for the EVH1 domains alone. *Right*, %identity/similarity between the EVH1 domains of cENA and other EVH1-containing proteins.

A

```
cENA     1  S S E A C I A T A M A R V M T Y N E S T K G - W V L L G G N  29
Ena      1  M T E Q S I I G A R A S V M V Y D D N Q K K - W V P S G - S  28
Mena     1  M S E Q S I C Q A R A A V M V Y D D A N K K - W V P A G - G  28
EVL      1  M S E Q S I C Q A R A S V M V Y D D T S K K - W V P I K P G  29
VASP     1  M S E T V I C S S R A T V M L Y D D S N K R - W L P A G T G  29
Homer    1  M G E Q P I F S T R A H V F Q I D P N T K K N W V P T S - -  28
WASP     1  L G R K C W T L A T T V V Q L Y L A L P P G - - A E H W - T  27
            M . E Q . I .   A R A . V M . Y D D . . K K   W V P . G   .

cENA    30  D D S M T N V R L I Q D I R R P E F R I V S N R A D - - S T  57
Ena     29  S S G L S K V Q I Y H H Q Q N N T F R V V G R K L Q - D H E  57
Mena    29  S T G F S R V H I Y H H T G N N T F R V V G R K I Q - D H Q  57
EVL     30  Q Q G F S R I N I Y H N T A S S T F R V V G V K L Q - D Q Q  58
VASP    30  P Q A F S R V Q I Y H N P T A N S F R V V G R K M Q P D Q Q  59
Homer   29  - K H A V T V S Y F Y D S T R N V Y R I I S L D G S - - - K  54
WASP    28  M E H C G A V C F V K D N P Q K S Y F I R L Y G L Q - A G R  56
              S . V . I Y H .     N . F R V V G   K . Q   D . .

cENA    58  N I L N C N I Y R G I K Y H K A T P M F H Q W R T E Q - R R  86
Ena     58  V V I N C S I L K G L K Y N Q A T A T F H Q W R D S - - K F  85
Mena    58  V V I N C A I P K G L K Y N Q A T Q T F H Q W R D A - - R Q  85
EVL     59  V V I N Y S I V K G L K Y N Q A T P T F H Q W R D A - - R Q  86
VASP    60  V V I N C A I I R G V K Y N Q A T P I F H Q W R D A - - R Q  87
Homer   55  A I I N S T I T P N M T F T K T S Q K F G Q W A D S R A N T  84
WASP    57  L L W E Q E L Y S Q L V Y L T P T P F F H T F A G D - - D C  84
            V V I N C . I   . G L K Y N Q A T P   F H Q W R D .     . .

cENA    87  V Y G L N F E N E Q D A T M F L S I V L Q A I E T L         112
Ena     86  V Y G L N F S S Q N D A E N F A R A M M H A L E V L         111
Mena    86  V Y G L N F G S K E D A N V F A S A M M H A L E V L N S Q E 115
EVL     87  V Y G L N F A S K E E A T T F S N A M L F A L N I M N S Q E 116
VASP    88  V W G L N F G S K E D A I Q F A T G M A N A L E A L E G - -  115
Homer   85  V Y G L G F S S E H H L S K F A E K F Q E F K                107
WASP    85  Q V G L N F A D E S E A Q A F R A L V Q E K I Q K R N Q - -  112
            V Y G L N F . S . . D A   F A .  M .  A L E  L
```

B

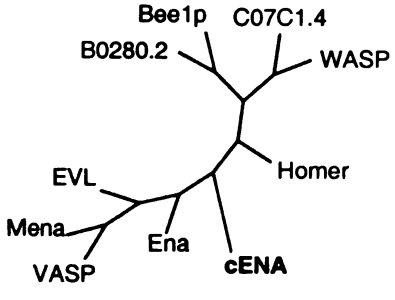

%identity/similarity	cENA	Ena	Mena	EVL	VASP	Homer	WASP
cENA		36/57	38/62	34/57	37/62	28/44	20/38
Ena			74/85	63/80	57/77	31/48	15/34
Mena				72/84	63/74	30/49	25/43
EVL					59/75	27/52	30/47
VASP						28/50	24/41
Homer							15/39
WASP							

Figure 2-8

c-ena cDNA coding sequence. The *c-ena* coding sequence is 1404 bp in length and encodes a protein with an EVH1 domain, a central proline-rich domain and a C-terminal EVH2 domain. Boundaries of EVH1 and EVH2 domains are bracketed and labeled. Proline residues in the central domain are in bold. Primers used for amplifying sequences for RNAi are indicated by arrows. Potential phosphorylation sites for cAMP- and cGMP-dependent kinases ([RK]-[RK]-X-[ST]) are italicized.

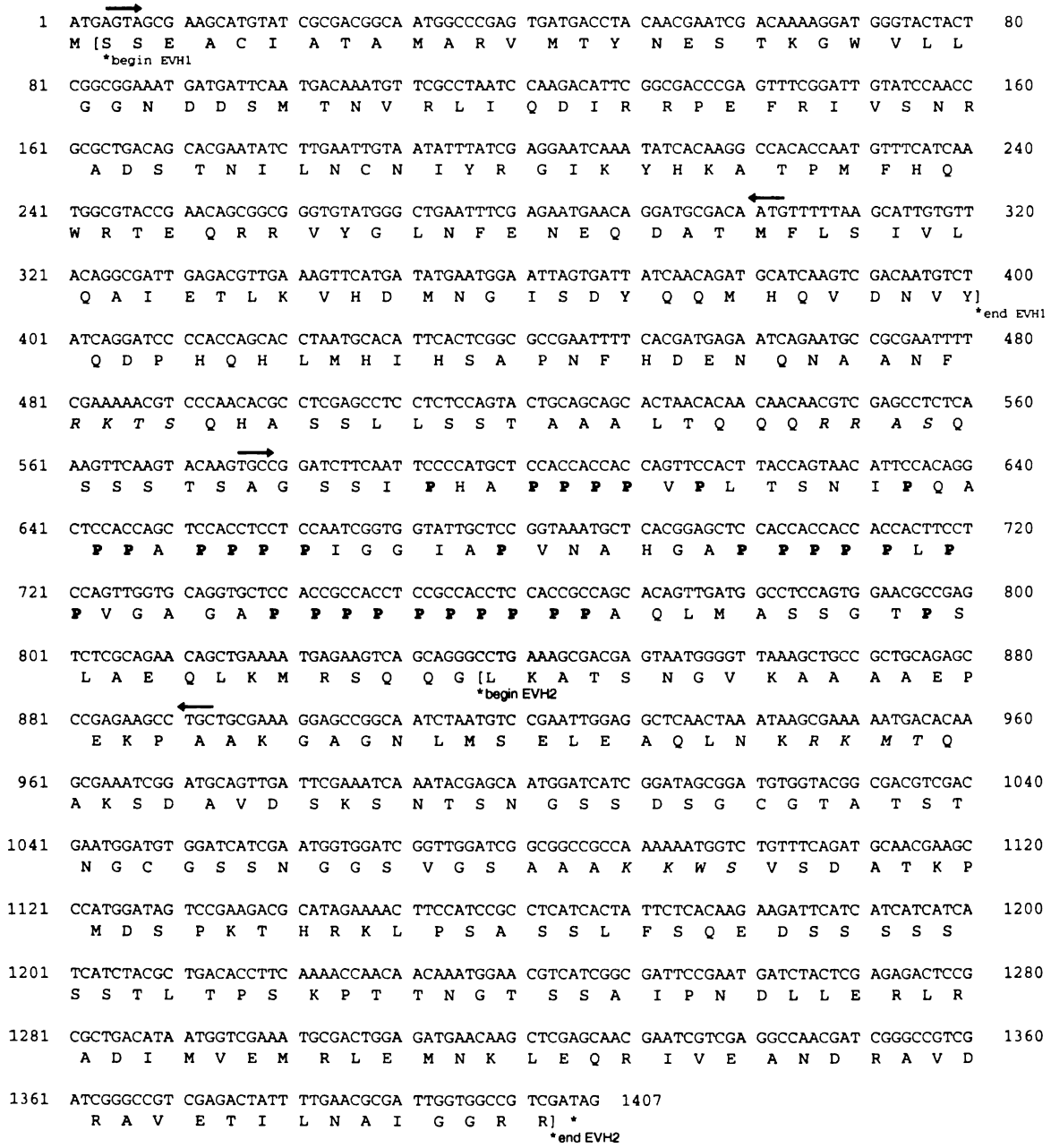
1 ATGAGTAGCG AAGCATGTAT CGCGACGGCA ATGGCCCGAG TGATGACCTA CAACGAATCG ACAAAAGGAT GGGTACTACT 80
M [S S E A C I A T A M A R V M T Y N E S T K G W V L L
*begin EVH1
81 CGGCGGAAAT GATGATTCAA TGACAAATGT TCGCCTAATC CAAGACATTC GGCGACCCGA GTTTCGGATT GTATCCAACC 160
G G N D D S M T N V R L I Q D I R R P E F R I V S N R
161 GCGCTGACAG CACGAATATC TTGAATTGTA ATATTTATCG AGGAATCAAA TATCACAAGG CCACACCAAT GTTTCATCAA 240
A D S T N I L N C N I Y R G I K Y H K A T P M F H Q
241 TGGCGTACCG AACAGCGGCG GGTGTATGGG CTGAATTTCG AGAATGAACA GGATGCGACA ATGTTTTTAA GCATTGTGTT 320
W R T E Q R R V Y G L N F E N E Q D A T M F L S I V L
321 ACAGGCGATT GAGACGTTGA AAGTTCATGA TATGAATGGA ATTAGTGATT ATCAACAGAT GCATCAAGTC GACAATGTCT 400
Q A I E T L K V H D M N G I S D Y Q Q M H Q V D N V Y]
*end EVH1
401 ATCAGGATCC CCACCAGCAC CTAATGCACA TTCACTCGGC GCCGAATTTT CACGATGAGA ATCAGAATGC CGCGAATTTT 480
Q D P H Q H L M H I H S A P N F H D E N Q N A A N F
481 CGAAAAACGT CCCAACACGC CTCGAGCCTC CTCTCCAGTA CTGCAGCAGC ACTAACACAA CAACAACGTC GAGCCTCTCA 560
R K T S Q H A S S L L S S T A A A L T Q Q Q R R A S Q
561 AAGTTCAAGT ACAAGTGCCG GATCTTCAAT TCCCCATGCT CCACCACCAC CAGTTCCACT TACCAGTAAC ATTCCACAGG 640
S S S T S A G S S I P H A P P P P V P L T S N I P Q A
641 CTCCACCAGC TCCACCTCCT CCAATCGGTG GTATTGCTCC GGTAAATGCT CACGGAGCTC CACCACCACC ACCACTTCCT 720
P P A P P P P I G G I A P V N A H G A P P P P P L P
721 CCAGTTGGTG CAGGTGCTCC ACCGCCACCT CCGCCACCTC CACCGCCAGC ACAGTTGATG GCCTCCAGTG GAACGCCGAG 800
P V G A G A P P P P P P P P P A Q L M A S S G T P S
801 TCTCGCAGAA CAGCTGAAAA TGAGAAGTCA GCAGGGCCTG AAAGCGACGA GTAATGGGGT TAAAGCTGCC GCTGCAGAGC 880
L A E Q L K M R S Q Q G [L K A T S N G V K A A A A E P
*begin EVH2
881 CCGAGAAGCC TGCTGCGAAA GGAGCCGGCA ATCTAATGTC CGAATTGGAG GCTCAACTAA ATAAGCGAAA AATGACACAA 960
E K P A A K G A G N L M S E L E A Q L N K R K M T Q
961 GCGAAATCGG ATGCAGTTGA TTCGAAATCA AATACGAGCA ATGGATCATC GGATAGCGGA TGTGGTACGG CGACGTCGAC 1040
A K S D A V D S K S N T S N G S S D S G C G T A T S T
1041 GAATGGATGT GGATCATCGA ATGGTGGATC GGTTGGATCG GCGGCCGCCA AAAAATGGTC TGTTTCAGAT GCAACGAAGC 1120
N G C G S S N G G S V G S A A A K K K W S V S D A T K P
1121 CCATGGATAG TCCGAAGACG CATAGAAAAC TTCCATCCGC CTCATCACTA TTCTCACAAG AAGATTCATC ATCATCATCA 1200
M D S P K T H R K L P S A S S L F S Q E D S S S S S
1201 TCATCTACGC TGACACCTTC AAAACCAACA ACAAATGGAA CGTCATCGGC GATTCCGAAT GATCTACTCG AGAGACTCCG 1280
S S T L T P S K P T T N G T S S A I P N D L L E R L R
1281 CGCTGACATA ATGGTCGAAA TGCGACTGGA GATGAACAAG CTCGAGCAAC GAATCGTCGA GGCCAACGAT CGGGCCGTCG 1360
A D I M V E M R L E M N K L E Q R I V E A N D R A V D
1361 ATCGGGCCGT CGAGACTATT TTGAACGCGA TTGGTGGCCG TCGATAG 1407
R A V E T I L N A I G G R R] *
*end EVH2

Figure 2-9

RNAi-mediated disruption of *c-ena* causes cell migration defects. (**A**) In wild-type animals, the CAN neuron (*arrow*) migrates posteriorly from the head to stop at the midbody (marked by the vulva, *v*). (**B**) In *c-ena* RNAi-injected animals, the CAN neuron (*arrow*) does not complete its migration and is found displaced anteriorly relative to the vulva (*v*). (**C**) Quantitation of CAN migration defects in *c-ena* RNAi-injected animals. The final positions of the CAN cell are shown for 30 animals injected with *c-ena* RNAi, with mean position indicated by the arrow. Mean positions of the CAN cell in *sax-3* mutants and in animals bearing the GFP marker alone are shown for comparison. CAN cells were visualized using *ceh-23::GFP*.

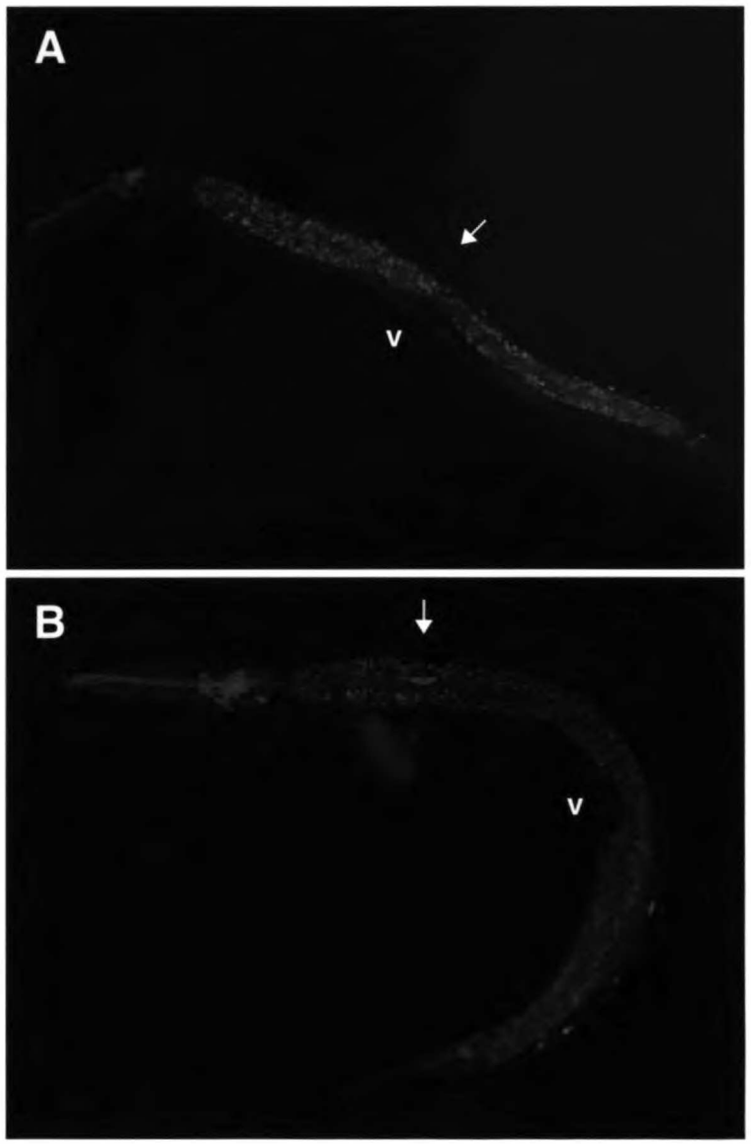
A
V
B
V
C
CAN migration in c-ena RNAi animals
0%
100%
0%
25%
50%
75%
100%
c-ena RNAi
mean position
sax-3(ky123)
GFP marker alone

Figure 2-10

Structure-function analysis of the SAX-3 cytoplasmic domain supports a role for motifs B and C in SAX-3 guidance. (**A**) *sax-3* mutants affect ventral guidance of the AVM neuron. In wild-type animals, the AVM axon initially projects ventrally to join the ventral nerve cord. In *sax-3* mutants, AVM often fails to migrate ventrally. (**B**) Summary of effects of cytoplasmic deletions on SAX-3 rescue of ventral guidance. Average %ventral guidance defect across all transgenic lines analyzed is shown. Deletions in motif A have minimal effect on SAX-3 rescue (average defect 6% over 10 lines), while deletions of motifs B and C lead to greater disruption of SAX-3 function (11% and 15% for B and C individually, 21% when both B and C are deleted). (C) Effects of cytoplasmic deletions on SAX-3 rescue, broken down by individual line. 2/4 and 3/10 *mec-7*::SAX-3 and *mec-7*::SAX-3ΔA lines rescue to 5% defects or better, compared to 0/8, 0/5 and 0/5 lines generated with *mec-7*::SAX-3ΔB, *mec-7*::SAX-3ΔC and *mec-7*::SAX-3ΔBC, respectively.

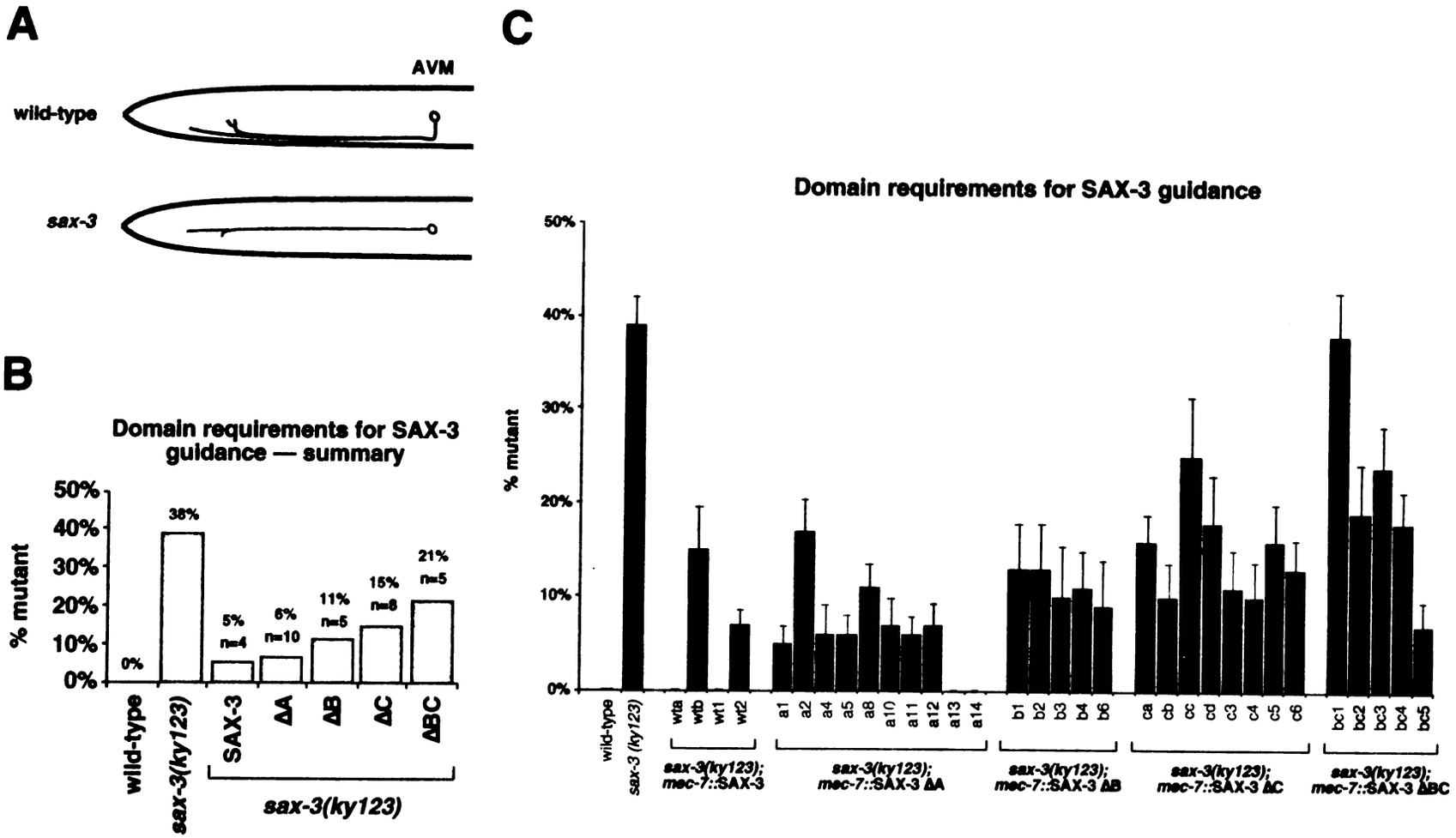
A
AVM
wild-type
sax-3
B
Domain requirements for SAX-3 guidance — summary
% mutant
50%
40%
30%
20%
10%
0%
0%
38%
5% n=4
6% n=10
11% n=5
15% n=8
21% n=5
wild-type
sax-3(ky123)
SAX-3
ΔA
ΔB
ΔC
ΔBC
sax-3(ky123)
C
Domain requirements for SAX-3 guidance
% mutant
50%
40%
30%
20%
10%
0%
wild-type
sax-3 (ky123)
wta
wtb
wt1
wt2
a1
a2
a4
a5
a8
a10
a11
a12
a13
a14
b1
b2
b3
b4
b6
ca
cb
cc
cd
c3
c4
c5
c6
bc1
bc2
bc3
bc4
bc5
sax-3(ky123); mec-7::SAX-3
sax-3(ky123); mec-7::SAX-3 ΔA
sax-3(ky123); mec-7::SAX-3 ΔB
sax-3(ky123); mec-7::SAX-3 ΔC
sax-3(ky123); mec-7::SAX-3 ΔBC

2.6 References

Anton, I. M., Lu, W., Mayer, B. J., Ramesh, N., and Geha, R. S. (1998). The Wiskott-Aldrich syndrome protein-interacting protein (WIP) binds to the adaptor protein Nck. *J Biol Chem* **273**, 20992-20995.

Bashaw, G. J., Kidd, T., Murray, D., Pawson, T., and Goodman, C. S. (2000). Repulsive axon guidance: Abelson and Enabled play opposing roles downstream of the roundabout receptor. *Cell* **101**, 703-715.

Bear, J. E., Krause, M., and Gertler, F. B. (2001). Regulating cellular actin assembly. *Curr Opin Cell Biol* **13**, 158-166.

Bear, J. E., Loureiro, J. J., Libova, I., Fassler, R., Wehland, J., and Gertler, F. B. (2000). Negative regulation of fibroblast motility by Ena/VASP proteins. *Cell* **101**, 717-728.

Brose, K., Bland, K. S., Wang, K. H., Arnott, D., Henzel, W., Goodman, C. S., Tessier-Lavigne, M., and Kidd, T. (1999). Slit proteins bind Robo receptors and have an evolutionarily conserved role in repulsive axon guidance. *Cell* **96**, 795-806.

Cowan, C. A., and Henkemeyer, M. (2001). The SH2/SH3 adaptor Grb4 transduces B-ephrin reverse signals. *Nature* **413**, 174-179.

Feller, S. M., Ren, R., Hanafusa, H., and Baltimore, D. (1994). SH2 and SH3 domains as molecular adhesives: the interactions of Crk and Abl. *Trends Biochem Sci* **19**, 453-458.

Fire, A., Xu, S., Montgomery, M. K., Kostas, S. A., Driver, S. E., and Mello, C. C. (1998). Potent and specific genetic interference by double-stranded RNA in *Caenorhabditis elegans*. *Nature* **391**, 806-811.

Frischknecht, F., Moreau, V., Rottger, S., Gonfloni, S., Reckmann, I., Superti-Furga, G., and Way, M. (1999). Actin-based motility of vaccinia virus mimics receptor tyrosine kinase signalling. *Nature* **401**, 926-929.

Garrity, P. A., Rao, Y., Salecker, I., McGlade, J., Pawson, T., and Zipursky, S. L. (1996). *Drosophila* photoreceptor axon guidance and targeting requires the dreadlocks SH2/SH3 adapter protein. *Cell* **85**, 639-650.

Gertler, F. B., Niebuhr, K., Reinhard, M., Wehland, J., and Soriano, P. (1996). Mena, a relative of VASP and *Drosophila* Enabled, is implicated in the control of microfilament dynamics. *Cell* **87**, 227-239.

Hao, J. C., Yu, T. W., Fujisawa, K., Culotti, J. G., Gengyo-Ando, K., Mitani, S., Moulder, G., Barstead, R., Tessier-Lavigne, M., and Bargmann, C. I. (2001). *C. elegans* Slit Acts in Midline, Dorsal-Ventral, and Anterior-Posterior Guidance via the SAX-3/Robo Receptor. *Neuron* **32**, 25-38.

Kidd, T., Bland, K. S., and Goodman, C. S. (1999). Slit is the midline repellent for the robo receptor in *Drosophila*. *Cell* **96**, 785-794.

Kidd, T., Brose, K., Mitchell, K. J., Fetter, R. D., Tessier-Lavigne, M., Goodman, C. S., and Tear, G. (1998). Roundabout controls axon crossing of the CNS midline and defines a novel subfamily of evolutionarily conserved guidance receptors. *Cell* **92**, 205-215.

Li, H. S., Chen, J. H., Wu, W., Fagaly, T., Zhou, L., Yuan, W., Dupuis, S., Jiang, Z. H., Nash, W., Gick, C., *et al.* (1999). Vertebrate slit, a secreted ligand for the transmembrane protein roundabout, is a repellent for olfactory bulb axons. *Cell* **96**, 807-818.

Loisel, T. P., Boujemaa, R., Pantaloni, D., and Carlier, M. F. (1999). Reconstitution of actin-based motility of *Listeria* and Shigella using pure proteins. *Nature* **401**, 613-616.

Lu, W., Katz, S., Gupta, R., and Mayer, B. J. (1997). Activation of Pak by membrane localization mediated by an SH3 domain from the adaptor protein Nck. *Curr Biol* 7, 85-94.

Machesky, L. M. (1997). Cell motility: complex dynamics at the leading edge. *Curr Biol* 7, R164-167.

McCarty, J. H. (1998). The Nck SH2/SH3 adaptor protein: a regulator of multiple intracellular signal transduction events. *Bioessays* **20**, 913-921.

Naqvi, S. N., Zahn, R., Mitchell, D. A., Stevenson, B. J., and Munn, A. L. (1998). The WASp homologue Las17p functions with the WIP homologue End5p/verprolin and is essential for endocytosis in yeast. *Curr Biol* **8**, 959-962.

Niebuhr, K., Ebel, F., Frank, R., Reinhard, M., Domann, E., Carl, U. D., Walter, U., Gertler, F. B., Wehland, J., and Chakraborty, T. (1997). A novel proline-rich motif present in ActA of *Listeria monocytogenes* and cytoskeletal proteins is the ligand for the EVH1 domain, a protein module present in the Ena/VASP family. *Embo J* **16**, 5433-5444.

Pawson, T., and Scott, J. D. (1997). Signaling through scaffold, anchoring, and adaptor proteins. *Science* **278**, 2075-2080.

Reinhard, M., Jarchau, T., and Walter, U. (2001). Actin-based motility: stop and go with Ena/VASP proteins. *Trends Biochem Sci* **26**, 243-249.

Rivero-Lezcano, O. M., Marcilla, A., Sameshima, J. H., and Robbins, K. C. (1995). Wiskott-Aldrich syndrome protein physically associates with Nck through Src homology 3 domains. *Mol Cell Biol* **15**, 5725-5731.

She, H. Y., Rockow, S., Tang, J., Nishimura, R., Skolnik, E. Y., Chen, M., Margolis, B., and Li, W. (1997). Wiskott-Aldrich syndrome protein is associated with the adapter protein Grb2 and the epidermal growth factor receptor in living cells. *Mol Biol Cell* **8**, 1709-1721.

White, J. G., Southgate, E., Thomson, J. N., and Brenner, S. (1986). The structure of the nervous system of the nematode *Caenorhabditis elegans. Philos Trans R Soc Lond B Biol Sci* **314**, 1-340.

Zallen, J. A., Kirch, S. A., and Bargmann, C. I. (1999). Genes required for axon pathfinding and extension in the *C. elegans* nerve ring. *Development* **126**, 3679-3692.

Zallen, J. A., Yi, B. A., and Bargmann, C. I. (1998). The conserved immunoglobulin superfamily member SAX-3/Robo directs multiple aspects of axon guidance in *C. elegans*. *Cell* **92**, 217-227.

Chapter 3

SAX-3/Robo signaling mediated by UNC-34/Enabled and a Netrin-independent function of UNC-40/DCC

Chapter 3 is modified from the following manuscript:

Yu, T. W., Hao, J. C., Lim, W., Tessier-Lavigne, M., and Bargmann, C. I.

Shared receptors in axon guidance: SAX-3/Robo signaling is mediated by UNC-34/Enabled and a Netrin-independent function of UNC-40/DCC.

Submitted.

3.1 Summary

The *C. elegans* SAX-3/Robo receptor acts in anterior-posterior, dorsal-ventral and midline guidance decisions. Here we show that SAX-3 signaling involves the *C. elegans* Enabled protein UNC-34 and an unexpected Netrin-independent function of the Netrin receptor UNC-40/DCC. Genetic interactions with gain and loss of function mutations in the *sax-3* pathway suggest that *unc-34* and *unc-40* act together with *sax-3* in several guidance decisions. The *C. elegans* Netrin gene *unc-6* does not act in the same genetic pathways. The SAX-3 cytoplasmic domain associates with UNC-34 and UNC-40 *in vitro,* suggesting the existence of a signaling complex. Our results support a role for UNC-34/Enabled proteins in SAX-3-mediated repulsion, and define a novel ability of UNC-40/DCC to potentiate SAX-3/Robo signaling via a mechanism that may involve direct binding of the two guidance receptors. A combinatorial logic dictates alternative functions for UNC-40/DCC, which can act in attraction to UNC-6/Netrin, repulsion from Netrin (with UNC-5), or repulsion from Slit (with SAX-3).

3.2 Introduction

The growth cones of developing neurons navigate through their environments in response to attractive and repulsive guidance cues (Tessier-Lavigne and Goodman, 1996). Several conserved families of ligands and receptors participate in axon guidance, including UNC-6/Netrin and its receptors UNC-40/DCC/Frazzled and UNC-5, Slit and its receptor Robo/SAX-3, Ephrins and the Eph receptors, and Semaphorins and their receptors Neuropilin and Plexin (Brose and Tessier-Lavigne, 2000; Culotti and Merz, 1998; Flanagan and Van Vactor, 1998; Flanagan and Vanderhaeghen, 1998; Nakamura *et al.*, 2000). The signaling mechanisms by which these molecules modulate the cytoskeleton are not well understood. The cytoplasmic domains of most guidance receptors are devoid of obvious catalytic motifs or similarity to one another, and even within a particular receptor family homology is often limited to short amino acid motifs of unknown function. Yet when the cytoplasmic sequences of UNC-40/DCC/Frazzled and SAX-3/Robo are fused to heterologous ligand-binding domains, they can drive axon attraction or repulsion, respectively (Bashaw and Goodman, 1999; Stein and Tessier-Lavigne, 2001).

The function of a particular guidance receptor can vary depending on the cell and its environment. For example, UNC-40/DCC is required for attraction to the UNC-6/Netrin guidance cue, but some cells that express UNC-40 are not attracted to Netrin, suggesting that UNC-40 requires additional cofactors to mediate attractive guidance (Chan *et al.*, 1996). In addition to its role in attraction, UNC-40 also potentiates repulsion from Netrin mediated by the UNC-5 receptor (Colavita and Culotti, 1998). This potentiation occurs through a direct interaction between the UNC-40 and UNC-5 cytoplasmic domains that is stimulated by Netrin binding (Hong *et al.*, 1999). There are also Netrin-independent functions of UNC-40 in cell and axon migration (Hedgecock *et al.*, 1990; Hedgecock *et al.*,

1987; Honigberg and Kenyon, 2000; Kim *et al.*, 1999). These results suggest that UNC-40 can participate in several different kinds of signaling complexes with different properties.

We are studying mechanisms of axon repulsion mediated by *C. elegans sax-3*, a member of the Robo family of guidance receptors. The nematode, fly and human SAX-3/Robo proteins are transmembrane receptors with five Immunoglobulin domains, three Fibronectin type III domains, and cytoplasmic domains from 377 to 733 amino acids in size (Kidd *et al.*, 1998a; Zallen *et al.*, 1998). *Drosophila Robo* and *C. elegans sax-3* mutants have defects in axon guidance at the ventral midline that suggest a role for these genes in preventing midline crossing (Kidd *et al.*, 1998a; Kidd *et al.*, 1998b; Tear *et al.*, 1993; Zallen *et al.*, 1998). In *Drosophila,* the secreted Robo ligand Slit is expressed at the midline, where it acts to repel Robo-expressing axons (Kidd *et al.*, 1999). Vertebrate Robos and Slits also act in repulsion, and vertebrate Slit is expressed at the ventral midline of the spinal cord (Brose *et al.*, 1999; Zou *et al.*, 2000). In addition to their midline defects, *C. elegans sax-3* mutants have defects in long-range cell migrations, in the formation of the nerve ring in the head, and in ventral axon guidance in the body (Zallen *et al.*, 1999). A *C. elegans* Slit homolog, *slt-1*, is one probable ligand for *sax-3* in several guidance decisions (Hao *et al.*, 2001).

Genetic screens in *C. elegans* and *Drosophila* have led to the identification of several genes that are candidate downstream components of axon guidance signaling pathways (Gallo and Letourneau, 1999; Lin and Greenberg, 2000; Merz and Culotti, 2000). One of these genes, *enabled,* was first identified in *Drosophila* as a genetic suppressor of lethal mutations in the cytoplasmic tyrosine kinase *abl* (Gertler *et al.*, 1990); subsequent analysis of *ena* mutants revealed significant axon guidance defects in the developing *Drosophila* nervous system (Gertler *et al.*, 1995). Dose-dependent interactions between *ena, abl,* and genes for receptor tyrosine phosphatases (RPTPs) also suggested that these proteins act in a common regulatory pathway for axon guidance (Wills *et al.*, 1999).

We show here that the *C. elegans* Enabled protein UNC-34 is a mediator of SAX-3 signaling in repulsive guidance from SLT-1. Robo and Enabled also act together in *Drosophila* midline guidance (Bashaw *et al.*, 2000). We also report the unexpected finding that SAX-3 function is potentiated by a Netrin-independent function of the Netrin receptor UNC-40. Our results suggest that SAX-3, UNC-34, and UNC-40 may interact directly in guidance complexes that contribute to repulsive guidance.

3.3 Results

sax-3 and *unc-34* have overlapping mutant phenotypes

There are several conserved proline-rich motifs in the cytoplasmic domains of *C. elegans* SAX-3, *Drosophila* Robo1, and human Robo1 receptors. One of these motifs resembles a consensus binding site for EVH1 domains, domains characteristic of Enabled proteins and their family members (Kidd *et al.*, 1998a). This motif, designated CC2, has a core of seven conserved prolines flanked by hydrophobic amino acids (in SAX-3, FIPPPPSNPPP). The evidence implicating Enabled in *Drosophila* axon guidance and the presence of this recognition site led us to study interactions between *sax-3* and *C. elegans* EVH1 domain-containing proteins.

We searched *C. elegans* sequence databases for potential EVH1 domain-containing proteins. *C. elegans* has three predicted EVH1 domain proteins: a single predicted Enabled homolog on chromosome V (*c-ena*), a Bee1p relative on chromosome III (B0280.2), and a N-WASP relative on chromosome IV (C07G1.4). To ask whether the *C. elegans* Enabled protein affects cell and axon migrations, its function was disrupted using double-stranded RNA-mediated interference (Fire *et al.*, 1998). RNAi of *c-ena* in wild-type *C. elegans* resulted in cell migration defects in the CAN neuron, a withered tail phenotype, and an

uncoordinated (Unc) phenotype (data not shown). Similar CAN migration and withered tail phenotypes are observed in *sax-3* mutants. These defects are also observed in *unc-34* mutants, which map to the same region of Chromosome V as *c-ena,* suggesting that *c-ena* might correspond to *unc-34.* This possibility has been confirmed by Dell and Garriga (personal communication) who demonstrated that *unc-34* encodes the *C. elegans* Enabled homolog and identified the allele *unc-34(gm104)* as a molecular null allele.

To ask whether *unc-34* has a role in *sax-3* signaling, we first compared the mutant phenotypes of *sax-3* and *unc-34* mutants. *sax-3* and *unc-34* mutants share a number of known defects, including aberrant axon bundling in the ventral nerve cord and shortened posterior migrations of the CAN neurons (Table 3-1) (Forrester and Garriga, 1997; McIntire *et al.*, 1992; Zallen *et al.*, 1998). We observed that they shared several other defects that were not previously described. First, the two PVQ axons in the ventral cord inappropriately crossed the midline in *unc-34* mutants, as they do in *sax-3* mutants (Figure 3-1A-F, Table 3-1). Second, *glr-1*-expressing interneurons migrated along the lateral body wall, instead of the ventral nerve cord, in both *unc-34* and *sax-3* mutants (S. G. Clark and C. I. B., unpublished). Third, *unc-34* mutants had defects in the ventral migration of the AVM sensory neuron that were similar to those of *sax-3* mutants (Zallen *et al.*, 1999) (Figure 3-1G-L). However, the phenotypes of *sax-3* and *unc-34* mutants were not identical. *sax-3* mutants have anteriorly misrouted sensory axons in the nerve ring (Zallen *et al.*, 1998), a defect not present in *unc-34* mutants. *unc-34* mutants exhibit misguidance of motor axons and premature termination of axons in the ventral nerve cord (McIntire *et al.*, 1992), defects that were not present in *sax-3* mutants. We conclude that *sax-3* and *unc-34* mutants share some, but not all, axon and cell migration defects.

sax-3 and _unc-34_ interact in a common genetic pathway for axon guidance

We used genetic criteria to test the involvement of *unc-34* in SAX-3 signaling, beginning with double mutant analysis. If two genes act exclusively in the same pathway, a double mutant should be similar to the strongest single null mutant. The phenotype of the strong *sax-3(ky123)* allele, which lacks the start ATG and signal sequence of SAX-3, served as a standard for the presumed *sax-3* null phenotype. A strong *sax-3* phenotype is also caused by the *sax-3(ky200ts)* mutant at 25°C. The strong *slt-1(eh15)* allele, which truncates SLT-1 in the leucine rich repeat domain, was used to inactivate SLT-1 function (Hao *et al.*, 2001), and the *unc-34(gm104)* null allele was used.

sax-3, *slt-1*, and *unc-34* were examined in detail for effects on the ventral guidance of the AVM mechanosensory neuron, the best-characterized *sax-3*-dependent guidance decision. The AVM cell body lies on the lateral body wall; at the end of the first larval stage (L1), its axon grows ventrally to the ventral nerve cord, whereupon it turns anteriorly and extends to the nerve ring (Figure 3-1G, L, Figure 3-2A) (White *et al.*, 1986). The initial ventral guidance of the AVM axon is mediated in part by repulsion from SLT-1, which is expressed by dorsal muscles. *sax-3* is required in AVM for repulsion from SLT-1 (Zallen *et al.*, 1999); in strong *sax-3* or *slt-1* mutants, 30-40% of AVM neurons fail in the initial ventral component of their trajectory and instead take an anterior path appropriate for the second part of their trajectory (Figure 3-1H, K, Figure 3-2B). On their own, *unc-34* mutants had a mild defect in AVM ventral guidance (Figure 3-1I, L, Figure 3-2B). AVM defects in *unc-34; slt-1* double mutants were similar to those of strong *slt-1* single mutants, and a similar result was observed for *unc-34; sax-3(ky200)* (Figure 3-2B) (*unc-34; sax-3(ky123)* double mutants were inviable, precluding analysis of AVM axon guidance). These results are consistent with a role for *unc-34* in the *slt-1/sax-3* guidance decision.

A second test for similar functions of *sax-3* and *unc-34* is to examine their effects when mutations are combined with mutations in an independent guidance pathway. *slt-1* and Netrin/*unc-6* guidance systems act in parallel to direct AVM ventral guidance: AVM is simultaneously repelled by dorsal SLT-1 and attracted to ventral UNC-6 (Hao *et al.*, 2001; Wadsworth *et al.*, 1996). In the strong *unc-6(ev400)* allele, 40% of AVM axons fail to grow ventrally (Hedgecock *et al.*, 1990) (Figure 3-2B). The defect in *unc-6 slt-1* double mutants is enhanced to over 90%, suggesting a loss of all dorsal-ventral guidance information (Figure 3-2B) (Hao *et al.*, 2001). We reasoned that if *unc-34* acts specifically in the *slt-1* pathway, *unc-34* mutants should act like *slt-1* mutants to enhance the AVM ventral guidance defects of null mutants in *unc-6*. Indeed, the ventral guidance defects of *unc-34; unc-6* mutants were much more severe than those of single mutants (Figure 3-2B). These results place *unc-34* in the Slit pathway for AVM ventral guidance and in parallel to the Netrin pathway.

Additional evidence for a role of *unc-34* in SAX-3/Robo signaling was provided by its ability to suppress a gain-of-function of the *sax-3* pathway caused by a *myo-3::SLT-1* transgene. SLT-1 is normally expressed in dorsal muscles. Ubiquitous muscle expression of SLT-1 under the *myo-3* promoter causes both dorsal-ventral defects and anterior-posterior defects in AVM axon guidance, whereas loss-of-function of *sax-3* or *slt-1* cause only dorsal-ventral defects in AVM (Figure 3-3) (Hao *et al.*, 2001). The anterior-posterior defects caused by *myo-3::SLT-1* were diagnostic of overactivated SAX-3/SLT-1 signaling. Since these defects were present in *myo-3::SLT-1,* but absent in *sax-3* mutants, they provided a distinguishable gain-of-function phenotype for epistasis analysis. *sax-3* loss-of-function mutations are strong suppressors of the anterior-posterior defect of *myo-3::SLT-1*, as expected since loss of a receptor should suppress the effects of excess ligand (Figure 3-3D) (Hao *et al.*, 2001). Posterior defects of *myo-3::SLT-1* animals were also suppressed by mutations in *unc-34* (Figure 3-3D, Table 3-2). Suppression was observed in several

independent *myo-3::SLT-1* strains (Table 3-2). These epistasis results suggest that *unc-34* acts with *sax-3* downstream of *slt-1* in AVM guidance.

Finally, in a genetic background sensitized by weak mutations in one gene, mutation of a second gene in the pathway can synergize to yield a stronger phenotype. This criterion was used to test *unc-34* for enhancement of a weak *sax-3* allele in nerve ring axon guidance. In strong *sax-3* mutants such as *sax-3(ky123),* sensory axons exit the nerve ring to take abnormal anterior trajectories in the head (Figure 3-4A, B). This defect is not observed in animals bearing the temperature-sensitive *sax-3* allele *sax-3(ky200)* at 20°C, the permissive temperature, nor is it observed in *unc-34* mutants (Figure 3-4C, D). The temperature-sensitive *sax-3(ky200)* allele served as a sensitized background for enhancement studies. Removing a single copy of *unc-34* in a *sax-3(ky200)* background at 20°C caused anterior sensory axon defects (Figure 3-4E). Removing both copies of *unc-34* in a *sax-3(ky200)* background had an even stronger effect, resulting in a defect that was comparable to *sax-3* null mutants (Figure 3-4F). Similar synergistic interactions were observed in interneuron axons in the nerve ring. Using the interneuron marker *glr-1::GFP,* no defects were observed in *sax-3(ky200)* at 20°C, but 93% of *sax-3(ky123)* animals had anterior axon defects (Figure 3-4G-I, K). *unc-34* had mild anterior axon defects, which were strongly enhanced in *unc-34; sax-3(ky200)* double mutants at 20°C (Figure 3-4J, K). These results demonstrate that UNC-34 contributes to nerve ring axon guidance, a role not evident from analysis of *unc-34* mutants alone. They therefore reveal another function shared by *sax-3* and *unc-34*, and support the model that *unc-34* and *sax-3* function in a common guidance pathway.

unc-40 has a *unc-6/Netrin*-independent interaction with *sax-3* and *slt-1*

To seek additional components of the *sax-3* guidance pathway, we examined the functions of other axon guidance genes using the same genetic assays described for *unc-34*. Surprisingly,

we observed that mutations in the Netrin receptor *unc-40* strongly suppressed anterior-posterior AVM defects in the *myo-3:SLT-1* strain (Figure 3-3D, Table 3-2). Since the anterior-posterior defects are a specific result of SLT-1 misexpression, this result suggested that the gain-of-function SLT-1 phenotype requires the UNC-40 guidance receptor in addition to the SAX-3 guidance receptor. Mutations in *unc-6/Netrin* did not suppress the gain-of-function SLT-1 phenotype (Figure 3-3D, Table 3-2).

In *Drosophila*, neurons expressing the *unc-40* homolog *frazzled* can bind Netrin and present it to developing axons (Hiramoto *et al.*, 2000). If UNC-40 binds and redistributes the UNC-6 protein, mutations in *unc-40* could cause *unc-6*-dependent defects in pathfinding. To ask if the suppression of *myo-3::SLT-1* by *unc-40* was secondary to a redistribution of UNC-6, we examined an *unc-40; unc-6 myo-3::SLT-1* triple mutant. The triple mutant phenotype was identical to *unc-40; myo-3::SLT-1*, demonstrating that mutations in *unc-40* suppressed the posterior axon phenotypes of *myo-3::SLT-1* regardless of the presence of *unc-6* (Figure 3-3D). Thus the ability to suppress *myo-3::SLT-1* is not due to UNC-6 redistribution, and is an *unc-6*-independent function of *unc-40*.

To test whether *unc-40* plays a role in other *sax-3*-dependent guidance pathways, we examined the enhancement of nerve ring axon guidance defects in animals harboring the weak *sax-3(ky200)* allele, as described above for *unc-34*. *unc-40* mutants did not have anterior guidance defects in the nerve ring. However, *unc-40; sax-3(ky200)* mutants at 20°C exhibited a dramatic enhancement of anterior nerve ring phenotypes compared to *sax-3(ky200)* alone, yielding a phenotype similar to that of strong *sax-3* mutants (Figure 3-5). No enhancement was observed in *unc-6(ev400) sax-3(ky200)* double mutants (Figure 3-5). Thus, the nerve ring defect, like the *myo-3::SLT-1* defect, results from a Netrin-independent function of *unc-40*.

In summary, like *unc-34/Enabled* mutations, *unc-40/DCC* mutations suppressed a SLT-1 gain-of-function defect in AVM guidance and enhanced weak *sax-3* loss-of-function defects in the nerve ring. Therefore, in two different cell types and two different genetic assays, UNC-40 had the properties expected of a component in the SAX-3 guidance pathway. Neither of these *unc-40* functions was shared with *unc-6.*

UNC-34 and UNC-40 bind directly to the SAX-3 cytoplasmic domain

Genetic interactions do not distinguish whether two proteins interact directly or indirectly. To ask whether SAX-3, UNC-40, and UNC-34 could interact directly in a guidance complex, we used *in vitro* binding assays to ask whether UNC-34 and UNC-40 proteins can bind SAX-3.

In vitro translated UNC-34 associated with a bacterially expressed GST::SAX-3 protein, but not with a GST::UNC-40 protein or with GST alone (Figure 3-6A). Full-length UNC-34 also bound ActA (Figure 3-6A), a *Listeria* protein that is a ligand for the EVH1 domains of vertebrate Enabled/VASP family members (Chakraborty *et al.*, 1995). UNC-34 has several unusual amino acid substitutions compared to other EVH1 domain proteins, but these results confirm that it acts as a typical ActA-binding EVH1 protein.

The UNC-40 cytoplasmic domain associated with GST::SAX-3, but not with GST alone or GST::ActA (Figure 3-6B). This binding interaction is evolutionarily conserved, since vertebrate DCC and Robo can bind one another (Stein and Tessier-Lavigne, 2001). *In vitro* translated UNC-40 also associated with GST::UNC-40 (Figure 3-6B), consistent with observations that vertebrate DCC can dimerize (Stein *et al.*, 2001). Similarly, *in vitro* translated SAX-3 associated with GST::SAX-3 as well as with GST::UNC-40, but not GST or GST::ActA (Figure 3-6C). These results show that SAX-3 and UNC-40 have the potential to form homomeric and heteromeric complexes, and suggest that the observed

genetic interactions could be mediated by direct interactions between SAX-3, UNC-34 and UNC-40 proteins.

3.4 Discussion

Our results demonstrate that axon guidance by SAX-3, the *C. elegans* Robo protein, is potentiated by UNC-34/Enabled and UNC-40/DCC. The UNC-34/Enabled function is similar to a recently reported role of *Drosophila* Enabled in Robo function at the midline (Bashaw *et al.*, 2000). Our results extend these observations to a variety of non-midline axon guidance decisions. The UNC-40/DCC function is unexpected, and suggests that SAX-3/Robo and UNC-40 cooperate in a guidance process that is distinct from the known roles of UNC-40 in Netrin responses.

unc-34/Enabled acts in repulsive axon guidance pathways

unc-34 and *sax-3* affect several of the same axon guidance and cell migration decisions. In addition to shared mutant defects, four results suggest that *unc-34* interacts with *sax-3*. First, *unc-34* mutants in double mutant combinations have defects in AVM ventral guidance that are diagnostic of reduced SLT-1/SAX-3 activity. Second, loss of *unc-34* function suppresses SLT-1 gain of function phenotypes. Third, *unc-34* mutations enhance *sax-3*-like phenotypes in a sensitized weak *sax-3* mutant background. Fourth, UNC-34 binds directly to the SAX-3 cytoplasmic domain. SAX-3 and Robo share very little overall sequence similarity in their intracellular domains, but their genetic and biochemical interactions are conserved between *Drosophila* and *C. elegans,* providing strong support for their biological relevance (Bashaw *et al.*, 2000).

The involvement of Enabled proteins in actin polymerization during *Listeria* intracellular motility suggests a role for UNC-34/Enabled as an effector that links SAX-3 to the actin cytoskeleton (Chakraborty *et al.*, 1995; Laurent *et al.*, 1999). In addition, mammalian Ena-family proteins can inhibit cell motility, consistent with roles of SAX-3 in axon repulsion (Bear *et al.*, 2000). However, our experiments do not formally distinguish whether UNC-34 acts upstream or downstream of SAX-3 (though both act downstream of SLT-1), so it is possible that UNC-34 acts as a regulator and not an effector of SAX-3 during guidance.

unc-34 mutants have considerably weaker phenotypes than *sax-3* mutants in AVM ventral guidance and in the nerve ring. Therefore, UNC-34 cannot be the sole mediator of SAX-3-mediated guidance decisions. Evidence from *Drosophila* also suggests that additional factors, including kinases and phosphatases as well as *son of sevenless* and calmodulin pathways, may contribute to Robo-mediated guidance events (Bashaw *et al.*, 2000; Fritz and VanBerkum, 2000; Sun *et al.*, 2000). Conversely, UNC-34 has SAX-3-independent roles in guidance. *unc-34* mutants have defects in motor neuron guidance that resemble those of *unc-5* mutants, which lack the repulsive Netrin receptor. *unc-34* also suppresses an UNC-6-dependent, UNC-5 gain-of-function axon guidance defect (Colavita and Culotti, 1998). Thus *unc-34* acts in two different repulsive guidance pathways: avoidance of SLT-1 (mediated by SAX-3) and avoidance of UNC-6/Netrin (mediated by UNC-5). *unc-34* does not appear to act in AVM attraction to UNC-6, so it is not required for all forms of axon guidance. It is possible that *unc-34* acts specifically in repulsive axon guidance pathways.

UNC-40/DCC has an UNC-6/Netrin-independent role in SAX-3 signaling

It has long been appreciated that *C. elegans unc-40* has functions that are independent of *unc-6/Netrin* (Hedgecock *et al.*, 1990; Hedgecock *et al.*, 1987; Honigberg and Kenyon,

2000; Kim *et al.*, 1999). Our observations demonstrate an UNC-6-independent function of UNC-40 in SAX-3 signaling. Mutations that diminish *unc-40* function can suppress SLT-1 gain-of-function defects, but mutations in *unc-6* do not suppress these defects. Moreover, *unc-40* mutations suppress SLT-1 gain-of-function in animals lacking *unc-6*, demonstrating that this effect of *unc-40* is independent of Netrin. *unc-40* but not *unc-6* mutations also enhance weak *sax-3* mutations in nerve ring axon guidance. The genetic interactions between *unc-40* and *sax-3* are very similar to the interactions between *unc-34* and *sax-3*, and point to a role for UNC-40 in SAX-3 guidance. Such a role is further supported by the direct interaction between UNC-40 and SAX-3 cytoplasmic domains.

These results suggest that SAX-3/UNC-40 complexes are required for efficient axon guidance by SAX-3. SAX-3 can mediate guidance decisions without UNC-40, just as it can without UNC-34, but in the absence of either gene guidance is less efficient and more sensitive to perturbation. This proposed SAX-3/UNC-40 receptor complex is analogous in some respects to the UNC-5/UNC-40 complex that acts in repulsion from Netrin. UNC-5 can mediate repulsion on its own, although efficient repulsion from Netrin requires both UNC-5 and UNC-40 (Colavita and Culotti, 1998; Hedgecock *et al.*, 1990; Hong *et al.*, 1999). Thus UNC-40 can act to assist two repulsive receptors, SAX-3 and UNC-5, in addition to its role in Netrin attraction. Unlike UNC-5/UNC-40, however, the proposed SAX-3/UNC-40 complex crosses ligand boundaries, by linking UNC-40 to Slit responses.

An interaction between UNC-40 and SAX-3 is also observed with their vertebrate counterparts, DCC and Robo (Stein and Tessier-Lavigne, 2001), where it is implicated in a different guidance decision. In Stage 22 *Xenopus* spinal cord neurons, Slit acting through Robo silences the ability of DCC to mediate turning towards Netrin, but those axons are not repelled by Slit. Thus Robo can act as a negative regulator of DCC in *Xenopus* or as a collaborator with UNC-40/DCC in *C. elegans*. We speculate that the outcome of the

Robo/DCC interaction is regulated by other proteins that are present or absent in particular neurons at particular developmental stages. Mouse DCC mutants have more severe defects in axon guidance in the spinal cord than do Netrin mutants, suggesting a Netrin-independent role for DCC (Fazeli *et al.*, 1997); perhaps this involves an interaction with Robo proteins as well.

The existence of a shared guidance complex such as SAX-3/UNC-40 could help explain why there is little similarity among cytoplasmic domains of different guidance receptors. SAX-3 does not need to have the same domains as UNC-40 if it can simply recruit UNC-40 into decisions when those domains are useful. For example, a SAX-3/UNC-40 complex could promote motility in certain regions of the growth cone, propelling it away from a source of repellent. In *Xenopus* studies of Robo-mediated silencing, Robo binding to DCC abolishes Netrin-stimulated turning, but not outgrowth (Stein and Tessier-Lavigne, 2001). We suggest that local interactions between guidance receptors optimize the ability of growth cones to perform local integration of guidance cues. Turning requires the growth cone to make a decision across its surface, and during turning different regions of the growth cone behave quite differently — one filopodium may be retracting as another advances. These highly local decisions may be best accomplished by integrating guidance decisions immediately at the level of the receptor, maximizing the interpretation of spatial information across the growth cone.

3.5 Materials and Methods

Strains

Wild-type animals were *C. elegans* variety Bristol, strain N2. The following strains were utilized for these studies: CX3171 [*sax-3(ky200) X*], CX3198 [*sax-3(ky123) X*], CX5001 [*slt-*

1(eh15) X], CB315 [*unc-34(e315) V*], CX4374 [*unc-34(gm104) V*], CX4345 [*unc-34(e951) V*], CX3099 [*unc-34(ky155) V; kyIs4 X*], NW434 [*unc-6(ev400) X*], CX5353 [*unc-40(e1430) I*], CB271 [*unc-40(e271) I*], CX5088 [*zdIs5 I; dpy-20(e1282) IV; myo-3::SLT-1(kyIs213)*], CX5078 [*zdIs5 I; dpy-20(e1282) IV; myo-3::SLT-1(kyIs218) X*], CX5083 [*zdIs5 I; dpy-20(e1282) IV; myo-3::SLT-1(kyIs223)*], CX2627 [*kyIs4(ceh-23::GFP) X*], CX5334 [*oyIs14(sra-6::GFP) V; lin-15(n765) X*], and CX4971 [*mec-4::GFP(zdIs5)*]. *sax-3(ky123)* deletes the start ATG and signal sequence of SAX-3, whereas *sax-3(ky200)* encodes a P37S point mutation in the first immunoglobulin repeat (Zallen *et al.*, 1998). *unc-34(gm104)* introduces an early stop codon in the UNC-34 coding sequence, and *unc-34(e951)* is a deletion that removes the EVH1 domain (Megan Dell and Gian Garriga, personal communication). *slt-1(eh15)* is a deletion that truncates SLT-1 after the first leucine rich repeat (Hao *et al.*, 2001). *unc-6(ev400), unc-40(e1430)* and *unc-40(e271)* are canonical strong loss-of-function alleles (Chan *et al.*, 1996; Hedgecock *et al.*, 1990; Wadsworth *et al.*, 1996). Strains were maintained using standard methods. Animals were grown at 20°C except for the *sax-3(ky200)* strain, which was grown at either 20°C or 25°C, as noted. *unc-34(gm104)* and *unc-34(e951)* strains were kindly provided by Megan Dell and Gian Garriga. Some strains were provided by the *Caenorhabditis* Genetic Center.

Construction of double mutants

Double mutants were constructed using standard genetic procedures. In general, *unc-34*, *unc-6* and *unc-40* were followed based on visible phenotypes and *sax-3* and *slt-1* mutations were scored by PCR. Double Unc mutants were crossed to N2 to confirm segregation of the appropriate single mutants. The following strains were created: CX4350 [*unc-34(ky155) V; sax-3 (ky200) kyIs29 X*], CX4347 [*unc-34(ky155) V; sax-3(ky200) kyIs4 X*], CX4337 [*unc-34(e315) V; sax-3(ky200) kyIs4 X*], CX4756 [*unc-34(gm104) V; sax-3(ky200) X*], CX4774

[*zdIs5 I; unc-34(gm104) V; sax-3(ky200) X*], CX5226 [*zdIs5 I; unc-34(gm104) V; slt-1(eh15) X*], and CX5474 [*zdIs5 I; unc-34(gm104) V; unc-6(ev400) X*]. *myo-3::SLT-1* homozygotes were selected based on expression of *str-1::GFP*, a marker present on the integrated *myo-3::SLT-1* array. The following *myo-3::SLT-1* strains were constructed: CX5113 [*zdIs5 I; sax-3(ky123) myo-3::SLT-1(kyIs218) X*], CX5103 [*zdIs5 I; unc-34(e951) V; kyIs218(myo-3::SLT-1)*], CX5115 [*zdIs5 I; unc-34(gm104) V; kyIs218(myo-3::SLT-1)*], CX5303 [*zdIs5 I; unc-34(gm104) V; kyIs223(myo-3::SLT-1)*], CX5374 [*zdIs5 unc-40(e1430) I; kyIs218(myo-3::SLT-1) X*], CX5224 [*zdIs5 unc-40(e271) I; kyIs218(myo-3::SLT-1)X*], CX5371 [*zdIs5 I; unc-6(ev400) kyIs218(myo-3::SLT-1) X*], and CX5372 [*unc-40(e271) zdIs5 I; unc-6(ev400) kyIs218(myo-3::SLT-1) X*].

Characterization of neuronal phenotypes

Axons visualized with integrated GFP transgenes were scored in live adult animals. Nerve ring sensory axons were visualized with an integrated *ceh-23::GFP* transgene (*kyIs4 X*), and nerve ring interneurons were visualized with an integrated *glr-1::GFP* transgene (*kyIs29 X*). The PVQ interneurons were visualized with an integrated *sra-6::GFP* transgene (*oyIs14 V*), a generous gift of Piali Sengupta). AVM axons were visualized with an integrated *mec-4::GFP* transgene (*zdIs5*, a generous gift of Scott Clark). Images were photographed on a Zeiss Axiocam cooled CCD. For some phenotypes, stacks of images were obtained using laser scanning confocal microscopy and projected into a single plane for presentation.

Generation of proteins for binding analysis

Expression vectors for *in vitro* translation of SAX-3, UNC-40, and UNC-34 probes were constructed in pCITE-4c (Novagen) by standard methods. To generate the UNC-34 probe, a full-length UNC-34 cDNA was first obtained by RT-PCR from wild-type N2 RNA

prepared by Trizol extraction (GIBCO), using primers from the UNC-34 coding region and the *C. elegans* splice leader SL1. The following probes were generated: CITE::SAX-3(898-1273), CITE::UNC-40(1106-1415), and CITE::UNC-34(1-467). *In vitro translation* reactions were carried out with the TNT T7 Quick Coupled Transcription/Translation kit (Promega) in the presence of 35[S]-methionine according to the manufacturer's instructions. Expression vectors for GST-fusion proteins were constructed in pGEX-4T-1 (Pharmacia Biotech) by standard methods. The following GST-fusion proteins were produced (amino acids listed in parentheses): GST::SAX-3(898-1273), GST::SAX-3(978-1224), GST::UNC-40(1106-1415), GST::ActA. GST-fusions were expressed in *E. coli* BL21-CodonPlus RIL (Stratagene), purified using glutathione agarose beads (Sigma), and quantitated by SDS-PAGE and Coomassie staining. For binding assays, 2 µg of GST fusion protein was mixed with 20 µl of 35[S]-methionine-labelled probe in 10 mM Tris 7.5, 150 mM NaCl, 0.1% Triton, 0.05% BSA. Samples were incubated for six hours at 4°C and then washed three times in the same buffer. BSA was omitted from the last wash. Bound proteins were separated by SDS-PAGE, soaked in Amplify (Amersham), dried down under vacuum and exposed to film.

Table 3-1 Neuronal guidance in wild-type, *sax-3* mutants and *unc-34* mutants

	wild-type	*sax-3*	*unc-34*
Cell migration			
CAN cells	posterior migration	**stop short**[1]	**stop short**[2]
Ventral nerve cord			
PVQ interneurons	do not cross midline	**cross midline**[3]	**cross midline**
glr-1 interneurons	ventral	**lateral**[3]	**lateral**[4]
HSN motor neurons	anterior to head	**anterior to head**	**terminate**[5]
Dorsal/ventral guidance			
AVM axon	ventral guidance	**guidance defect**[1]	**guidance defect**
VD and DD axons	dorsal guidance	dorsal guidance	**guidance defect**[5]
Nerve ring			
ceh-23 sensory neurons	nerve ring	**anterior misguidance**[1]	nerve ring
glr-1 interneurons	nerve ring	**anterior misguidance**[1]	nerve ring

[1]Zallen *et al*, 1999. [2]Forrester and Garriga, 1997. [3]Zallen *et al*, 1998. [4]S. Clark and C. I. B, unpubl. [5]McIntire *et al*, 1992.

Table 3-2 **Suppression of *SLT-1* gain-of-function phenotype by *sax*-3, *unc-34* and *unc-40***

Genotype	% posterior axons	n
wild-type	0	>300
sax-3(ky123)	0	383
unc-34(gm104)	1	252
unc-40(e271)	1	186
unc-6(ev400)	7	275
kyIs218(myo-3::SLT-1)	13	213
kyIs218(myo-3::SLT-1); sax-3(ky123)	1*	223
kyIs218(myo-3::SLT-1); unc-34(gm104)	3*	330
kyIs218(myo-3::SLT-1); unc-34(e951)	4*	167
kyIs218(myo-3::SLT-1); unc-40(e271)	1*	139
kyIs218(myo-3::SLT-1); unc-40(e1430)	2**	53
kyIs218(myo-3::SLT-1); unc-6(ev400)	23	203
kyIs218(myo-3::SLT-1); unc-40(e1430); unc-6(ev400)	1*	133
kyIs223(myo-3::SLT-1)	14	658
kyIs223(myo-3::SLT-1); unc-34(gm104)	1*	146
kyIs213(myo-3::SLT-1)	9	225
kyIs213(myo-3::SLT-1); unc-40(e271)	0	39

Asterisks denote double mutants that were significantly suppressed compared to *myo-3::SLT-1* alone (*$p<0.01$, **$p<0.05$)

Figure 3-1

unc-34 and *sax-3* mutants share axon guidance phenotypes at the ventral midline and in ventral guidance. (**A-F**) Ventral views of ventral cord axons expressing *sra-6::gfp* in wild-type (**A, D**), *sax-3* (**B, E**) and *unc-34* (**C, F**) backgrounds. (**A, D**) In wild-type animals, axons from the two PVQ interneurons extend in the ventral nerve cord where they are restricted to the ipsilateral nerve cord. (**B, E**) In a *sax-3(ky123)* mutant animal, the PVQ axons cross the midline. Here both PVQ axons run on the right side of the vulva (arrows). (**C, F**) In an *unc-34(gm104)* mutant animal, the PVQ axons also cross the midline (arrows). (**G-L**) Ventral guidance phenotypes visualized by *mec-4::gfp* in wild-type (**G, J**), *sax-3* (**H, K**), and *unc-34* (**I, L**) mutant backgrounds. (**G, J**) In wild-type animals, AVM (*arrow*) grows ventrally to the ventral cord, and then extends anteriorly to the nerve ring. (**H, K**) In *sax-3* mutant animals, AVM has ventral guidance defects. Shown is a *sax-3(ky123)* animal in which AVM fails to grow ventrally and extends directly anteriorly. (**I, L**) *unc-34* mutants also have ventral guidance defects in AVM. Anterior is left in all panels. *Scale bars*, 20 μm.

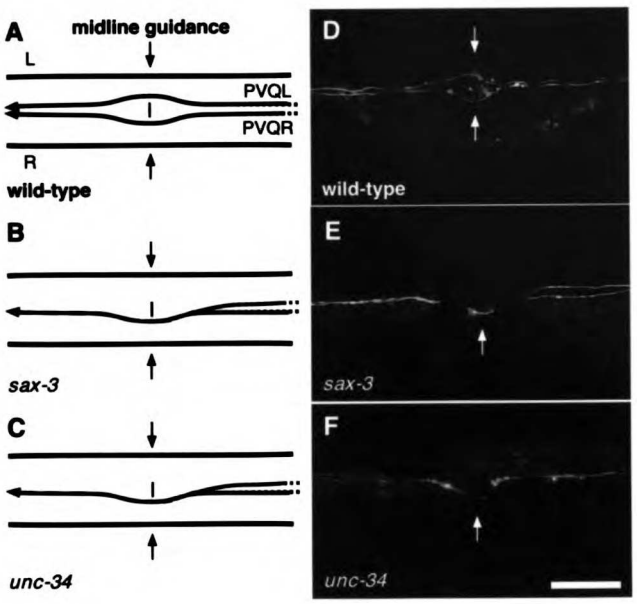
A
midline guidance
L
PVQL
PVQR
R
wild-type
B
sax-3
C
unc-34
D
wild-type
E
sax-3
F
unc-34

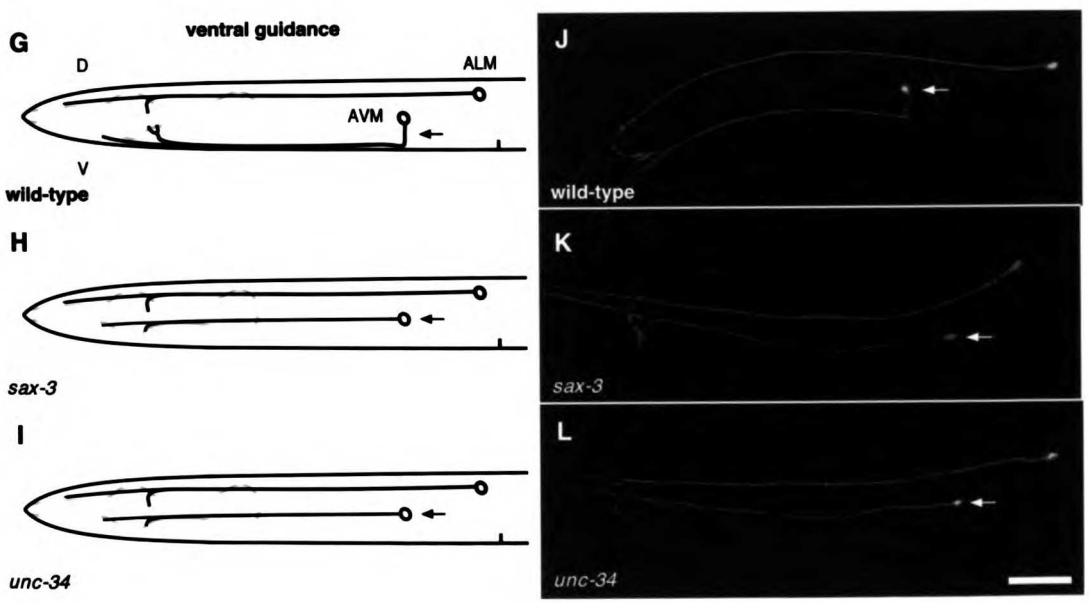
G
ventral guidance
D
ALM
AVM
V
wild-type
H
sax-3
I
unc-34
J
wild-type
K
sax-3
L
unc-34

Figure 3-2

unc-34 double mutant analysis in AVM ventral guidance. (**A**) Organization of guidance cues for AVM ventral guidance in *C. elegans*. SLT-1 is expressed dorsally in muscle (red), whereas UNC-6 is expressed ventrally in the ventral nerve cord (blue). AVM (green) expresses both SAX-3 and UNC-40 guidance receptors. (**B**) Quantitation of ventral guidance defects in *sax-3*, *slt-1*, *unc-6*, and *unc-34* single and double mutants. Asterisks denote defects greater than the *unc-6* single mutant at $p<0.01$. *unc-6 slt-1* data are from Hao *et al.*, 2001.

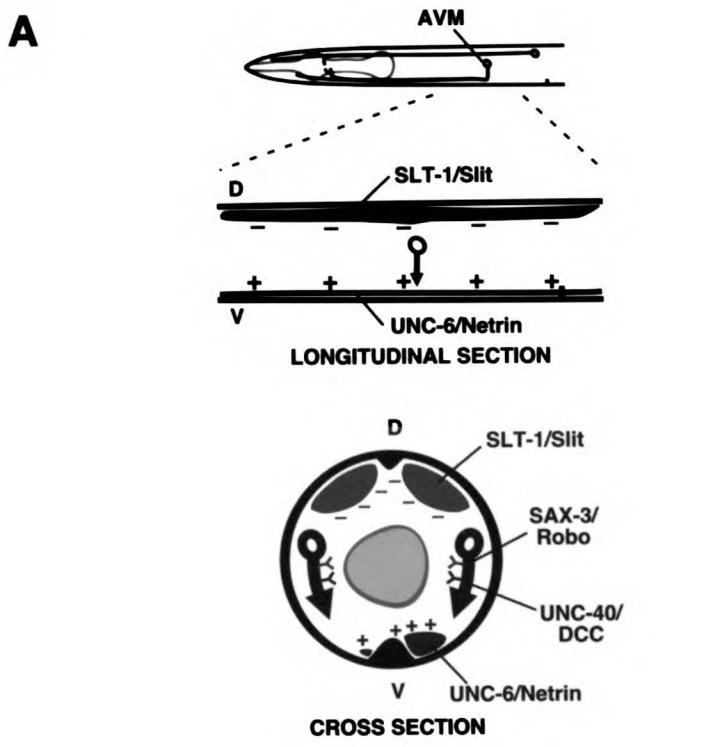
A
AVM
SLT-1/Slit
D
V
UNC-6/Netrin
LONGITUDINAL SECTION
D
SLT-1/Slit
SAX-3/
Robo
UNC-40/
DCC
V
UNC-6/Netrin
CROSS SECTION

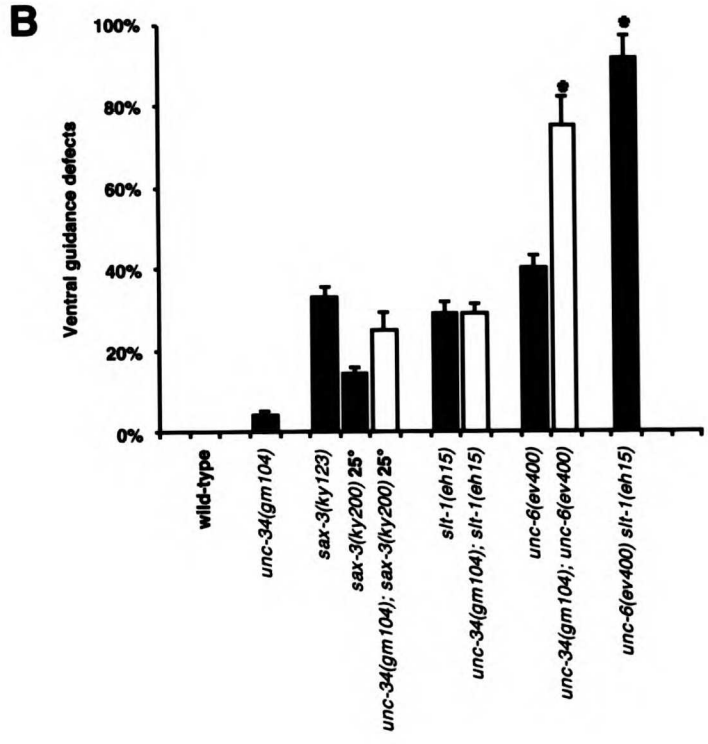
B
Ventral guidance defects
100%
80%
60%
40%
20%
0%
wild-type
unc-34(gm104)
sax-3(ky123)
sax-3(ky200) 25°
unc-34(gm104); sax-3(ky200) 25°
slt-1(eh15)
unc-34(gm104); slt-1(eh15)
unc-6(ev400)
unc-34(gm104); unc-6(ev400)
unc-6(ev400) slt-1(eh15)

Figure 3-3

Suppression of Slit gain-of-function phenotypes by *unc-34* and *unc-40*. (**A**) A wild-type ventral AVM axon projection (*arrow*) visualized with *mec-4::gfp*. ALM (*white arrowhead*) is also visible with this marker. Position of the vulva (*red arrowhead*) is shown. (**B**) Expression pattern of the *myo-3* promoter, as visualized by GFP. The *myo-3* promoter drives expression in dorsal and ventral body wall muscle cells. Position of the vulva (*red arrowhead*) is shown for comparison. (**C**) Posteriorly-directed AVM axon (*arrow*) caused by misexpression of SLT-1 under the *myo-3* promoter, with positions of ALM (*white arrowhead*) and the vulva (*red arrowhead*) shown for reference. (**D**) Quantitation of posterior axon phenotypes using an integrated *myo-3::SLT-1* transgene (*kyIs218*). Data are shown ± SEM. Asterisks denote double mutants that are significantly suppressed compared to *myo-3::SLT-1* alone ($p<0.01$). *Scale bars,* 20 μm.

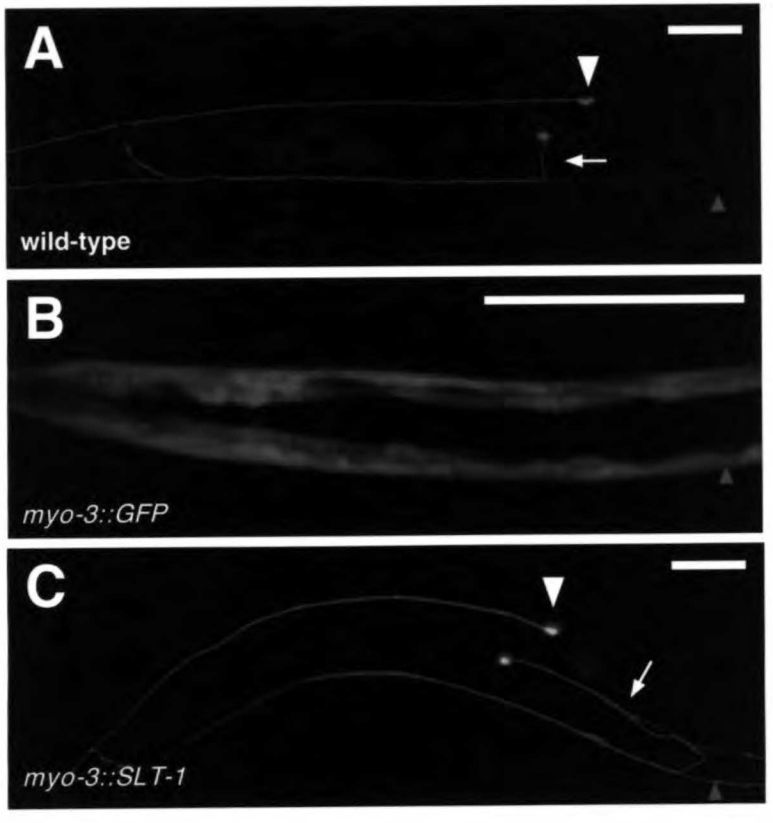
A
wild-type
B
myo-3::GFP
C
myo-3::SLT-1

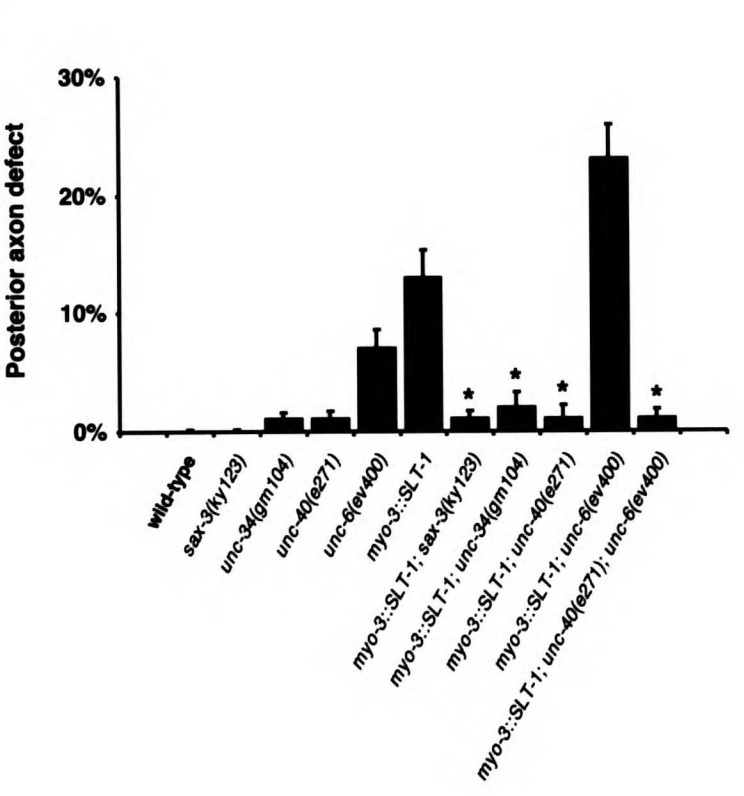
D
Posterior axon defect
30%
20%
10%
0%
wild-type
sax-3(ky123)
unc-34(gm104)
unc-40(e271)
unc-6(ev400)
myo-3::SLT-1
myo-3::SLT-1; sax-3(ky123)
myo-3::SLT-1; unc-34(gm104)
myo-3::SLT-1; unc-40(e271)
myo-3::SLT-1; unc-6(ev400)
myo-3::SLT-1; unc-40(e271); unc-6(ev400)

Figure 3-4

Genetic interactions between *sax-3* and *unc-34* in the nerve ring: phenotypes of sensory axons (**A-F**), as visualized with the *ceh-23::gfp* marker, and interneurons (**G-J**), as visualized with the *glr-1::gfp* marker. (**A**) Wild-type nerve ring, in which sensory axons extend ventrally from their cell bodies into the nerve ring (*schematic: green arrowheads*). Anterior processes are sensory dendrites. (**B**) *sax-3(ky123)*, a strong loss-of-function mutant. Nearly all axons (*schematic: red axons*) travel anteriorly beyond the normal confines of the ring. (**C**) *unc-34* animals have no axon guidance defects in the nerve ring (although some axons terminate prematurely within the nerve ring). (**D**) *sax-3(ky200ts)* at the permissive temperature (20°C). Sensory axons are normal. (**E**) *sax-3(ky200ts) unc-34/+* at the permissive temperature (20°C). One axon grows anteriorly beyond the confines of the nerve ring. (**F**) *sax-3(ky200ts) unc-34* at the permissive temperature (20°C). A highly disorganized, anterior nerve ring reminiscent of the strong *sax-3* phenotype. (**G**) Wild-type animals, in which interneuron axons extend within the nerve ring en route to or from the ventral cord. (**H**) *sax-3(ky200ts)* at the permissive temperature (20°C). Interneuron axons are normal. (**I**) *sax-3(ky123)* animal. *glr-1*-expressing axons leave the nerve ring to travel anteriorly. (**J**) *sax-3(ky200ts) unc-34* at the permissive temperature (20°C), with anterior axon phenotype reminiscent of the strong *sax-3* phenotype. (**K**) Quantitation of anterior guidance defects in the nerve ring. Asterisks denote double mutants that are enhanced compared to *sax-3(ky200ts)* alone ($p<0.01$). Data are shown ± SEM for proportions. *Scale bars*, 20 μm.

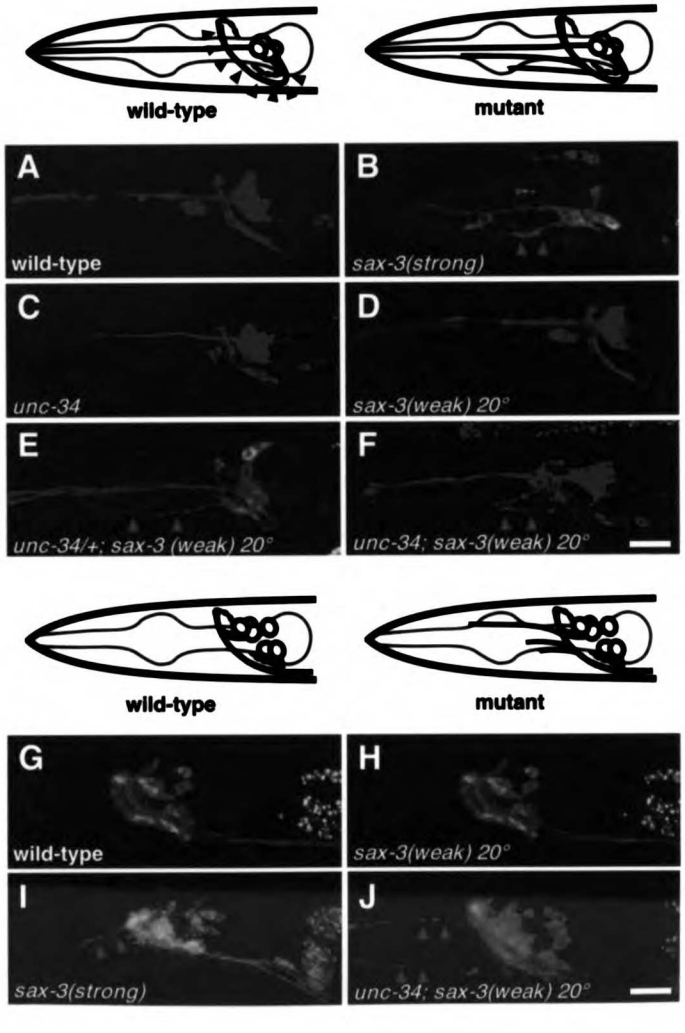
wild-type
mutant
A
wild-type
B
sax-3(strong)
C
unc-34
D
sax-3(weak) 20°
E
unc-34/+; sax-3 (weak) 20°
F
unc-34; sax-3(weak) 20°
wild-type
mutant
G
wild-type
H
sax-3(weak) 20°
I
sax-3(strong)
J
unc-34; sax-3(weak) 20°

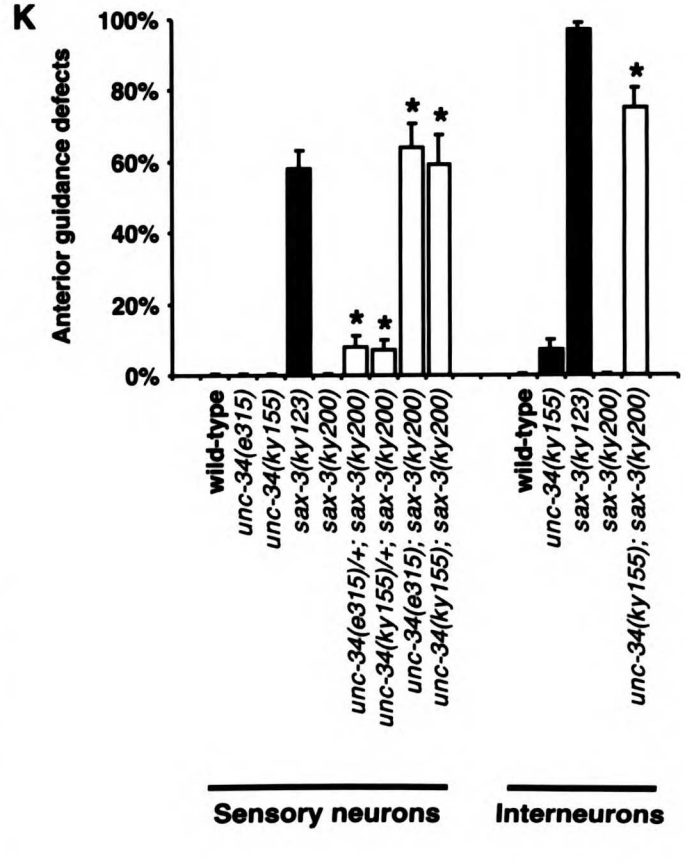
K
Anterior guidance defects
100%
80%
60%
40%
20%
0%
wild-type
unc-34(e315)
unc-34(ky155)
sax-3(ky123)
sax-3(ky200)
unc-34(e315)/+; sax-3(ky200)
unc-34(ky155)/+; sax-3(ky200)
unc-34(e315); sax-3(ky200)
unc-34(ky155); sax-3(ky200)
wild-type
unc-34(ky155)
sax-3(ky123)
sax-3(ky200)
unc-34(ky155); sax-3(ky200)
Sensory neurons
Interneurons

Figure 3-5

Genetic interactions between *sax-3* and *unc-40* in the nerve ring. Like *unc-34*, *unc-40* mutations have no anterior axon guidance defects in the nerve ring on their own; however, a contribution of *unc-40* to anterior nerve ring guidance is revealed in a sensitized *sax-3(ky200ts)* background. Asterisks denote double mutants that are enhanced compared to *sax-3(ky200ts)* alone ($p<0.01$). Data are shown ± SEM.

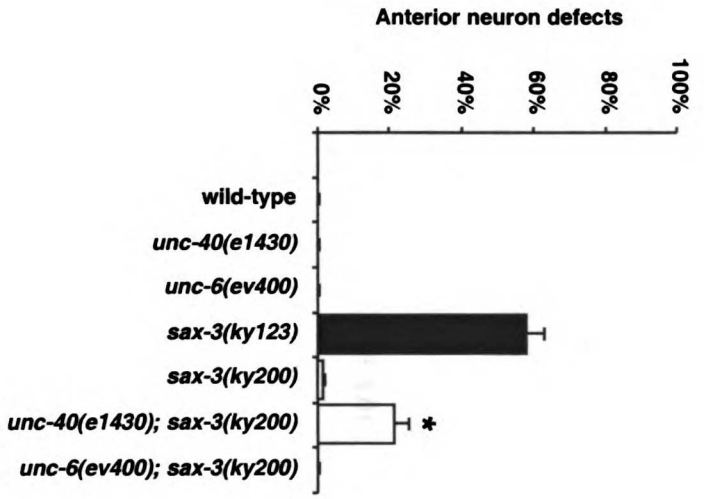
Anterior neuron defects
0%
20%
40%
60%
80%
100%
wild-type
unc-40(e1430)
unc-6(ev400)
sax-3(ky123)
sax-3(ky200)
unc-40(e1430); sax-3(ky200)
unc-6(ev400); sax-3(ky200)
*

Figure 3-6

SAX-3, UNC-34 and UNC-40 proteins can associate. (**A**) UNC-34 associates *in vitro* with the SAX-3 cytoplasmic domain, but not with either GST alone or the UNC-40 cytoplasmic domain. UNC-34 also associates with the *Listeria* protein ActA. *arrow,* band corresponding to full-length 35[S]-labelled UNC-34 probe. (**B**) The UNC-40 cytoplasmic domain associates with itself and with the SAX-3 cytoplasmic domain *in vitro*, but not with GST alone or with *Listeria* ActA protein. *arrow,* band corresponding to 35[S]-labelled UNC-40 cytoplasmic domain probe. (**C**) The SAX-3 cytoplasmic domain associates with itself and with the UNC-40 cytoplasmic domain *in vitro*, but not with GST alone or with *Listeria* ActA protein. *double arrow*, bands corresponding to 35[S]-labelled SAX-3 cytoplasmic domain probe. *input*, 1/20th of input probe; --, blank, *GST*, GST alone; *UNC40*, GST fused to the UNC-40 cytoplasmic domain (amino acids 1106-1415); *SAX3*, GST fused to the SAX-3 cytoplasmic domain (amino acids 898-1273); *SAX3 ABC*, GST fused to a subdomain of the SAX-3 cytoplasmic domain (amino acids 978-1224); *ActA*, GST fused to the *Listeria* protein ActA. In all cases, 35[S]-labelled probe was incubated with GST fusion proteins, co-precipitated with glutathione-agarose beads, and run out by SDS-PAGE and autoradiographed.

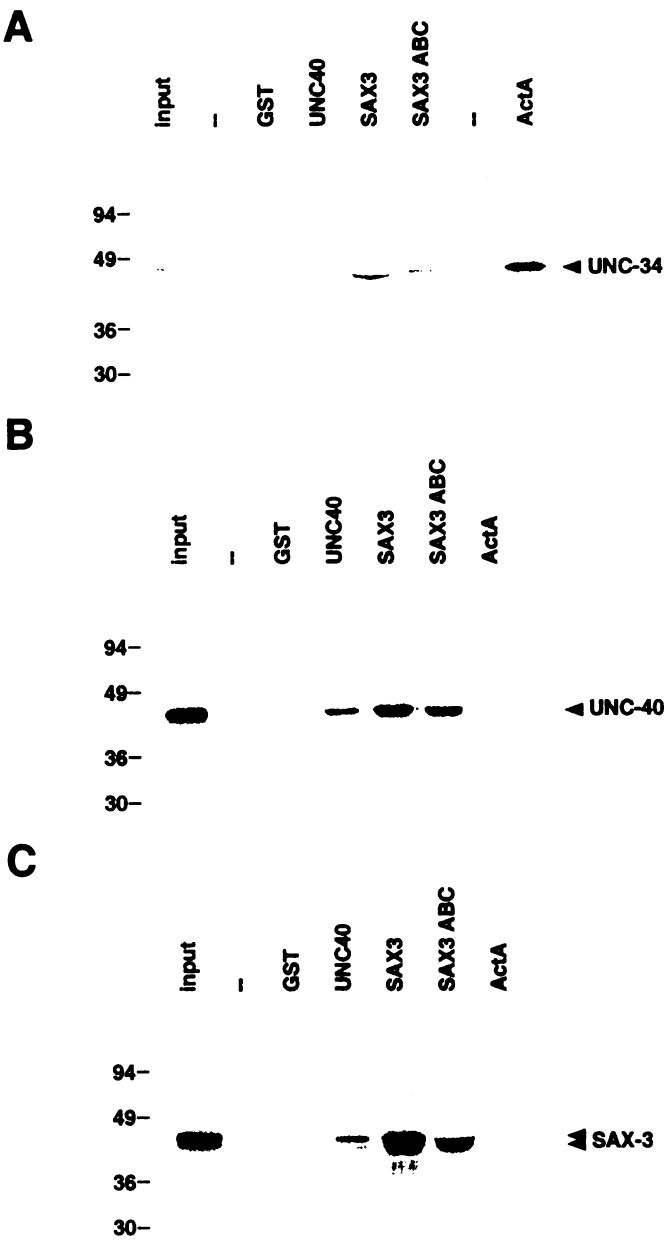
A
input
–
GST
UNC40
SAX3
SAX3 ABC
–
ActA
94–
49–
36–
30–
UNC-34
B
input
–
GST
UNC40
SAX3
SAX3 ABC
ActA
94–
49–
36–
30–
UNC-40
C
input
–
GST
UNC40
SAX3
SAX3 ABC
ActA
94–
49–
36–
30–
SAX-3

3.6 References

Bashaw, G. J., and Goodman, C. S. (1999). Chimeric axon guidance receptors: the cytoplasmic domains of slit and netrin receptors specify attraction versus repulsion. *Cell* **97**, 917-926.

Bashaw, G. J., Kidd, T., Murray, D., Pawson, T., and Goodman, C. S. (2000). Repulsive axon guidance: Abelson and Enabled play opposing roles downstream of the roundabout receptor. *Cell* **101**, 703-715.

Bear, J. E., Loureiro, J. J., Libova, I., Fassler, R., Wehland, J., and Gertler, F. B. (2000). Negative regulation of fibroblast motility by Ena/VASP proteins. *Cell* **101**, 717-728.

Brose, K., Bland, K. S., Wang, K. H., Arnott, D., Henzel, W., Goodman, C. S., Tessier-Lavigne, M., and Kidd, T. (1999). Slit proteins bind Robo receptors and have an evolutionarily conserved role in repulsive axon guidance. *Cell* **96**, 795-806.

Brose, K., and Tessier-Lavigne, M. (2000). Slit proteins: key regulators of axon guidance, axonal branching, and cell migration. *Current Opinion in Neurobiology* **10**, 95-102.

Chakraborty, T., Ebel, F., Domann, E., Niebuhr, K., Gerstel, B., Pistor, S., Temm-Grove, C. J., Jockusch, B. M., Reinhard, M., Walter, U., and Wehland, J. A. (1995). A focal adhesion factor directly linking intracellularly motile *Listeria monocytogenes* and *Listeria ivanovii* to the actin-based cytoskeleton of mammalian cells. *Embo J* **14**, 1314-1321.

Chan, S. S., Zheng, H., Su, M. W., Wilk, R., Killeen, M. T., Hedgecock, E. M., and Culotti, J. G. (1996). UNC-40, a *C. elegans* homolog of DCC (Deleted in Colorectal Cancer), is required in motile cells responding to UNC-6 netrin cues. *Cell* **87**, 187-195.

Colavita, A., and Culotti, J. G. (1998). Suppressors of ectopic UNC-5 growth cone steering identify eight genes involved in axon guidance in *Caenorhabditis elegans. Developmental Biology* **194**, 72-85.

Culotti, J. G., and Merz, D. C. (1998). DCC and netrins. *Curr Opin Cell Biol* **10**, 609-613.

Fazeli, A., Dickinson, S. L., Hermiston, M. L., Tighe, R. V., Steen, R. G., Small, C. G., Stoeckli, E. T., Keino-Masu, K., Masu, M., Rayburn, H., *et al.* (1997). Phenotype of mice lacking functional *Deleted in colorectal cancer* (*Dcc*) gene. *Nature* **386**, 796-804.

Fire, A., Xu, S., Montgomery, M. K., Kostas, S. A., Driver, S. E., and Mello, C. C. (1998). Potent and specific genetic interference by double-stranded RNA in *Caenorhabditis elegans. Nature* **391**, 806-811.

Flanagan, J. G., and Van Vactor, D. (1998). Through the looking glass: axon guidance at the midline choice point. *Cell* **92**, 429-432.

Flanagan, J. G., and Vanderhaeghen, P. (1998). The ephrins and Eph receptors in neural development. *Annu Rev Neurosci* **21**, 309-345.

Forrester, W. C., and Garriga, G. (1997). Genes necessary for *C. elegans* cell and growth cone migrations. *Development* **124**, 1831-1843.

Fritz, J. L., and VanBerkum, M. F. (2000). Calmodulin and *son of sevenless* dependent signaling pathways regulate midline crossing of axons in the *Drosophila* CNS. *Development* **127**, 1991-2000.

Gallo, G., and Letourneau, P. C. (1999). Axon guidance: A balance of signals sets axons on the right track. *Current Biology* **9**, R490-492.

Gertler, F. B., Comer, A. R., Juang, J. L., Ahern, S. M., Clark, M. J., Liebl, E. C., and Hoffmann, F. M. (1995). *enabled*, a dosage-sensitive suppressor of mutations in the *Drosophila* Abl tyrosine kinase, encodes an Abl substrate with SH3 domain-binding properties. *Genes and Development* **9**, 521-533.

Gertler, F. B., Doctor, J. S., and Hoffmann, F. M. (1990). Genetic suppression of mutations in the *Drosophila abl* proto-oncogene homolog. *Science* **248**, 857-860.

Hao, J. C., Yu, T. W., Fujisawa, K., Culotti, J. G., Gengyo-Ando, K., Mitani, S., Moulder, G., Barstead, R., Tessier-Lavigne, M., and Bargmann, C. I. (2001). *C. elegans* Slit Acts in Midline, Dorsal-Ventral, and Anterior-Posterior Guidance via the SAX-3/Robo Receptor. *Neuron* **32**, 25-38.

Hedgecock, E. M., Culotti, J. G., and Hall, D. H. (1990). The *unc-5*, *unc-6*, and *unc-40* genes guide circumferential migrations of pioneer axons and mesodermal cells on the epidermis in *C. elegans*. *Neuron* **4**, 61-85.

Hedgecock, E. M., Culotti, J. G., Hall, D. H., and Stern, B. D. (1987). Genetics of cell and axon migrations in *Caenorhabditis elegans*. *Development* **100**, 365-382.

Hiramoto, M., Hiromi, Y., Giniger, E., and Hotta, Y. (2000). The *Drosophila* Netrin receptor Frazzled guides axons by controlling Netrin distribution. *Nature* **406**, 886-889.

Hong, K., Hinck, L., Nishiyama, M., Poo, M. M., Tessier-Lavigne, M., and Stein, E. (1999). A ligand-gated association between cytoplasmic domains of UNC5 and DCC family receptors converts netrin-induced growth cone attraction to repulsion. *Cell* **97**, 927-941.

Honigberg, L., and Kenyon, C. (2000). Establishment of left/right asymmetry in neuroblast migration by UNC- 40/DCC, UNC-73/Trio and DPY-19 proteins in *C. elegans*. *Development* **127**, 4655-4668.

Kidd, T., Bland, K. S., and Goodman, C. S. (1999). Slit is the midline repellent for the robo receptor in *Drosophila*. *Cell* **96**, 785-794.

Kidd, T., Brose, K., Mitchell, K. J., Fetter, R. D., Tessier-Lavigne, M., Goodman, C. S., and Tear, G. (1998a). Roundabout controls axon crossing of the CNS midline and defines a novel subfamily of evolutionarily conserved guidance receptors. *Cell* **92**, 205-215.

Kidd, T., Russell, C., Goodman, C. S., and Tear, G. (1998b). Dosage-sensitive and complementary functions of *roundabout* and *commissureless* control axon crossing of the CNS midline. *Neuron* **20**, 25-33.

Kim, S., Ren, X. C., Fox, E., and Wadsworth, W. G. (1999). SDQR migrations in *Caenorhabditis elegans* are controlled by multiple guidance cues and changing responses to netrin UNC-6. *Development* **126**, 3881-3890.

Laurent, V., Loisel, T. P., Harbeck, B., Wehman, A., Grobe, L., Jockusch, B. M., Wehland, J., Gertler, F. B., and Carlier, M. F. (1999). Role of proteins of the Ena/VASP family in actin-based motility of *Listeria monocytogenes. J Cell Biol* **144**, 1245-1258.

Lin, M. Z., and Greenberg, M. E. (2000). Orchestral maneuvers in the axon: trio and the control of axon guidance. *Cell* **101**, 239-242.

McIntire, S. L., Garriga, G., White, J., Jacobson, D., and Horvitz, H. R. (1992). Genes necessary for directed axonal elongation or fasciculation in *C. elegans. Neuron* **8**, 307-322.

Merz, D. C., and Culotti, J. G. (2000). Genetic analysis of growth cone migrations in *Caenorhabditis elegans. J Neurobiol* **44**, 281-288.

Nakamura, F., Kalb, R. G., and Strittmatter, S. M. (2000). Molecular basis of semaphorin-mediated axon guidance. *J Neurobiol* **44**, 219-229.

Stein, E., and Tessier-Lavigne, M. (2001). Hierarchical organization of guidance receptors: silencing of netrin attraction by slit through a Robo/DCC receptor complex. *Science* **291**, 1928-1938.

Stein, E., Zou, Y., Poo, M., and Tessier-Lavigne, M. (2001). Binding of DCC by netrin-1 to mediate axon guidance independent of adenosine A2B receptor activation. *Science* **291**, 1976-1982.

Sun, Q., Bahri, S., Schmid, A., Chia, W., and Zinn, K. (2000). Receptor tyrosine phosphatases regulate axon guidance across the midline of the *Drosophila* embryo. *Development* **127**, 801-812.

Tear, G., Seeger, M., and Goodman, C. S. (1993). To cross or not to cross: a genetic analysis of guidance at the midline. *Perspect Dev Neurobiol* **1**, 183-194.

Tessier-Lavigne, M., and Goodman, C. S. (1996). The molecular biology of axon guidance. *Science* **274**, 1123-1133.

Wadsworth, W. G., Bhatt, H., and Hedgecock, E. M. (1996). Neuroglia and pioneer neurons express UNC-6 to provide global and local netrin cues for guiding migrations in *C. elegans*. *Neuron* **16**, 35-46.

White, J. G., Southgate, E., Thomson, J. N., and Brenner, S. (1986). The structure of the nervous system of the nematode *Caenorhabditis elegans*. *Philos Trans R Soc Lond B Biol Sci* **314**, 1-340.

Wills, Z., Bateman, J., Korey, C. A., Comer, A., and Van Vactor, D. (1999). The tyrosine kinase Abl and its substrate enabled collaborate with the receptor phosphatase Dlar to control motor axon guidance. *Neuron* **22**, 301-312.

Zallen, J. A., Kirch, S. A., and Bargmann, C. I. (1999). Genes required for axon pathfinding and extension in the *C. elegans* nerve ring. *Development* **126**, 3679-3692.

Zallen, J. A., Yi, B. A., and Bargmann, C. I. (1998). The conserved immunoglobulin superfamily member SAX-3/Robo directs multiple aspects of axon guidance in *C. elegans*. *Cell* **92**, 217-227.

Zou, Y., Stoeckli, E., Chen, H., and Tessier-Lavigne, M. (2000). Squeezing axons out of the gray matter: a role for slit and semaphorin proteins from midline and ventral spinal cord. *Cell* **102**, 363-375.

Chapter 4

Untangling attractive and repulsive pathways in the guidance of the AVM axon

4.1 Summary

The secreted molecules Netrin and Slit influence a wide variety of axonal migrations. The signaling pathways utilized by these guidance cues, however, remain poorly understood. Few of the signaling components that act downstream of Netrin or Slit have been identified; furthermore, it is unknown whether their signaling pathways share components in common, or whether they are relatively insulated. In this chapter, I describe the genetic analysis of guidance of the AVM axon, whose migration towards the ventral midline depends upon the parallel actions of attractive Netrin (UNC-6) and repulsive Slit (SLT-1). Double mutant analyses with twenty candidate axon guidance genes in combination with *slt-1* or *unc-6* provide evidence for considerable specificity in axon guidance signaling pathways in the AVM growth cone. Mutations in eleven genes, *ced-2, ced-5, ced-10, unc-115, ephexin, unc-33, unc-53, max-1, mig-17, unc-129,* and *unc-130,* appear to disrupt Netrin- but not Slit-dependent guidance. In contrast, mutations in *unc-34* have strong effects on Slit-dependent AVM guidance. Four genes, *abl-1, mig-2, unc-73,* and *unc-71*, appear to be required for both Netrin attraction and Slit repulsion of AVM, while two genes, *vab-1* and *unc-14*, are either not involved in or redundant for AVM guidance. These results reveal an underlying organization of growth cone signaling pathways, and provide a foundation for the comprehensive analysis of genetic pathways underlying Slit and Netrin guidance.

4.2 Introduction

The UNC-6/Netrin and Slit families of extracellular molecules play important instructive roles in axon migrations, guiding axon growth along the dorsal/ventral axis of nematodes, flies and vertebrates (Brose *et al.*, 1999; Hao *et al.*, 2001; Hedgecock *et al.*, 1990; Kidd *et al.*, 1999; Mitchell *et al.*, 1996; Serafini *et al.*, 1996; Serafini *et al.*, 1994). UNC-6/Netrin signals growth cone attraction through the receptor UNC-40/DCC (Culotti and Merz, 1998), while Slit repels growth cones through the SAX-3/Robo receptor (Brose *et al.*, 1999; Hao *et al.*, 2001; Kidd *et al.*, 1999). The cytoplasmic domains of UNC-40/DCC and SAX-3/Robo receptors are sufficient to specify attraction or repulsion, respectively, when fused to heterologous ligand binding domains (Bashaw and Goodman, 1999; Stein and Tessier-Lavigne, 2001), indicating that attraction and repulsion are largely specified by cytoplasmic mechanisms within the growing axon. Identifying components of the intracellular signaling pathways that mediate attraction and repulsion remains an important goal for understanding of axon guidance.

Guidance signaling to the growth cone must ultimately be translated into changes in the cytoskeleton. Genetic, biochemical, and molecular approaches have succeeded in identifying a large number of molecules that are likely to play key roles in cytoskeletal signaling and growth cone motility. For example, studies of cytoskeletal regulation in Swiss 3T3 cells showed that the Rho, Rac, and Cdc42 GTPases coordinate the formation of actin stress fibers, lamellipodia and filopodia respectively (Dickson, 2001; Hall and Nobes, 2000; Nobes and Hall, 1995). Genetic screens in *C. elegans* and *Drosophila* have led to the cloning of candidate cytoskeletal regulatory proteins, such as the UNC-73/Trio, a guanine nucleotide exchange factor that regulates Rac GTPase activity (Newsome *et al.*, 2000; Steven *et al.*, 1998). Meanwhile, biochemical studies have pointed to roles of molecules such as the

Ena/VASP family of proteins, the Arp2/3 complex, and WASP in regulating actin assembly (Chakraborty *et al.*, 1995; May *et al.*, 1999; Rohatgi *et al.*, 1999).

The cytoskeletal regulators interact with each other and with other cytoskeletal players. Cdc42 may activate Rac (Nobes and Hall, 1995). *Drosophila Trio* interacts genetically with the SH2-SH3 adapter protein *Dock* (Garrity *et al.*, 1996; Newsome *et al.*, 2000), which itself interacts genetically and physically with the kinases *PAK* and *Misshapen* (Hing *et al.*, 1999; Ruan *et al.*, 1999). Grb4, a vertebrate relative of Dock, binds to a host of other cytoskeletal components (Cowan and Henkemeyer, 2001). Enabled binds to and is a substrate for phosphorylation by the Abl tyrosine kinase (Gertler *et al.*, 1995). A WASP-Arp2/3 complex is required for actin polymerization stimulated by Cdc42 or phosphatidylinositol (4,5) bisphosphate (Rohatgi *et al.*, 1999). WASP also binds Nck, another vertebrate relative of Dock (Rivero-Lezcano *et al.*, 1995).

An underlying functional logic to the organization of these cytoskeletal pathways has yet to emerge. In particular, it is unclear how they are functionally coupled to attractive or repulsive guidance cues. At one extreme, attractive and repulsive pathways may be inseparable, involving the orchestrated activity of many intertwined cytoskeletal pathways. At the opposite extreme, guidance cues may activate well-insulated signaling cassettes, recruiting components that are relatively specific to one cue or another.

In these studies we analyze the growth of the AVM axon, whose ventral growth is controlled by two partially redundant Netrin and Slit guidance pathways. Through double mutant analysis, we demonstrate specific roles for a wide variety of axon guidance genes in UNC-6/Netrin or Slit-mediated guidance. These results demonstrate that components of UNC-6 attractive and Slit-repulsive pathways are genetically separable, and provide a foundation for the comprehensive identification and analysis of molecules mediating Slit and Netrin guidance.

4.3 Results

Axon guidance of the AVM neuron

AVM is a mechanosensory neuron that arises from the QR lineage (QR.paa). It is born during the first larval stage, approximately 1200 minutes after first cleavage. Its axon grows towards the ventral midline, insinuating itself between hypodermis and ventral body wall muscle (Figure 4-1) (White *et al.*, 1986). AVM has several advantages for study. First, its cell body and axon are relatively well separated from those of other neurons, and easily identifiable with well-defined transgenic markers. Second, the timing of its migration is relatively well isolated from that of other neurons, allowing more selective analysis of its outgrowth in temperature-sensitive backgrounds. Finally, its axon does not fasciculate with other axons along its ventral trajectory, and is therefore is not likely to depend upon other axons for its guidance. The axon guidance receptors SAX-3 and UNC-40 act cell-autonomously in AVM to mediate ventral axon guidance (Chan *et al.*, 1996; Zallen *et al.*, 1998), consistent with AVM acting as a pioneer axon.

Proper ventral guidance of the AVM axon requires repulsion from SLT-1, which is expressed in dorsal muscles (Hao *et al.*, 2001), and attraction towards UNC-6/Netrin (Hedgecock *et al.*, 1990), which is expressed in the ventral nerve cord (Wadsworth *et al.*, 1996). Slit repulsion and Netrin attraction are partially redundant for ventral AVM axon growth: 34% (n=238) and 40% (n=275) of AVM axons fail to migrate ventrally in the predicted null mutants *slt-1(eh15)* and *unc-6(ev400)*. Over 90% of AVM axons fail to migrate ventrally in *unc-6(ev400) slt-1(eh15)* double mutants, suggesting a complete loss of dorsal-ventral guidance information.

A candidate-based screen for components of Netrin- and Slit-dependent AVM guidance

To identify additional components of Slit and Netrin signaling pathways, we utilized a candidate-based approach, taking advantage of the partial redundancy of Slit and Netrin pathways in AVM guidance. We analyzed ventral guidance defects of candidates alone and in combination with either *slt-1(eh15)* or *unc-6(ev400)*. Mutations that failed to enhance defects in either *slt-1* or *unc-6* backgrounds were classified as dispensable or redundant for AVM axon guidance. Mutations that enhanced defects of both *slt-1* and *unc-6* were classified as belonging to either both instructive Slit and Netrin pathways or a third, possibly permissive pathway. Mutations that selectively enhanced *slt-1* but not *unc-6*, were classified as belonging primarily to the Netrin pathway, while mutations that selectively enhanced *unc-6* but not *slt-1* were classified as belonging primarily to the Slit pathway. This general strategy is summarized in Figure 4-2.

The genes we chose for analysis are listed in Table 4-1. We primarily focused on genes known to be required for axon guidance in *C. elegans* and/or other organisms, with a particular emphasis on intracellular molecules with known or predicted roles in cytoskeletal regulation. When available, we utilized existing strong loss-of-function alleles. The resulting list of candidates (Table 4-1) includes a wide variety of molecules, including tyrosine kinases, cell engulfment genes, Racs and Rac GEFs, other cytoskeletal genes, genes implicated in CAN axon outgrowth, and genes required for motor axon guidance. Absent from this list were a number of candidate guidance factors that have embryonic or early larval lethal phenotypes, precluding analysis of AVM axon guidance (data not shown).

A summary of the mutant strains used for this study is shown in Table 4-2. A summary of the double mutants constructed and analyzed for this study is shown in Table 4-3. An overview of the results obtained is provided in Figure 4-10, while specific results for

each category of candidates are presented in Figures 4-3 through 4-9 and are described in more detail below.

unc-34 and the _abl-1_ tyrosine kinase may play distinct roles in AVM guidance

Mutations in the *C. elegans* Enabled homolog *unc-34* cause weakly penetrant axon guidance defects in AVM (Figure 4-3, Chapter 3). These defects are greatly enhanced by mutations in *unc-6*, but not by *slt-1*, demonstrating that *unc-34* is required for Slit but not Netrin guidance. In *Drosophila*, *enabled* was originally identified as a suppressor of lethality caused by mutations in the *Abl* tyrosine kinase (Gertler *et al.*, 1995), and is a substrate for phosphorylation by Abl (Ahern-Djamali *et al.*, 1998; Gertler *et al.*, 1995). In flies, *abl* mutants have mild axon guidance defects on their own (Wills *et al.*, 1999b). *abl* mutants also display dosage-sensitive genetic interactions with *ena*, *robo*, and *slit* in a manner which suggests that *abl-1* may downregulate signaling downstream of Slit (Bashaw *et al.*, 2000). *abl-1* also has dosage-sensitive and complementary genetic interactions with *ena* and the receptor tyrosine phosphatase *Dlar* (Wills *et al.*, 1999a).

To investigate whether *abl* plays a role in Netrin or Slit pathways, deletion mutants of the *C. elegans abl-1* were obtained from the *C. elegans* Knockout Consortium and analyzed for AVM guidance defects, alone and in combination with *unc-6* or *slt-1* (Figure 4-3). *abl-1(ok171)* mutants exhibited very infrequent AVM guidance defects on their own (1%, n=194). *abl-1 slt-1* double mutants appeared slightly enhanced (42%, n= 121) relative to *slt-1* mutants (34%, n=294), although this result did not reach statistical significance (p=0.15). *unc-6 abl-1* double mutants were similarly only mildly worse (51%, n=83) than *unc-6* alone (40%, n=275) (p=0.113). *abl-1* mutations also enhanced AVM guidance defects of a weak loss-of-function allele of *sax-3(ky200)*: 20% of animals (n=88) exhibited guidance defects in the *sax-3(ky200) abl-1* double, compared to 11% (n=397) in *sax-3(ky200)* (p<0.03). These

results are consistent with models in which *abl-1* makes a small contribution to both Netrin and Slit AVM axon guidance, or in which *abl-1* acts in an unidentified parallel pathway that may be permissive for axon guidance.

The cell engulfment genes *ced-2*, *ced-5* and *ced-10* are required for Netrin but not Slit pathways for AVM axon guidance

Cells undergoing programmed cell death in *C. elegans* are rapidly engulfed by surrounding cells. Engulfment of apoptotic cells is controlled by two groups of cell engulfment genes: group A, which includes the *ced-1*, *ced-6* and *ced-7* genes, and group B, which includes *ced-2*, *ced-5*, and *ced-10* (Ellis *et al.*, 1991). *ced-1*, *ced-6*, and *ced-7* encode a cell surface scavenger receptor, an adapter molecule and an ABC transporter respectively and are thought to be involved in recognition of cell corpses (Liu and Hengartner, 1998; Wu and Horvitz, 1998a; Zhou *et al.*, 2001). *ced-2*, *ced-5*, and *ced-10* encode CrkII, DOCK180, and Rac respectively (Reddien and Horvitz, 2000; Wu and Horvitz, 1998b). *ced-2*, *ced-5*, and *ced-10* are thought to direct cytoskeletal rearrangements in the engulfing cell that allow the extension of cell surfaces around dying cells. *ced-2*, *ced-5*, and *ced-10* also have defects in the migration of distal tip cells (DTCs) (Gumienny *et al.*, 2001; Reddien and Horvitz, 2000; Wu and Horvitz, 1998b).

To ask whether cell engulfment genes contribute to AVM axon guidance, *ced-2*, *ced-5*, *ced-5*, and *ced-10* were analyzed for AVM axon guidance defects alone and in combination with *slt-1* and *unc-6* (Figure 4-4). Guidance defects were not detected in *ced-2* or *ced-5* mutants alone (n=89 and 190, respectively). In *ced-10*, rare animals exhibited AVM ventral guidance defects (1%, n=83). *ced-2*, *ced-5*, and *ced-10* all failed to enhance defects in an *unc-6* background (Figure 4-3). In double mutant combination with *slt-1*, *ced-2* (48%, n=81), *ced-5* (50%, n=78), and *ced-10* (55%, n=91) all enhanced defects compared to *slt-1* alone

(34%) (p=0.02, p=0.017, p<0.001). These results suggest that the cell engulfment genes *ced-2*, *ced-5*, and *ced-10* may work together in AVM axon guidance as well, where they are required specifically for UNC-6/Netrin guidance.

Two Rac genes, *ced-10* and *mig-2*, have different contributions to AVM axon guidance

Rho family GTPases are thought to regulate growth cone morphology (Dickson, 2001), but their functions *in vivo* are poorly defined. The *C. elegans* genome encodes three Rac genes, *ced-10*, *rac-2*, and a divergent Rac family member, *mig-2*. While *ced-10* mutants exhibit defects in apoptotic cell engulfment and DTC migration, null *mig-2* mutations cause cell migration defects of Q cells, but no axon guidance defects (Zipkin *et al.*, 1997). Gain-of-function mutations in *mig-2* cause axon misguidance phenotypes, suggesting a possible role in axon outgrowth as well (Zipkin *et al.*, 1997).

To study the role of different Rac genes in axon guidance, we compared AVM guidance phenotypes caused by mutations in *ced-10* and *mig-2*. *ced-10* is required for Netrin-dependent guidance of AVM (Figure 4-4). The null mutation *mig-2(mu28)* was examined for effects on AVM guidance (Figure 4-5). Consistent with previous analyses of other neurons (Zipkin *et al.*, 1997), guidance errors were never observed in *mig-2(mu28)* mutants (n=27, and data not shown). However, *mig-2(mu28)* enhanced defects of *slt-1* (52%, n=91, vs. 34%, p=0.005). *mig-2(mu28)* also strongly enhanced defects of *unc-6* (72%, n=25, vs. 40%, p=0.004). These results provide evidence of axon guidance defects caused by loss of *mig-2* function, and put *mig-2* in both Slit and Netrin pathways for AVM guidance.

Rac-associated genes: Roles of the guanine nucleotide exchange factors *unc-73/Trio* and *ephexin*, and the actin-associated gene *unc-115*

Rho family GTPases function as binary switches, cycling between an inactive GDP-bound state and an active GTP-bound state. Their activity is regulated by the activities of guanine nucleotide exchange factors (GEFs) of the Dbl family, which promote conversion to the active GTP-bound state, and GTPase activating proteins (GAPs), which promote conversion to the inactive GDP-bound state. *unc-73* is a *C. elegans* homolog of Trio that contains two GEF domains and is required for a number of cell and axon migrations (Steven *et al.*, 1998). *unc-73(rh40)* encodes an inactivating point mutation in its first GEF domain, DH-1, which has been shown to have GEF activity for Rac GTPases. *ok253* is a deletion allele of K07D4.7, obtained from the *C. elegans* Knockout Consortium. K07D4.7 encodes a worm relative of ephexin, a vertebrate GEF implicated in Eph-A receptor signaling (Shamah *et al.*, 2001). *ok253* deletes 2.4 kB of a 3.0 kB genomic region spanning the predicted GEF, PH and SH3 domains of worm ephexin.

Lastly, the *unc-115* gene encodes cytoskeletal component containing a villin headpiece and LIM domains (Lundquist *et al.*, 1998). *unc-115* demonstrates genetic interactions with *ced-10* and *mig-2*, and may be an effector of Rac function (Erik Lundquist and Cori Bargmann, personal communication).

unc-73(rh40) mutants displayed mildly penetrant AVM guidance defects on their own (14%, n=79) (Figure 4-6). *unc-73(rh40)* mutants also occasionally had termination defects, multiple axons and extra axon branching (data not shown). *unc-73(rh40)* enhances guidance defects of both *slt-1* and *unc-6* mutants (70%, n=88, $p<0.001$ and 74%, n=31, $p<0.001$ in the double mutants, respectively). In contrast, no guidance defects were observed in *ephexin(ok253)* mutants alone (n=79) (Figure 4-6). *ephexin; slt-1* double mutants were strongly enhanced (61%, n=49) compared to *slt-1* (34%) ($p<0.001$). *ephexin;*

unc-6 double mutants were slightly more defective (47%, n=155) than *unc-6* (40%, n=275) but this difference was not statistically significant (p=0.18). Mutations in the Eph receptor *vab-1* do not disrupt AVM axon guidance, either alone (0%, n=80) or in combination with *slt-1* or *unc-6*.(n=120 or 55, respectively) backgrounds. These results suggest that the Trio-related GEF *unc-73* acts in both Netrin and Slit pathways or a parallel pathway, while GEF activity of *ephexin* is required relatively specifically for the Netrin pathway.

Loss of *unc-115* function alone results in rare AVM axon guidance defects (1%, n=40) (Figure 4-6). *unc-115* does not enhance defects of *unc-6* (38% in the double vs. 40%), but *unc-115 slt-1* double mutants (49%, n=71) are more severe than *slt-1* (34%) (p=0.028). *unc-115* is thus required for Netrin- and not for Slit-dependent guidance of AVM.

The axonal outgrowth genes unc-14, unc-33, unc-51, and unc-53

The genes *unc-14, unc-33, unc-51* and *unc-53* act to control cell migration of the sex myoblasts (SMs), which migrate from the ventral midposterior body region of the animal to the developing gonad in the center of the animal (Branda and Stern, 2000). These genes are also required for the guidance of growth cones along the ventral nerve cord (Wightman and Garriga, personal communication). *unc-14* encodes a protein without obvious structural motifs that interacts with UNC-51, a serine/threonine kinase (Ogura *et al.*, 1997; Ogura *et al.*, 1994). *unc-51* also has effects on synaptic vesicle clustering (Crump *et al.*, 2001). *unc-33* encodes a protein related to collapsin response mediator protein CRMP-62 (Goshima *et al.*, 1995; Li *et al.*, 1992). *unc-53* has been reported to encode a F-actin- and nucleotide-binding molecule with effects on neurite outgrowth *in vivo* and *in vitro* (Thierry Bogaert, personal communication).

unc-14 and *unc-51* display branching and termination defects of the AVM axon, and as well as guidance defects (Figure 4-7). In general, defects were more penetrant in *unc-51* than in *unc-14*. *unc-14* did not enhance axon guidance defects in either *slt-1* or *unc-6* backgrounds (21%, n=52, and 35%, n=62, respectively). *unc-51; slt-1* guidance defects were not significantly enhanced (43%, n=35, p=0.41) although this analysis was complicated by the severity of branching, extra axon and termination defects in *unc-51* mutants (data not shown) as well as low sample size. Guidance defects in the *unc-51; unc-6* double were not analyzed for this study.

unc-33 mutations cause frequent early termination of the AVM axon before it reaches the nerve ring (data not shown), as well as lower penetrance guidance defects (6%, n=53) (Figure 4-7). *unc-33* enhances *slt-1* (48%, n=91, p=0.014) but not *unc-6* (39%, n=80), indicating that it is required for Netrin- but not Slit-dependent AVM guidance.

unc-53 mutations result in a highly penetrant AVM termination defect in the nerve ring (data not shown), but no ventral guidance defects were observed (n=38) (Figure 4-7). *unc-53* significantly enhanced *slt-1* (54%, n=61, p=0.006) guidance defects. Interestingly, *unc-53* did not enhance *unc-6* guidance defects but rather appeared to suppress them (15%, n=54, p<0.001). These results suggest that *unc-53* may be a component of Netrin signaling that inhibits the Slit guidance pathway.

The ADAM family metalloproteases *unc-71* and *mig-17* may have separable roles in Netrin and Slit pathways

Metalloprotease inhibitors potentiate the activity of Netrin-stimulated neurite outgrowth *in vitro* (Galko and Tessier-Lavigne, 2000). The ADAM family metalloprotease Kuzbanian has also been shown to regulate the cleavage of the axonal repellents (Hattori *et al.*, 2000), and *kuz* mutants in *Drosophila* exhibit axon defects (Fambrough *et al.*, 1996). The *C. elegans*

genome encodes a number of ADAM metalloproteases, including *adm-1/unc-71* (Yishi Jin, personal communication) and *mig-17* (Nishiwaki *et al.*, 2000).

To ask whether ADAM family metalloproteases may play a role in Netrin and/or Slit signaling, we analyzed AVM in *unc-71* and *mig-17* mutants (Figure 4-8). *unc-71* mutations had rare guidance defects on their own (1%, n=91), but significantly enhanced *slt-1* (47%, n=91, p=0.037) and *unc-6* (64%, n=51, p=0.002). Guidance defects were not observed in *mig-17* (n=17), nor did *mig-17* enhance *unc-6* (39%, n=53). *mig-17* slightly enhanced *slt-1* (43%, n=37), although due to the low sample size, it was not clear whether this enhancement was significant (p=0.365). Nonetheless, these results demonstrate a role for *unc-71* in AVM guidance that is not specific to either Netrin or Slit signaling, and suggest a possible role for *mig-17* in Netrin-mediated guidance.

Motor axon guidance genes: *max-1, unc-129* and *unc-130* affect Netrin-dependent ventral guidance of AVM

Finally, misrouting of motor axons is observed in the mutants *unc-69* (Michael Hentgartner, personal communication), *max-1* (Hwai-Jong Cheng, personal communication), *unc-129* (Colavita *et al.*, 1998) and *unc-130* (Nash *et al.*, 2000). *unc-69* is required for axonal guidance, outgrowth, and fasciculation of many neurons, and encodes a novel 108 amino acid protein with a predicted coil-coil motif (Michael Hentgartner, personal communication). *max-1* encodes a novel protein with PH, MyTH4, and FERM domains (Hwai-Jong Cheng, personal communication). *unc-129* was originally identified as a suppressor of ectopic UNC-5-mediated repulsion (Colavita and Culotti, 1998), and encodes a TGF-beta that is expressed in specifically in dorsal body wall muscle (Colavita *et al.*, 1998). *unc-130* encodes a forkhead transcription factor required to maintain graded expression of *unc-129* along the dorsal-ventral axis (Nash *et al.*, 2000).

unc-69 mutants display occasional AVM guidance defects (2%, n=50). Double mutants of *unc-69* with *slt-1* or *unc-6* appeared slightly more severe than either single mutant alone (42%, n=57, and 47%, n=43, respectively) although these results did not reach statistical significance (p=0.323 and 0.522, respectively).

max-1 mutants demonstrate rare AVM axon guidance defects (2%, n=46). Strikingly, *max-1 slt-1* double mutants exhibited nearly complete failure of AVM ventral guidance (97% in the double mutant, n=59, p<0.001). *max-1* mutants enhanced *unc-6* to a lesser degree (63%, n=35, p=0.017). These results implicate *max-1* in AVM guidance, with a strong contribution to Slit signaling and a relatively weaker contribution to the Netrin pathway.

As previously reported, *unc-129* mutants did not exhibit AVM guidance defects on their own (n=85) (Colavita *et al.*, 1998), nor was *unc-129* required for guidance in the absence of *unc-6* (35%, n=91). However in a *slt-1* background, loss of *unc-129* function had dramatic effects on AVM guidance, with guidance defects (80%, n=100) more than twice that of *slt-1* alone (34%) (p<0.001). Consistent with previous reports, we also observed that *unc-130* possesses AVM guidance defects alone (11%, n=27). We find that *unc-130* greatly enhances defects of *slt-1* (87% in the double mutant, n=70, p<0.001) but has more equivocal effects in an *unc-6* background (50%, n=32, p=0.369). While we cannot at this time rule out a possible effect of *unc-130* on Slit guidance, these results indicate an important role for *unc-129* in Netrin-dependent guidance of AVM.

4.4 Discussion

The combined action of attractive and repulsive guidance cues is thought to specify the proper trajectory of axons in the developing nervous system (Tessier-Lavigne and Goodman,

1996). For example, multiple Netrin, Semaphorin, and Fasciclin II cues act together in a dosage-sensitive manner to regulate proper selection of muscle targets by motor neurons in *Drosophila* (Winberg *et al.*, 1998). However, previous studies of guidance signaling have focused upon guidance events in which only a single cue is involved (Bashaw *et al.*, 2000; Shamah *et al.*, 2001; Wahl *et al.*, 2000), or in which the instructive cue is unknown (Wills *et al.*, 1999a).

In *C. elegans*, ventral guidance of the AVM neuron relies upon the combined action of attractive UNC-6/Netrin and repulsive Slit guidance cues. AVM guidance therefore presents an opportunity to evaluate the specific contributions of genes to either Netrin or Slit guidance. The experiments presented here take advantage of this situation to probe the functions of twenty candidate axon guidance genes, and classify them into Netrin or Slit pathways. The data are summarized in Figure 4-10. General themes and major conclusions are discussed below.

Redundancy

Almost all of the candidate genes tested have subtle or very minor effects on AVM axon guidance when mutated alone. For example, misguided AVM axons were never detected in *vab-1* or *ced-5* mutants, and only rarely in *max-1*. In some cases (e.g., *vab-1*), the absence of defects may indicate that these genes do not contribute to AVM axon guidance. However, important roles for many of these genes were revealed in backgrounds sensitized by loss of *slt-1* or *unc-6* function. For example, in animals lacking *slt-1*, a requirement for *ced-5* was evident (50% in the double mutant vs. 34% for *slt-1* alone), as well as an even stronger requirement for *max-1* (97% in the double mutant). These results demonstrate the existence of considerable redundancy in axon guidance signaling. They also highlight the importance of using sensitized backgrounds to penetrate this redundancy.

Specificity vs. convergence in Netrin and Slit signaling pathways

Experiments using chimeric UNC-40/DCC and SAX-3/Robo show that growth cone attraction and repulsion by Netrin and Slit are initiated by distinct mechanisms involving their receptors' cytoplasmic domains (Bashaw and Goodman, 1999; Stein and Tessier-Lavigne, 2001). Analysis of the twenty genes described here indicate that Netrin and Slit signaling pathways can be separated further downstream as well. Specificity is seen for molecules that predicted to act at several different levels in the signaling cascade, from an adapter molecule (CED-2/CrkII) to a GEF (ephexin) to a Rac family member (CED-10) to a potential actin-binding Rac effector (UNC-115). While these examples indicate that portions of Netrin and Slit signaling modules may be relatively well insulated, they do not exclude the possibility of convergence in Netrin and Slit signaling. Indeed, this screen has identified components (e.g., UNC-73 and MIG-2) that are important for the function of both pathways.

Parallels between cell engulfment and axon guidance

The genes *ced-2/CrkII*, *ced-5/DOCK180*, and *ced-10/Rac*, act together to control the engulfment of dying cells (Reddien and Horvitz, 2000; Wu and Horvitz, 1998b). *ced-2*, *ced-5* and *ced-10* appear to work together in a Netrin pathway for AVM guidance. CED-2/CrkII binds to CED-5/DOCK180 (Reddien and Horvitz, 2000). Recently, the cloning of another member of the *ced-2/5/10* pathway, *ced-12* has been reported (Gumienny *et al.*, 2001). The *ced-12* gene product CED-12/ELMO-1 binds to CED-2/CED-5 in a ternary complex, and promotes phagocytosis and cell shape changes in mammalian cells (Gumienny *et al.*, 2001). It will be of interest to determine if *ced-12* acts in Netrin signaling as well.

The demonstration of underlying functional parallels between growth cone guidance and cell engulfment raises the possibility that other cell engulfment genes may act in axon guidance also. While *ced-1, ced-6,* and *ced-7* are in general thought to be involved in relaying a signal from the dying cell to the engulfing cell (Liu and Hengartner, 1998; Wu and Horvitz, 1998a; Zhou *et al.*, 2001), it is possible that they too contribute to growth cone signaling. Conversely, genes previously thought to be specific to growth cone guidance may have roles in cell engulfment. It is tempting to speculate that there may be an active guidance component to cell phagocytosis as well.

Functional specialization of Racs

There are three Rac genes in *C. elegans*, CED-10/Rac-1, Rac-2 and MIG-2. In previous reports, loss-of-function mutations in *ced-10* or *mig-2* were shown primarily to affect cell migrations (Reddien and Horvitz, 2000; Zipkin *et al.*, 1997). Activated *mig-2* alleles can disrupt axon guidance, leading to speculation that *mig-2* acts redundantly with other molecules in axon guidance (Zipkin *et al.*, 1997). Consistent with this hypothesis, *ced-10; mig-2* double mutants exhibit axon misguidance phenotypes (Erik Lundquist and Cori Bargmann, personal communication). Here, loss of *mig-2* function is shown to disrupt axon guidance in the presence of wild-type *ced-10*, demonstrating that *mig-2* and *ced-10* are not fully redundant.

The duplication of genes in gene families is thought not only to generate redundancy but to allow individual members to take on specialized roles. *ced-10* may act downstream of an activated UNC-40 transgene (Zemer Gitai, personal communication), and the results presented here provide strong evidence for a role for *ced-10* in axon guidance mediated by Netrin, but not by Slit. In contrast to *ced-10*, *mig-2* has a large contribution to Slit guidance. Thus, *ced-10* and *mig-2* have distinct roles in Netrin and Slit guidance. To our

knowledge, these are the first results linking different Racs to specific directional guidance systems.

Specificity of GEFs in axon guidance pathways

Guanine nucleotide exchange factors have been proposed to sit near the top of the cytoskeletal signaling cascade, linking guidance receptors to downstream Rac, Rho, and Cdc42 effectors and specific cytoskeletal responses (Mueller, 1999). Recently, a role for the GEF ephexin in repulsion downstream of EphA receptors has been described (Shamah *et al.*, 2001), Ephexin has stimulatory activity for RhoA, Rac1, and Cdc42. Activation of EphA receptors is thought to enhance the ability of ephexin to activate RhoA, and inhibit the ability of ephexin to activate Rac1 and Cdc42, thus resulting in a shift in the balance of rho family GTPase activity (Shamah *et al.*, 2001).

Little is known about the *in vivo* functions of GEFs downstream of specific guidance cues. The *C. elegans* genome includes at least eleven proteins with predicted GEF domains (data not shown). Our results point to functionally distinct roles for two of them, UNC-73/Trio and a *C. elegans* homolog of ephexin, in guidance downstream of Netrin and Slit. UNC-73/Trio has multiple roles in cell migration, axon outgrowth and axon guidance (Steven *et al.*, 1998). Our analysis of *unc-73(rh40)* mutation, which specifically disrupts the DH-1 GEF domain of *unc-73* but leaves the remaining protein intact, indicates that DH-1 GEF activity is likely to be required for multiple pathways for AVM axon guidance as well. Alternatively, this domain may supply a critical function that is required for growth cone guidance to occur at all.

In contrast, mutations in a *C. elegans* homolog of ephexin specifically disrupt Netrin but not Slit guidance. Mutations in the *C. elegans* Eph receptor VAB-1 do not affect AVM ventral guidance by Netrin or Slit. These results establish a role for ephexin in axon

guidance *in vivo*. While vertebrate ephexin is implicated in a repulsive Eph receptor pathway, these results indicate that *C. elegans* ephexin contributes to Eph receptor-independent attractive signaling.

ADAM family metalloproteases and axon guidance

ADAM family metalloproteases, also known as metalloprotease disintegrins, are cell surface molecules with domains implicating them in cell-cell and cell-matrix adhesion as well as proteolysis (Black and White, 1998). ADAM metalloproteases play roles in a wide variety of cell signaling events, including lateral inhibition (Pan and Rubin, 1997; Wen *et al.*, 1997), ectodomain shedding (Peschon *et al.*, 1998), and termination of signaling by repellent ligands (Hattori *et al.*, 2000). Metalloproteases may also modulate cell surface levels of the netrin receptor DCC, and inhibitors of metalloproteases potentiate Netrin-induced neurite outgrowth (Galko and Tessier-Lavigne, 2000).

We analyzed the potential roles of two ADAM family metalloproteases in *C. elegans, unc-71/adm-1* and *mig-17*, in Netrin and Slit guidance. Mutations in *unc-71* significantly disrupted AVM axon guidance in both *unc-6* and *slt-1* backgrounds, suggesting roles in both pathways or a third, parallel pathway. The UNC-71/ADM-1 protein is predicted to encode a nonfunctional protease domain (Chieh Chang, personal communication). UNC-71's role in AVM guidance may therefore be to promote growth cone adhesion. On the other hand, the ADAM metalloprotease family member *mig-17* may have a specific role in Netrin guidance, since it slightly enhances *slt-1* but not *unc-6* defects. Of note, previous reports indicate that *mig-17* possesses migration defects in distal tip cells, a defect also present in *unc-6*. Furthermore, *mig-17* enhances DTC migration defects of a weak allele of *unc-6* (Nishiwaki *et al.*, 2000).

Recently, the ADAM family metalloprotease Kuzbanian was shown to affect midline guidance in *Drosophila* by Slit (Schimmelpfeng *et al.*, 2001). It will be interesting to see whether the *C. elegans* SUP-17/Kuzbanian plays a similar role in SAX-3/Slit signaling. Experiments to address this possibility are underway.

Novel functions for *max-1*

max-1 is a novel gene identified in screens for mutants partially defective in motor axon projections but with wild-type locomotory movement. MAX-1 encodes a novel conserved protein with PH, MyTH4, and FERM domains. *max-1* is required for normal dorsal guidance of motor axons, which involves repulsion from UNC-6 via its receptors UNC-40 and UNC-5. Genetic and molecular data suggest models in which MAX-1 primarily through UNC-5 (Hwai-Jong Cheng, personal communication).

Analysis of the AVM axon in *max-1* mutants demonstrates that *max-1* plays vital roles in AVM ventral guidance as well. In AVM, *max-1* is required for both Slit- and Netrin-dependent guidance, although the severity of defects observed in *max-1; slt-1* double mutants points towards an especially large contribution to Netrin signaling. Interestingly, a *max-1* promoter fusion was previously reported to drive GFP expression in AVM (Hwai-Jong Cheng, personal communication). It is possible that MAX-1 acts with UNC-40 and SAX-3 in AVM guidance, but with UNC-5 in motorneurons. Alternatively, motor axon guidance defects may involve MAX-1 interactions with UNC-40 as well as UNC-5.

The UNC-129 TGF-beta and AVM axon guidance

The *unc-129* gene was identified in a screen for suppressors of axon defects caused by misexpression of the repulsive Netrin receptor UNC-5. In this screen, ectopic expression of UNC-5 in the AVM, ALM, PVM and PLM neurons resulted in the dorsal redirection of

their axons (Colavita and Culotti, 1998). *unc-129* mutants also have defects in dorsally-directed motor axon growth, leading to the hypothesis that UNC-129, a secreted TGF-beta molecule, is an attractive cue for motor axons (Colavita *et al.*, 1998).

The observation that *unc-129* is required for repulsion of AVM initially suggested that it may be involved in Slit repulsion as well. Instead, our results argue that *unc-129* is specifically required for AVM attraction towards Netrin. These results do not fit models in which UNC-129 itself acts as an attractive cue for AVM, since UNC-129 is expressed in dorsal but not ventral muscle (Colavita *et al.*, 1998).

Our observation that UNC-129 contributes to both dorsal and ventral guidance suggests that either UNC-129 acts in its own pathway as a bifunctional guidance cue, or that UNC-129 acts in the same pathway as a bifunctional guidance cue. In the first model, UNC-129 acts as an attractant for motor neurons, and a repellent for AVM axons. We do not favor this model, however, because of the near complete penetrance of guidance defects in *unc-6 slt-1* double mutants, and the fact that *unc-129* mutants alone do not have AVM axon guidance defects. Furthermore, preliminary results indicate that relative to AVM axon guidance defects are not enhanced in *unc-129; unc-6 slt-1* triple mutants relative to *unc-6 slt-1* double mutants (data not shown).

The observation that *unc-129* specifically and strongly enhances *slt-1* and not *unc-6* leads us to favor the second model, in which UNC-129 acts in the same pathway as the bifunctional guidance cue UNC-6. UNC-6 both repels motor neurons and attracts the AVM neuron (Hedgecock *et al.*, 1990). We propose that UNC-129 acts in UNC-6 signaling, by sharpening the UNC-6 gradient or facilitating interpretation of the UNC-6 gradient. In this model, dorsally-secreted UNC-129 may limit the physical diffusion of ventrally-secreted UNC-6. Alternatively, UNC-129 may act directly on growth cones, to polarize them along an UNC-129/UNC-6 axis. Such a polarization could in principle

represent the amplification step which has been postulated to be necessary for the interpretation of extracellular gradients.

Intriguingly, misexpression of UNC-129 in both dorsal and ventral body wall muscle, either by transgenic expression (Colavita *et al.*, 1998) or mutation of *unc-130* (Nash *et al.*, 2000), causes partially penetrant AVM guidance defects. In our interpretation of these results, misexpression of UNC-129 disrupts the UNC-6 signaling gradient. Consistent with this hypothesis, *unc-130* mutations strongly disrupt the Netrin component of AVM guidance. We cannot exclude the possibility that *unc-130* mutations have a slight effect on Slit guidance as well. However, *unc-129* mutations do not enhance *unc-6*. It remains possible that the *unc-130* transcription factor affects patterns of Slit as well as UNC-129 expression, although no obvious change in Slit::GFP expression was observed in *unc-130* mutants (Joe Hao, unpublished observations).

4.5 Conclusions

Table 4-4 summarizes the categorization of candidate genes into Netrin and Slit pathways, and a hypothesized genetic pathway for AVM guidance is illustrated in Figure 4-11.

How generalizable are these results? One important point is that the genes identified in this candidate screen have been analyzed only for their effects on axon guidance of a single neuron. Interactions between guidance components are likely to be regulated differently in different neurons. Furthermore, genes contributing to attractive pathways in AVM may act in repulsive pathways elsewhere, as illustrated by the example of *max-1*. Nonetheless, analysis of AVM reveals that while there is some convergence of Netrin and Slit signaling pathways, many of their components are distinct, a finding which may apply to other neurons as well.

Nine genes (*ced-2, ced-5, ced-10, ephexin, unc-115, unc-33, unc-53, max-1,* and *unc-129*) are relatively specific for Netrin-mediated attraction. Two genes (*unc-34* and *mig-2*) predominantly affect Slit-mediated repulsion. The reason for this asymmetry is not known, but it is clear that many of the genes that act in Slit guidance remain to be discovered. Future candidate-based attempts to uncover genes in the Slit signaling pathway may do well to focus on candidates with cell migration defects that are present in *slt-1* and *sax-3* but not *unc-6* (Hao *et al.*, 2001; Zallen *et al.*, 1998). In addition, saturating genetic screens for enhancers of *slt-1* and *unc-6* AVM defects may prove especially useful for discovering novel components of Netrin and Slit pathways. The results presented here provide a foundation for these and other future experiments aimed at uncovering the complete genetic pathways underlying Slit and Netrin axon guidance.

4.6 Materials and Methods

Strains

Wild-type animals were *C. elegans* variety Bristol, strain N2. The alleles and parent strains utilized for these studies are listed in Table 4-1 and 4-2, respectively. Strains were maintained using standard methods. Animals were grown at 20°C. Some strains were provided by the *Caenorhabditis* Genetic Center.

Construction of double mutants

Double mutants were constructed using standard genetic procedures. *abl-1(ok171), ephexin(ok253),* and *slt-1(eh15)* were scored by PCR. The strains generated for analysis in these studies are listed in Table 4-3.

Characterization of neuronal phenotypes

Axons visualized with integrated GFP transgenes were scored in live adult animals. AVM axons were visualized with an integrated *mec-4::GFP* transgene (*zdIs5*, a generous gift of Scott Clark). All strains analyzed were raised at 20°C for at least two generations unless otherwise noted.

Table 4-1 Genes analyzed for effects on AVM axon guidance

Gene(*allele*)	Encodes	Reference
slt-1(eh15)	extracellular guidance cue. *eh15*, deletion, truncates SLT-1 after the first LRR	(Hao *et al.*, 2001)
unc-6(ev400)	extracellular guidance cue. *ev400*, canonical strong loss-of-function, Q78STOP	(Hedgecock *et al.*, 1990; Wadsworth *et al.*, 1996)
unc-34(gm104)	Enabled/VASP family, genetic and biochemical interactions with SAX-3. *gm104*, early stop	(Chapter 3, and Megan Dell and Gian Garriga, personal communication)
abl-1(ok171)	Abl tyrosine kinase, opposes Ena function in *Drosophila*. *ok171*, deletion allele from *C. elegans* knockout consortium	
ced-2(n1994)	CrkII homolog, required for engulfment of cell corpses (engulfment group B). *n1994*, R102STOP	(Reddien and Horvitz, 2000)
ced-5(n1812)	DOCK180/Myoblast City, required for engulfment of cell corpses (engulfment group B). *n1812*, E28STOP	(Wu and Horvitz, 1998b)
ced-10(n1993)	Rac-1 homolog, required for engulfment of cell corpses, *n1993*, V190G, predicted to disrupt CaaX prenylation site	(Reddien and Horvitz, 2000)
mig-2(mu28)	divergent Rac-like protein. *mu28*, W60STOP	(Zipkin *et al.*, 1997)
unc-73(rh40)	related to vertebrate Trio and Kalirin, spectrin-like repeats, DH/PH, SH3, Ig, FN type III domains, GEF activity for Rac. *rh40*, point mutation, disrupts function of the first (DH-1) GEF domain.	(Steven *et al.*, 1998)

Table 4-1 Candidate AVM axon guidance genes (continued)

Gene(*allele*)	Encodes	Reference
ephexin(ok253)	related to Ephexin, a GEF downstream of EphA receptors. *ok253*, deletion allele from *C. elegans* knockout consortium, 2.4 kB deletion in 3 kB region containing GEF, PH and SH3 domains	(Shamah *et al.*, 2001)
vab-1(e2)	Eph receptor. *e2*, predicted weak allele, G917E	(George *et al.*, 1998)
unc-115(ky275)	cytoskeletal linker protein with villin headpiece and LIM-domains, genetic interactions with *ced-10* and *mig-2*. *ky275*, W489STOP	(Lundquist *et al.*, 1998) (Erik Lundquist and Cori Bargmann, personal communication)
unc-14(e57)	novel protein, binds UNC-51, abnormal axon elongation	(Ogura *et al.*, 1997)
unc-33(e204)	homologous to collapsin response mediator protein (CRMP-62)	(Goshima *et al.*, 1995; Li *et al.*, 1992)
unc-51(e369)	serine/threonine kinase, abnormal axon elongation	(Ogura *et al.*, 1994)
unc-53(e404)	genetic interactions with *unc-14, unc-51, unc-71* in outgrowth of the excretory canals	(Thierry Bogaert, personal communication)
unc-71(e541)	ADAM family metalloprotease	(Yishi Jin, personal communication)
mig-17(k174)	ADAM family metalloprotease, genetic interactions with *unc-6* in DTC migration. *k174*, Q111STOP	(Nishiwaki *et al.*, 2000)
max-1(cy1)	PH, MyTH4, FERM domains, required for motor axon guidance. *cy1*, Q803STOP	(Hwai-Jong Cheng, personal communication)
unc-69(e587)	108 aa protein with predicted coil-coil domain, required for motor axon guidance, outgrowth and fasciculation defects	(Michael Hentgartner, personal communication)

Table 4-1 Candidate AVM axon guidance genes (continued)

Gene(*allele*)	Encodes	Reference
unc-129(ev557)	TGF-beta required for motorneuron axon guidance, suppresses ectopic UNC-5 repulsion of AVM. *ev557*, Y242STOP	(Colavita *et al.*, 1998)
unc-130(oy10)	Forkhead transcription required for graded expression of UNC-129. *oy10*, R218C, predicted to disrupt DNA binding	(Nash *et al.*, 2000)

Table 4-2 Parent strains used for analysis of AVM axon guidance

Strain name	Genotype
CX5089	*zdIs5 I; slt-1(eh15) X*
CX5300	*zdIs5 I; unc-6(ev400) X*
CX5169	*zdIs5 I; unc-6(ev400) slt-1(eh15) X*
CX5226	*zdIs5 I; unc-34(gm104) V; slt-1(eh15) X*
CX5473	*zdIs5 I; unc-34(gm104) V; unc-6(ev400) X*
CZ1426	*abl-1(ok171) X*
LE208	*kyIs8 I; ced-2(n1994) IV*
MT4434	*ced-5(n1812) IV*
MT3013	*ced-10(n1993) IV*
CX4783	*mig-2(mu28) X*
LE128	*unc-73(rh40) I; kyIs4 X*
CX5696	*zdIs5 I; ephexin (ok253) II*
CB2	*vab-1(e2) II*
CX3709	*unc-115(ky275) X*
CB57	*unc-14(e57) I*
CB204	*unc-33(e204) IV*
MT1511	*unc-51(e369) V*
CB404	*unc-53(e404) II*
CB587	*unc-69(e587) III*
CX5729	*unc-71(e541) III*
NF198	*mig-17(k174) V*
TL5	*max-1(cy1) V; evIs82*
CX4383	*unc-129(ev557) IV*
PY1133	*unc-130(oy10) II*

Table 4-3 Strains constructed for analysis of AVM ventral guidance

Strain name	Genotype
CX4767	*zdIs5 I; unc-34(gm104) V*
CX5226	*zdIs5 I; unc-34(gm104) V; slt-1(eh15) X*
CX5473	*zdIs5 I; unc-34(gm104) V; unc-6(ev400) X*
CX5385	*zdIs5 I; abl-1(ok171) X*
CX5695	*zdIs5 I; abl-1(ok171) slt-1(eh15) X*
CX5708	*zdIs5 I; unc-6(ev400) abl-1(ok171) X*
CX5689	*zdIs5 I; ced-2(n1994) IV*
CX5687	*zdIs5 I; ced-2(n1994) IV; slt-1(eh15) X*
CX5688	*zdIs5 I; ced-2(n1994) IV; unc-6(ev400) X*
CX5378	*zdIs5 I; ced-5(n1812) IV*
CX5699	*zdIs5 I; ced-5(n1812) IV; slt-1(eh15) X*
CX5698	*zdIs5 I; ced-5(n1812) IV; unc-6(ev400) X*
CX5683	*zdIs5 I; ced-10(n1993) IV*
CX5682	*zdIs5 I; ced-10(n1993) IV; slt-1(eh15) X*
	zdIs5 I; ced-10(n1993) IV; unc-6(ev400) X
CX5723	*zdIs5 I; mig-2(mu28) X*
CX5725	*zdIs5 I; slt-1 (eh15) mig-2(mu28) X*
CX5675	*zdIs5 I; mig-2(mu28) unc-6(ev400) X*
CX5711	*zdIs5 I; unc-115(ky275) X*
CX5709	*zdIs5 I; unc-115(ky275) slt-1(eh15) X*
CX5710	*zdIs5 I; unc-6(ev400) unc-115(ky275) X*
CX5383	*zdIs5 unc-73(rh40) I*
CX5225	*zdIs5 unc-73(rh40) I; slt-1(eh15) X*
	zdIs5 unc-73(rh40) I; unc-6(ev400) X
CX5696	*zdIs5 I; ok253 II*
CX5727	*zdIs5 I; ok253 II; slt-1(eh15) kyIs104 X*
CX5694	*zdIs5 I; ok253 II; unc-6(ev400) X*
CX5719	*zdIs5 I; vab-1(e2) II*

Table 4-3 Strains constructed for analysis of AVM ventral guidance (continued)

Strain name	Genotype
CX5718	*zdIs5 I; vab-1(e2) II; slt-1(eh15) X*
CX5717	*zdIs5 I; vab-1(e2) II; unc-6(ev400) X*
CX5703	*zdIs5 unc-14(e57) I*
CX5716	*zdIs5 unc-14(e57) I; slt-1(eh15) X*
CX5722	*zdIs5 unc-14(e57) I; unc-6(ev400) X*
CX5377	*zdIs5 I; unc-33(e204) IV*
CX5680	*zdIs5 I; unc-33(e204) IV; slt-1(eh15) X*
	zdIs5 I; unc-33(e204) IV; unc-6(ev400) X
CX5715	*zdIs5 I; unc-51(e369) V*
CX5714	*zdIs5 I; unc-51(e369) V; slt-1(eh15) X*
	zdIs5 I; unc-51(e369) V; unc-6(ev400) X
CX5707	*zdIs5 I; unc-53(e404) II*
CX5706	*zdIs5 I; unc-53(e404) II; slt-1(eh15) X*
CX5700	*zdIs5 I; unc-53(e404) II; unc-6(ev400) X*
CX5686	*zdIs5 I; unc-71(e541) III*
CX5685	*zdIs5 I; unc-71(e541) III; slt-1(eh15) X*
CX5684	*zdIs5 I; unc-71(e541) III; unc-6(ev400) X*
CX5839	*zdIs5 I; mig-17(k174) V*
CX5808	*zdIs5 I; mig-17(k174) V; slt-1(eh15) X*
	zdIs5 I; mig-17(k174) V; unc-6(ev400) X
CX5807	*zdIs5 I; max-1(cy1) V*
CX5806	*zdIs5 I; max-1(cy1) V; slt-1(eh15) X*
	zdIs5 I; max-1(cy1) V; unc-6(ev400) X
	zdIs5 I; unc-69(e587) III
	zdIs5 I; unc-69(e587) III; slt-1(eh15) X
	zdIs5 I; unc-69(e587) III; unc-6(ev400) X
CX5704	*zdIs5 I; unc-129(ev557) IV*
CX5705	*zdIs5 I; unc-129(ev557) IV; slt-1(eh15) X*
CX5702	*zdIs5 I; unc-129(ev557) IV; unc-6(ev400) X*

Table 4-3 Strains constructed for analysis of AVM ventral guidance (continued)

Strain name	Genotype
CX5834	*zdIs5 I; unc-130(oy10) II*
CX5833	*zdIs5 I; unc-130(oy10) II; slt-1(eh15) X*
CX5832	*zdIs5 I; unc-130(oy10) II; unc-6(ev400) X*

Table 4-4 Classification of genes into UNC-6/Netrin or Slit pathways

Gene	Netrin pathway	Slit pathway
unc-34		√√
abl-1	(√)	(√)
ced-2	√	
ced-5	√	
ced-10	√	
mig-2	√	√√
unc-73	√√	√√
ephexin	√	
vab-1		
unc-115	√	
unc-14		
unc-33	√	
unc-51	(√)	n.d.
unc-53	√	
unc-71	√	√
mig-17	(√)	
max-1	√√	√
unc-69	(√)	(√)
unc-129	√√	

Checkmarks indicate that a gene acts within the pathway. Parentheses indicate results that did not reach statistical significance. Double checkmarks indicate a particularly strong contribution to a pathway. n.d., not determined.

Figure 4-1

The AVM axon is guided by dorsal SLT-1/Slit and ventral UNC-6/Netrin. The AVM cell body is situated on the lateral hypodermis; its axon migrates ventrally between hypodermis and ventral muscle to join the ventral nerve cord (White *et al.*, 1986). SLT-1 is expressed in dorsal muscles where it acts to repels the AVM axon ventrally (Hao *et al.*, 2001). UNC-6 is expressed in the ventral nerve cord and attracts the AVM axon (Hedgecock *et al.*, 1990; Wadsworth *et al.*, 1996). Abbreviations: *hyp*, hypodermis, *int*, intestine, *m*, body wall muscle, *nc*, nerve cord.

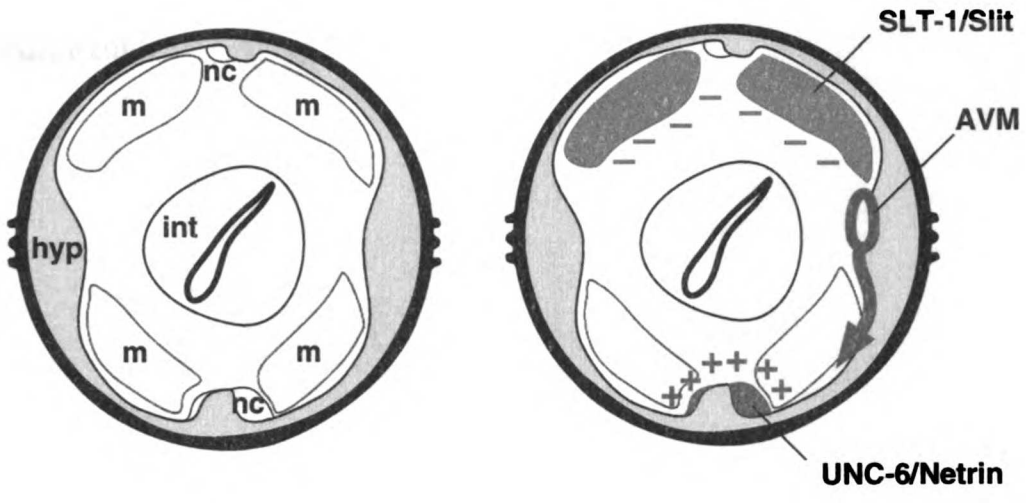
nc
m
m
int
hyp
m
m
nc
SLT-1/Slit
AVM
UNC-6/Netrin

Figure 4-2

Strategy for identifying components of Slit and Netrin signaling pathways. Disruption of either *slt-1* or *unc-6* guidance pathways alone cause only partially penetrant (30-40%) defects in AVM guidance, while disruption of both pathways cause >90% defects. Candidate genes are analyzed for ventral guidance defects in combination with *slt-1* or *unc-6*. Mutations in genes that act specifically in Netrin pathways are predicted to enhance *slt-1*, while mutations in genes that act specifically in Slit pathways are predicted to enhance *unc-6*. Mutations in genes that act in both pathways, or are permissive for axon guidance, enhance both *slt-1* and *unc-6*, while mutations in genes not involved in (or redundant for) Slit and Netrin guidance fail to enhance either.

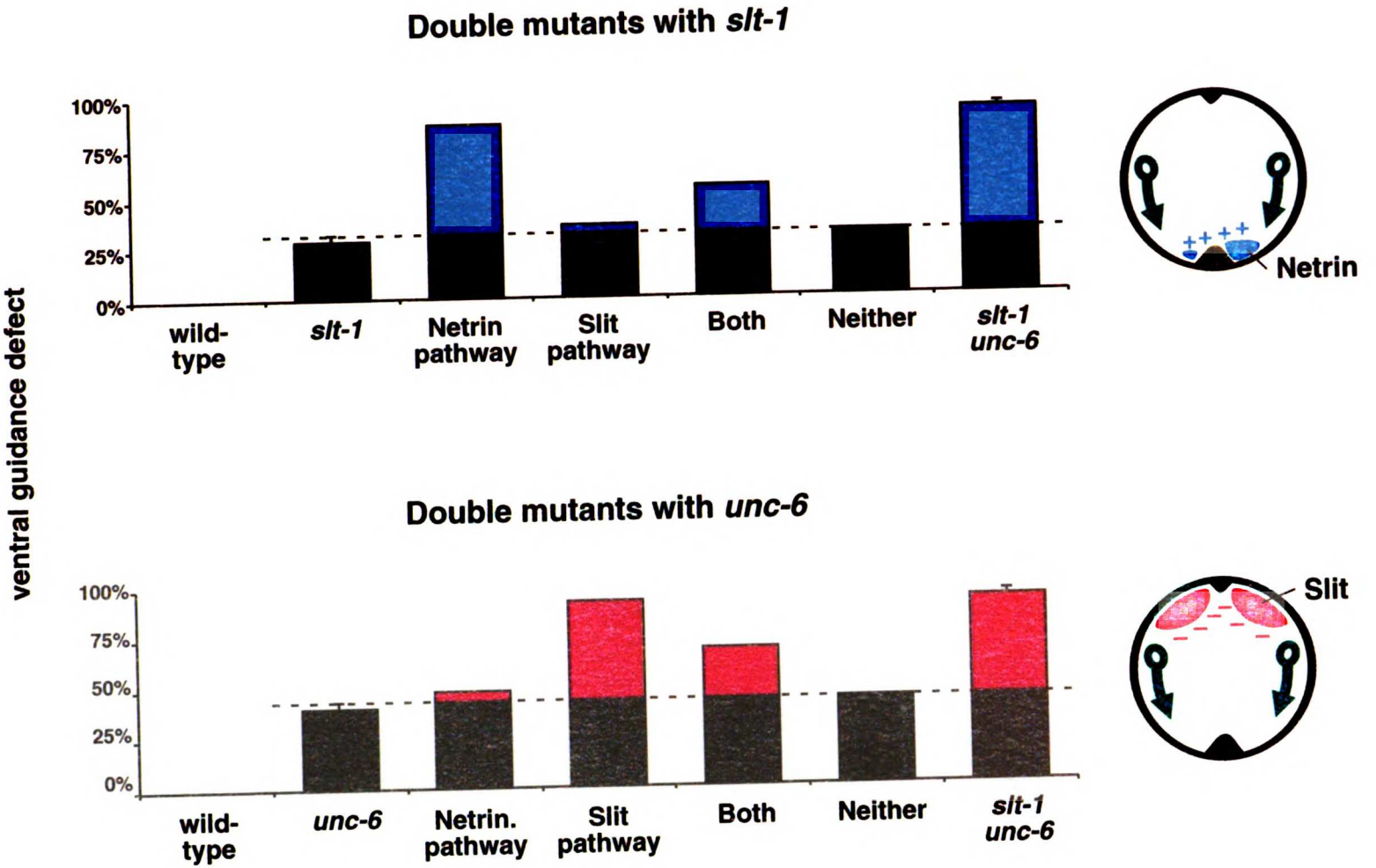
Double mutants with slt-1
ventral guidance defect
100%
75%
50%
25%
0%
wild-type
slt-1
Netrin pathway
Slit pathway
Both
Neither
slt-1 unc-6
Netrin
Double mutants with unc-6
100%
75%
50%
25%
0%
wild-type
unc-6
Netrin. pathway
Slit pathway
Both
Neither
slt-1 unc-6
Slit

Figure 4-3

Involvement of *unc-34/ena* and *abl-1* in Slit and Netrin signaling. Asterisks denote significant enhancement over single mutants at $p<0.05$ or better.

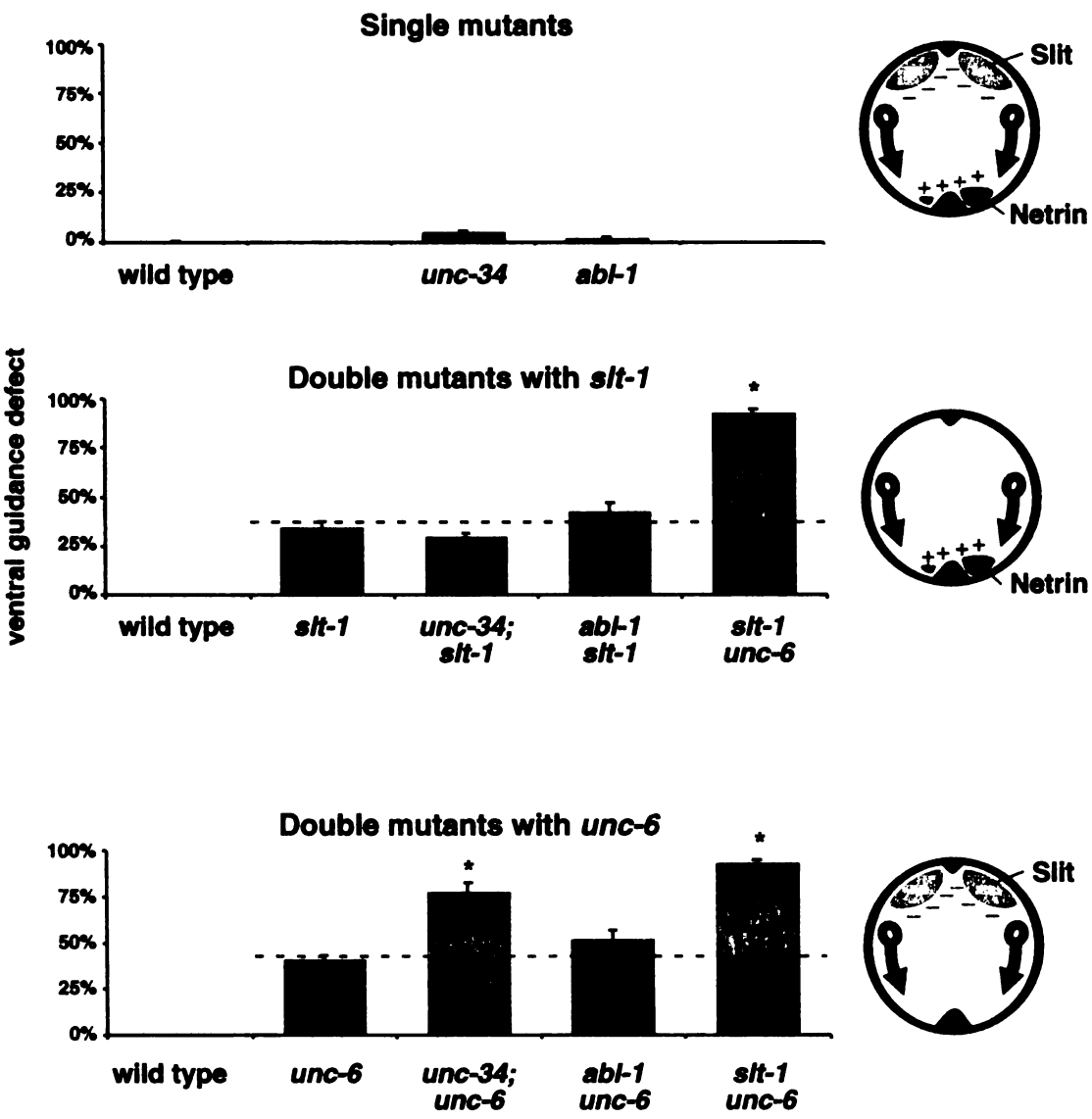
Single mutants
100%
75%
50%
25%
0%
wild type
unc-34
abl-1
Slit
Netrin
ventral guidance defect
Double mutants with slt-1
*
wild type
slt-1
unc-34; slt-1
abl-1 slt-1
slt-1 unc-6
Netrin
Double mutants with unc-6
*
*
wild type
unc-6
unc-34; unc-6
abl-1 unc-6
slt-1 unc-6
Slit

Figure 4-4

Involvement of the cell engulfment genes *ced-2, ced-5, and ced-10* in Slit and Netrin signaling. Asterisks denote significant enhancement over single mutants at $p<0.05$ or better.

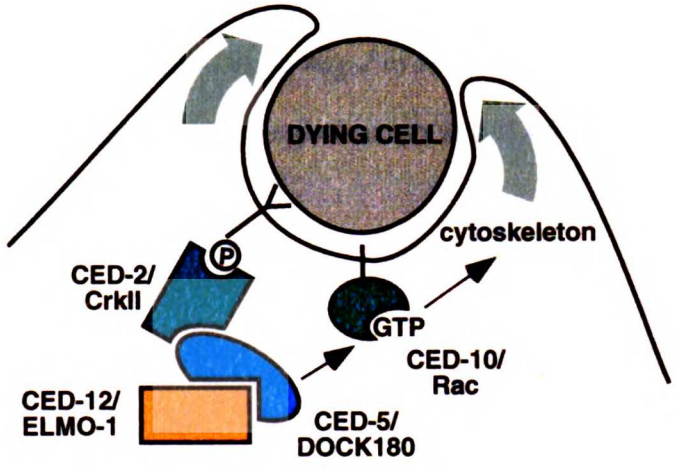
DYING CELL
cytoskeleton
P
CED-2/
CrkII
GTP
CED-10/
Rac
CED-12/
ELMO-1
CED-5/
DOCK180

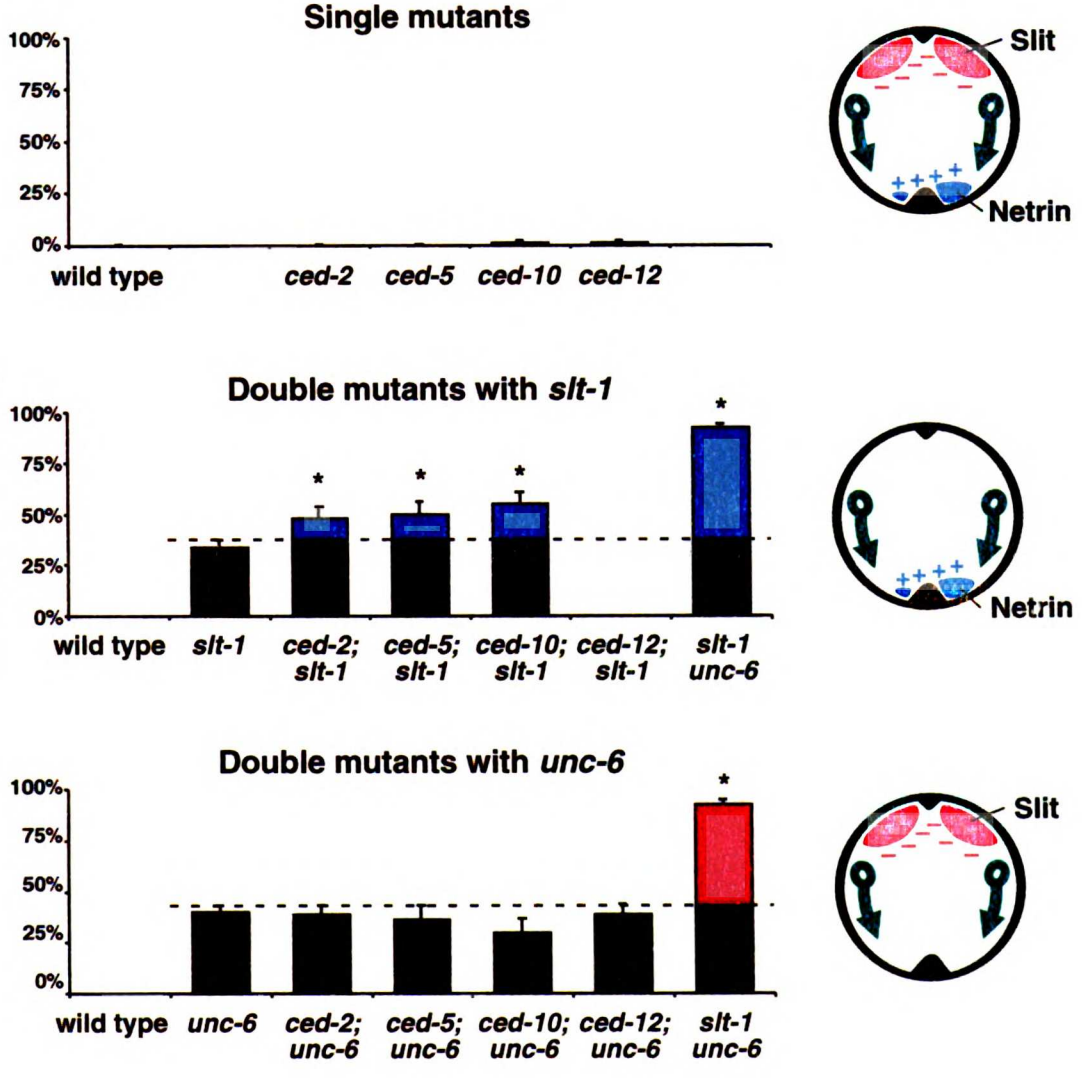
Single mutants
100%
75%
50%
25%
0%
wild type
ced-2
ced-5
ced-10
ced-12
Slit
Netrin
ventral guidance defect
Double mutants with slt-1
wild type
slt-1
ced-2; slt-1
ced-5; slt-1
ced-10; slt-1
ced-12; slt-1
slt-1 unc-6
Netrin
Double mutants with unc-6
wild type
unc-6
ced-2; unc-6
ced-5; unc-6
ced-10; unc-6
ced-12; unc-6
slt-1 unc-6
Slit

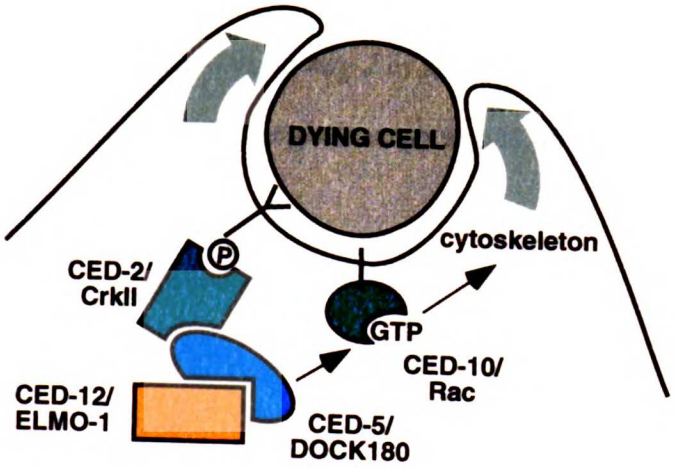
DYING CELL
cytoskeleton
CED-2/
CrkII
P
GTP
CED-10/
Rac
CED-12/
ELMO-1
CED-5/
DOCK180

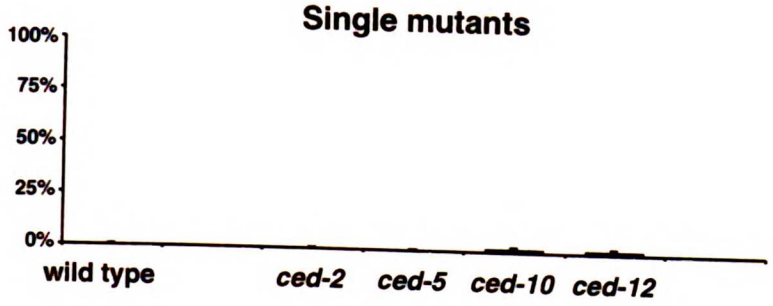
Single mutants
100%
75%
50%
25%
0%
wild type
ced-2
ced-5
ced-10
ced-12

Slit
Netrin

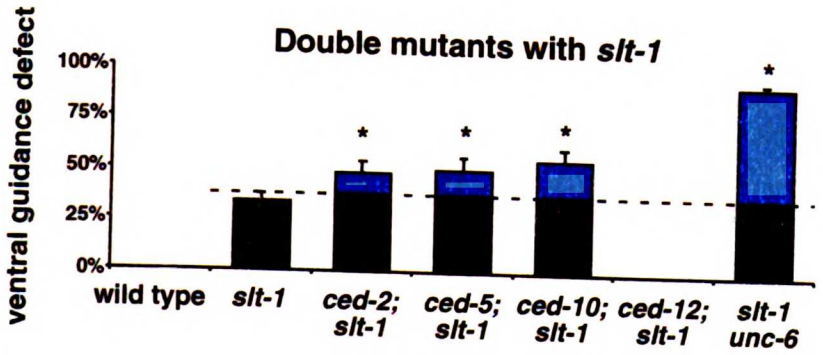
ventral guidance defect
Double mutants with slt-1
100%
75%
50%
25%
0%
wild type
slt-1
ced-2; slt-1
ced-5; slt-1
ced-10; slt-1
ced-12; slt-1
slt-1 unc-6

Netrin

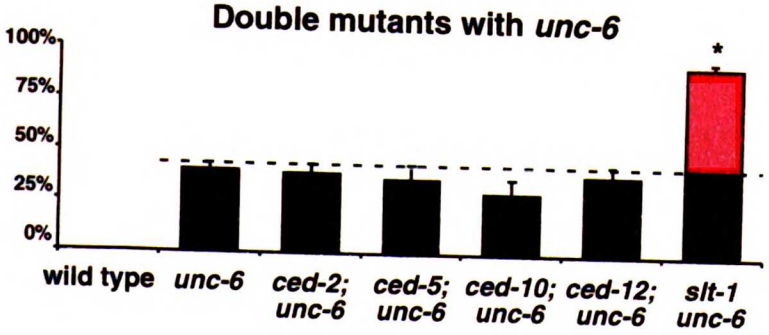
Double mutants with unc-6
100%
75%
50%
25%
0%
wild type
unc-6
ced-2; unc-6
ced-5; unc-6
ced-10; unc-6
ced-12; unc-6
slt-1 unc-6

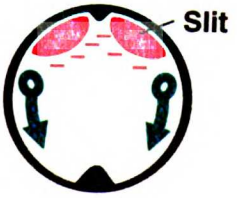
Slit

Figure 4-5

Involvement of the Rac genes *ced-10* and *mig-2* in Slit and Netrin signaling. Asterisks denote significant enhancement over single mutants at $p<0.05$ or better.

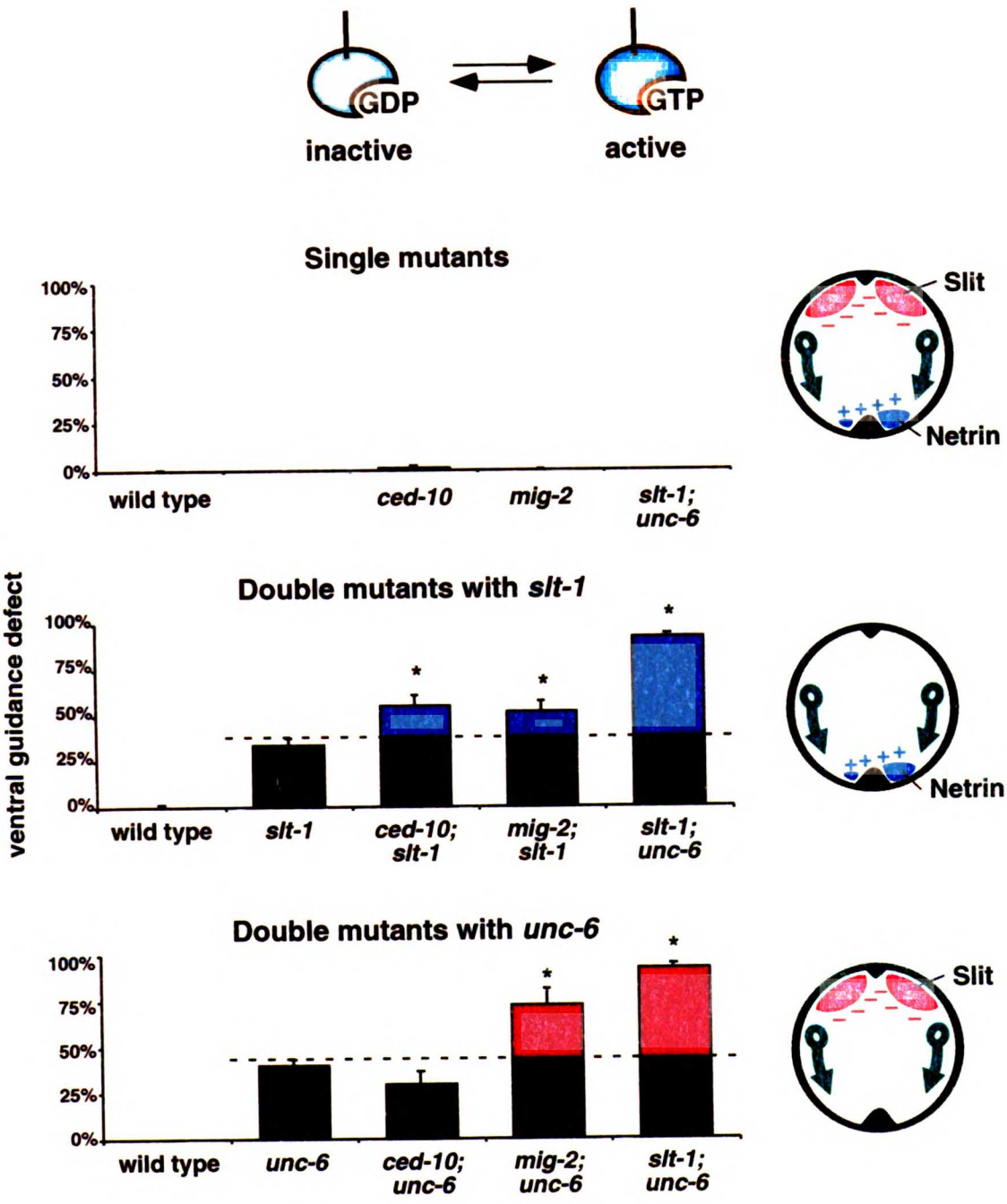
GDP
GTP
inactive
active
Single mutants
100%
75%
50%
25%
0%
wild type
ced-10
mig-2
slt-1; unc-6
Slit
Netrin
Double mutants with slt-1
ventral guidance defect
100%
75%
50%
25%
0%
wild type
slt-1
ced-10; slt-1
mig-2; slt-1
slt-1; unc-6
*
Netrin
Double mutants with unc-6
100%
75%
50%
25%
0%
wild type
unc-6
ced-10; unc-6
mig-2; unc-6
slt-1; unc-6
*
Slit

Figure 4-6

Involvement of the Rac-associated genes *unc-115, unc-73* and *ephexin* in Slit and Netrin signaling. Asterisks denote significant enhancement over single mutants at $p<0.05$ or better.

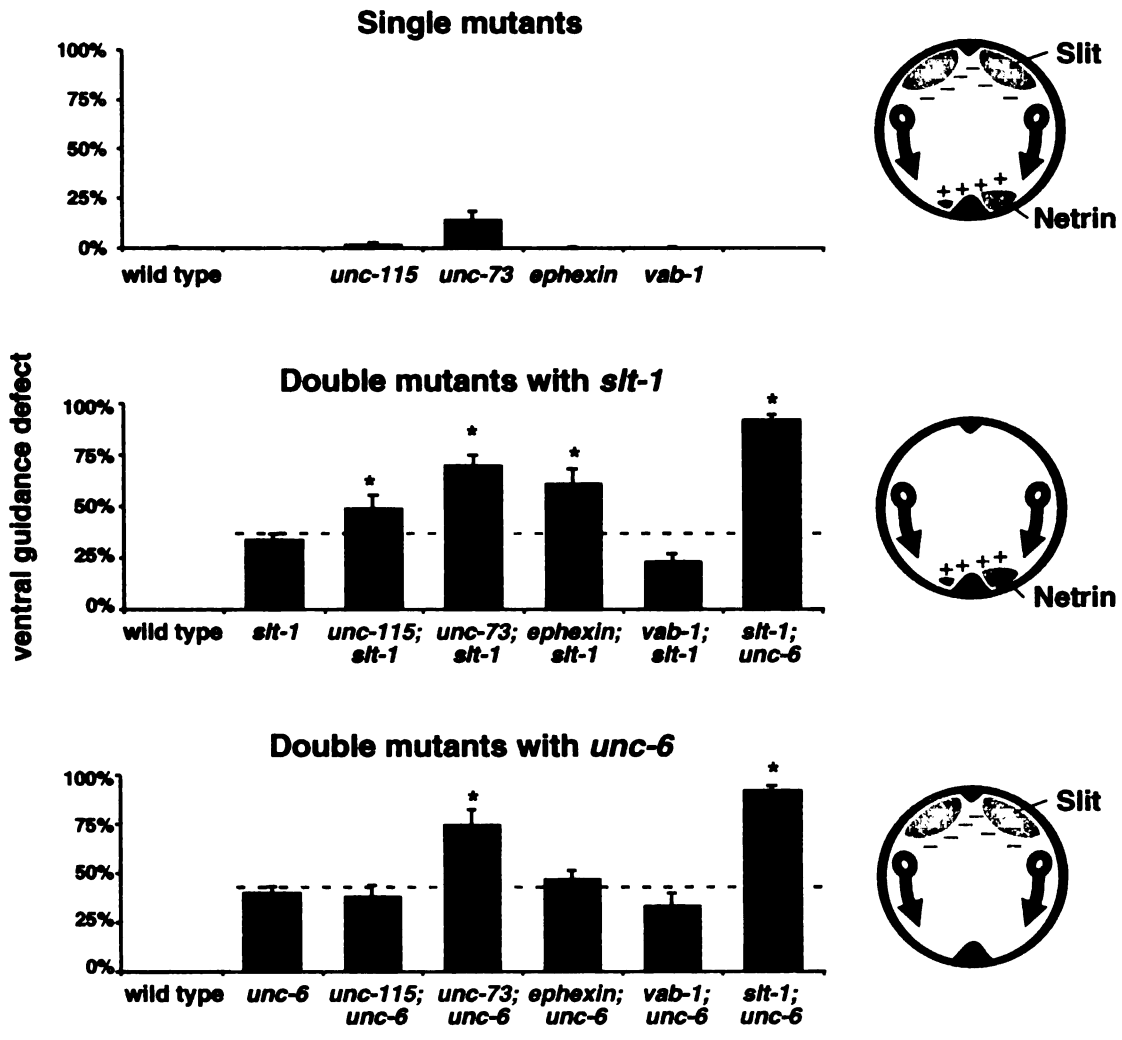
Single mutants
100%
75%
50%
25%
0%
wild type
unc-115
unc-73
ephexin
vab-1
Slit
Netrin
ventral guidance defect
Double mutants with slt-1
wild type
slt-1
unc-115; slt-1
unc-73; slt-1
ephexin; slt-1
vab-1; slt-1
slt-1; unc-6
Netrin
Double mutants with unc-6
wild type
unc-6
unc-115; unc-6
unc-73; unc-6
ephexin; unc-6
vab-1; unc-6
slt-1; unc-6
Slit

Figure 4-7

Involvement of the axonal outgrowth genes *unc-14*, *unc-33*, *unc-51* and *unc-53* in Slit and Netrin signaling. Asterisks denote significant enhancement over single mutants at $p<0.05$ or better.

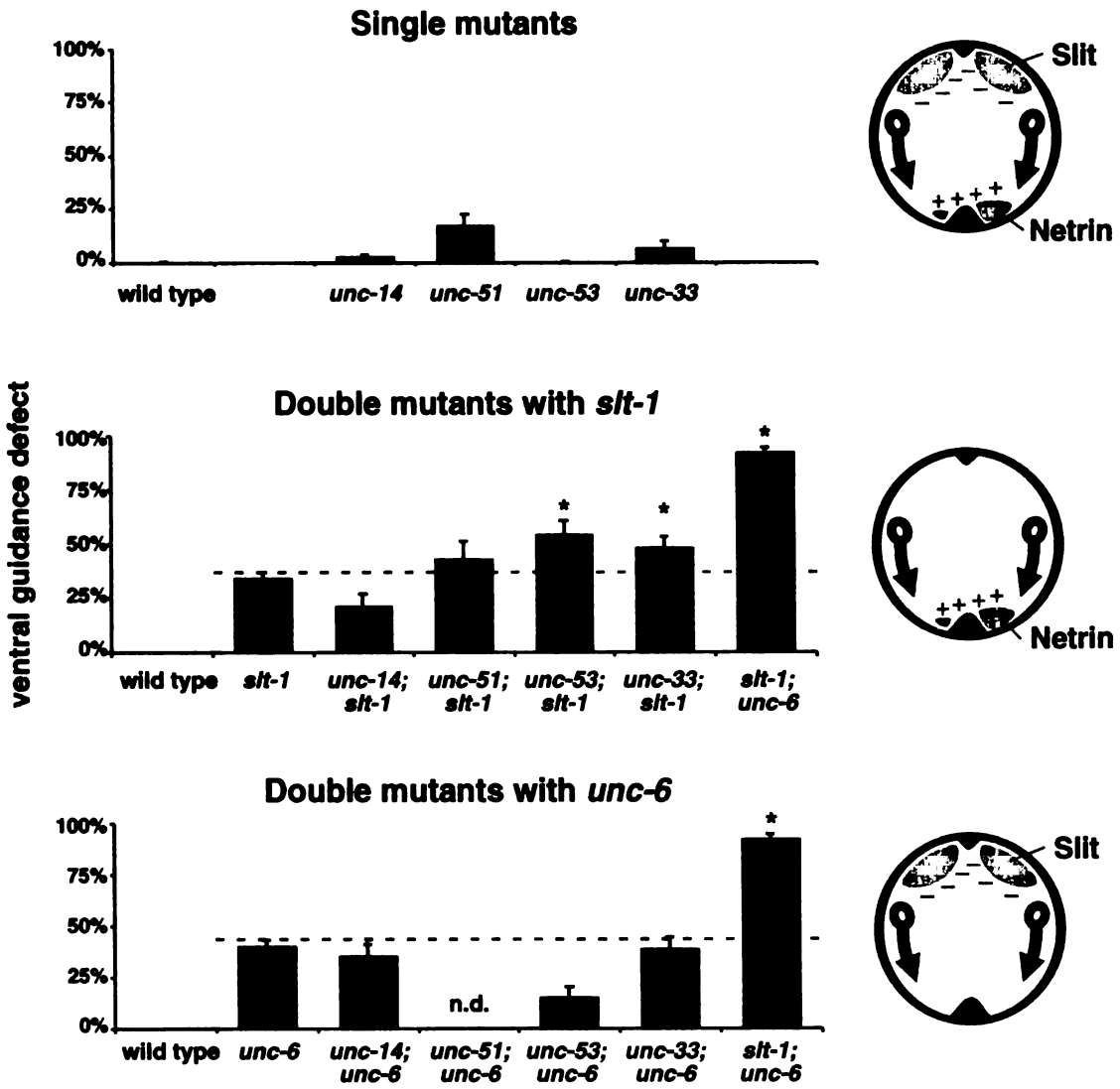
Single mutants
100%
75%
50%
25%
0%
wild type
unc-14
unc-51
unc-53
unc-33
Slit
Netrin
ventral guidance defect
Double mutants with slt-1
wild type
slt-1
unc-14; slt-1
unc-51; slt-1
unc-53; slt-1
unc-33; slt-1
slt-1; unc-6
Netrin
Double mutants with unc-6
n.d.
wild type
unc-6
unc-14; unc-6
unc-51; unc-6
unc-53; unc-6
unc-33; unc-6
slt-1; unc-6
Slit

Figure 4-8

Involvement of the ADAM metalloprotease genes *unc-71* and *mig-17* in Slit and Netrin signaling. Asterisks denote significant enhancement over single mutants at $p<0.05$ or better.

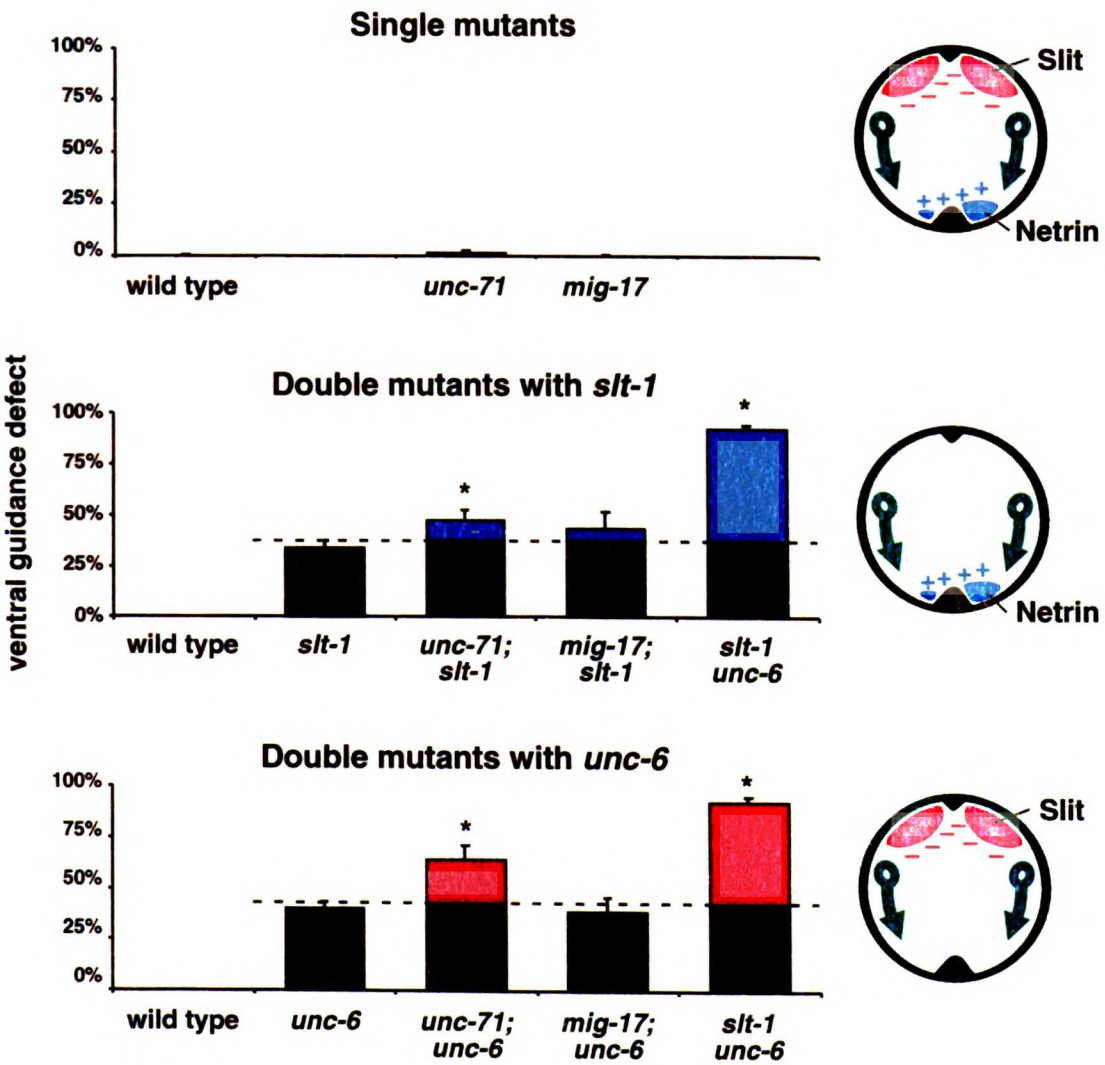
Single mutants
100%
75%
50%
25%
0%
wild type
unc-71
mig-17
Slit
Netrin
ventral guidance defect
Double mutants with slt-1
*
*
wild type
slt-1
unc-71; slt-1
mig-17; slt-1
slt-1 unc-6
Netrin
Double mutants with unc-6
*
*
wild type
unc-6
unc-71; unc-6
mig-17; unc-6
slt-1 unc-6
Slit

Figure 4-9

Involvement of motor axon guidance genes *max-1*, *unc-69, unc-129,* and *unc-130* in Slit and Netrin signaling. Asterisks denote significant enhancement over single mutants at $p<0.05$ or better.

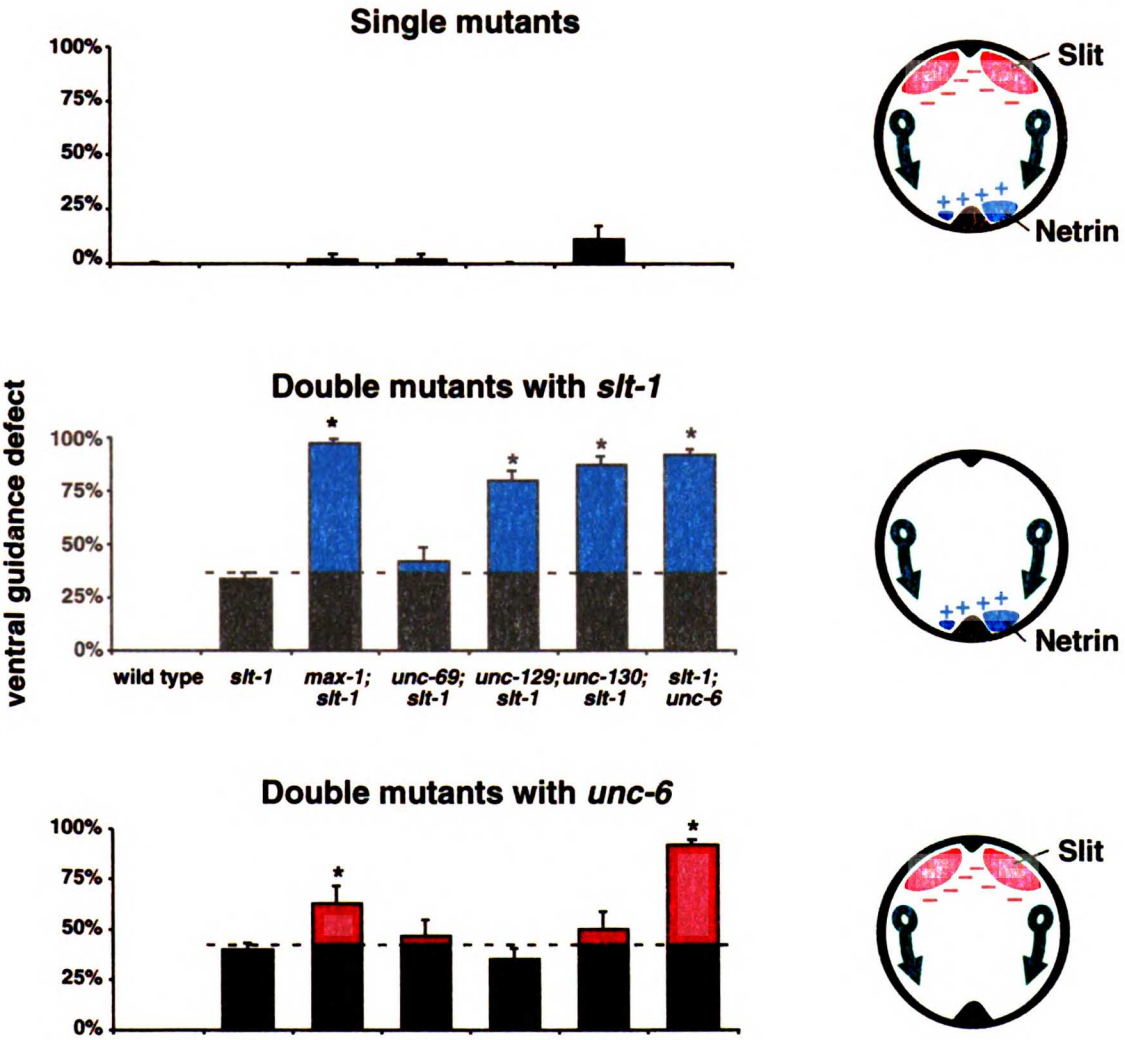
Single mutants
100%
75%
50%
25%
0%
Slit
Netrin
Double mutants with slit-1
ventral guidance defect
100%
75%
50%
25%
0%
wild type
slit-1
max-1; slit-1
unc-69; slit-1
unc-129; slit-1
unc-130; slit-1
slit-1; unc-6
Netrin
Double mutants with unc-6
100%
75%
50%
25%
0%
wild type
unc-6
max-1; unc-6
unc-69; unc-6
unc-129; unc-6
unc-130; unc-6
slit-1; unc-6
Slit

Figure 4-10

Summary of results of AVM analysis . Asterisks denote significant enhancement over single mutants at $p<0.05$ or better.

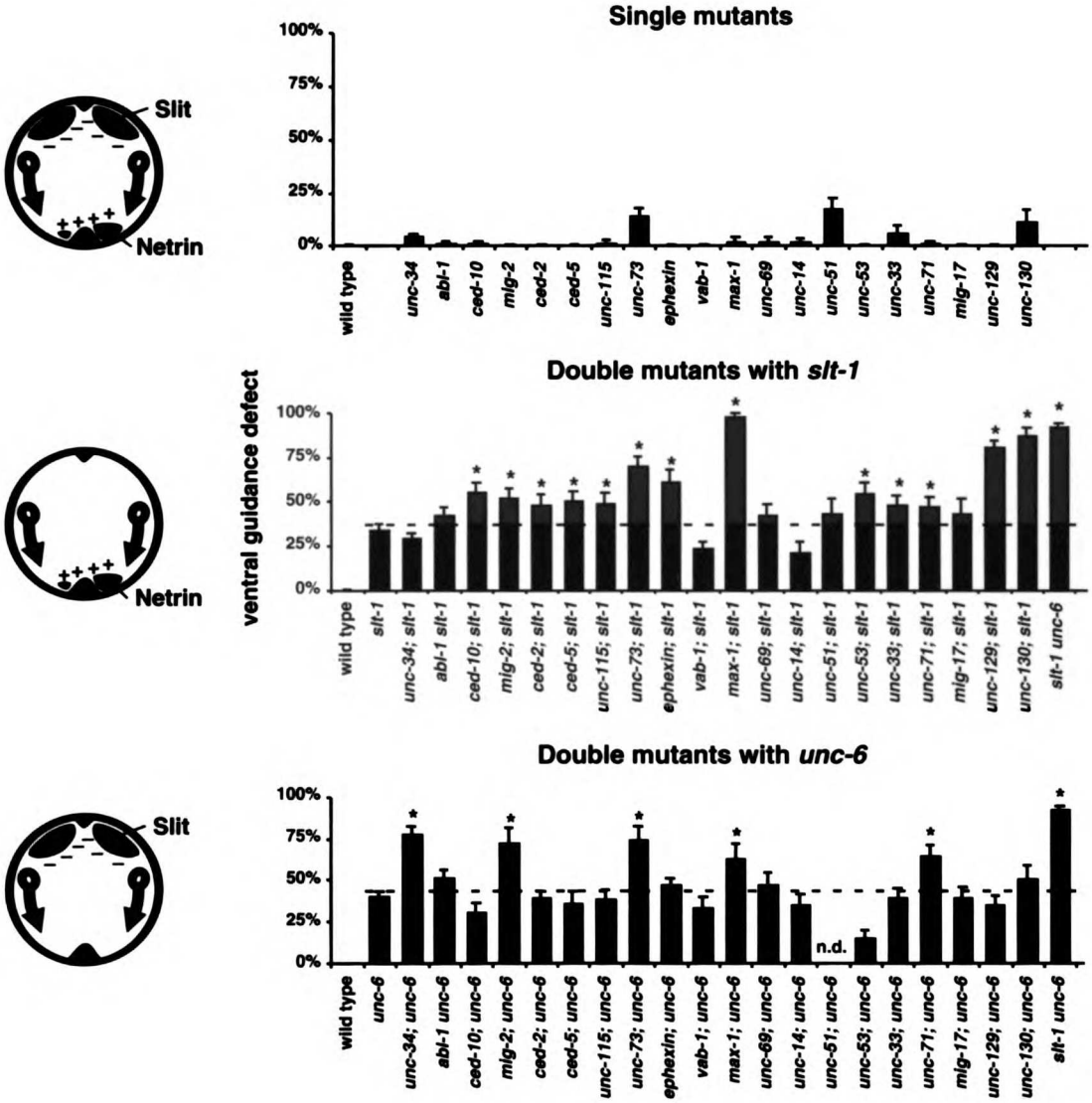
Slit
Netrin
Single mutants
100%
75%
50%
25%
0%
wild type
unc-34
abl-1
ced-10
mig-2
ced-2
ced-5
unc-115
unc-73
ephexin
vab-1
max-1
unc-69
unc-14
unc-51
unc-53
unc-33
unc-71
mig-17
unc-129
unc-130
Netrin
ventral guidance defect
Double mutants with slt-1
wild type
slt-1
unc-34; slt-1
abl-1 slt-1
ced-10; slt-1
mig-2; slt-1
ced-2; slt-1
ced-5; slt-1
unc-115; slt-1
unc-73; slt-1
ephexin; slt-1
vab-1; slt-1
max-1; slt-1
unc-69; slt-1
unc-14; slt-1
unc-51; slt-1
unc-53; slt-1
unc-33; slt-1
unc-71; slt-1
mig-17; slt-1
unc-129; slt-1
unc-130; slt-1
slt-1 unc-6
Slit
Double mutants with unc-6
wild type
unc-6
unc-34; unc-6
abl-1 unc-6
ced-10; unc-6
mig-2; unc-6
ced-2; unc-6
ced-5; unc-6
unc-115; unc-6
unc-73; unc-6
ephexin; unc-6
vab-1; unc-6
max-1; unc-6
unc-69; unc-6
unc-14; unc-6
unc-51; unc-6
unc-53; unc-6
unc-33; unc-6
unc-71; unc-6
mig-17; unc-6
unc-129; unc-6
unc-130; unc-6
slt-1 unc-6
n.d.

4.7 References

Ahern-Djamali, S. M., Comer, A. R., Bachmann, C., Kastenmeier, A. S., Reddy, S. K., Beckerle, M. C., Walter, U., and Hoffmann, F. M. (1998). Mutations in *Drosophila enabled* and rescue by human vasodilator-stimulated phosphoprotein (VASP) indicate important functional roles for Ena/VASP homology domain 1 (EVH1) and EVH2 domains. *Molecular Biology of the Cell* 9, 2157-2171.

Bashaw, G. J., and Goodman, C. S. (1999). Chimeric axon guidance receptors: the cytoplasmic domains of slit and netrin receptors specify attraction versus repulsion. *Cell* 97, 917-926.

Bashaw, G. J., Kidd, T., Murray, D., Pawson, T., and Goodman, C. S. (2000). Repulsive axon guidance: Abelson and Enabled play opposing roles downstream of the roundabout receptor. *Cell* 101, 703-715.

Black, R. A., and White, J. M. (1998). ADAMs: focus on the protease domain. *Curr Opin Cell Biol* 10, 654-659.

Branda, C. S., and Stern, M. J. (2000). Mechanisms controlling sex myoblast migration in *Caenorhabditis elegans* hermaphrodites. *Dev Biol* 226, 137-151.

Brose, K., Bland, K. S., Wang, K. H., Arnott, D., Henzel, W., Goodman, C. S., Tessier-Lavigne, M., and Kidd, T. (1999). Slit proteins bind Robo receptors and have an evolutionarily conserved role in repulsive axon guidance. *Cell* 96, 795-806.

Chakraborty, T., Ebel, F., Domann, E., Niebuhr, K., Gerstel, B., Pistor, S., Temm-Grove, C. J., Jockusch, B. M., Reinhard, M., Walter, U., and Wehland, J. A. (1995). A focal adhesion factor directly linking intracellularly motile *Listeria monocytogenes* and *Listeria ivanovii* to the actin-based cytoskeleton of mammalian cells. *Embo J* 14, 1314-1321.

Chan, S. S., Zheng, H., Su, M. W., Wilk, R., Killeen, M. T., Hedgecock, E. M., and Culotti, J. G. (1996). UNC-40, a *C. elegans* homolog of DCC (Deleted in Colorectal Cancer), is required in motile cells responding to UNC-6 netrin cues. *Cell* 87, 187-195.

Colavita, A., and Culotti, J. G. (1998). Suppressors of ectopic UNC-5 growth cone steering identify eight genes involved in axon guidance in *Caenorhabditis elegans. Developmental Biology* 194, 72-85.

Colavita, A., Krishna, S., Zheng, H., Padgett, R. W., and Culotti, J. G. (1998). Pioneer axon guidance by UNC-129, a *C. elegans* TGF-beta. *Science* 281, 706-709.

Cowan, C. A., and Henkemeyer, M. (2001). The SH2/SH3 adaptor Grb4 transduces B-ephrin reverse signals. *Nature* 413, 174-179.

Crump, J. G., Zhen, M., Jin, Y., and Bargmann, C. I. (2001). The SAD-1 kinase regulates presynaptic vesicle clustering and axon termination. *Neuron* 29, 115-129.

Culotti, J. G., and Merz, D. C. (1998). DCC and netrins. *Curr Opin Cell Biol* 10, 609-613.

Dickson, B. J. (2001). Rho GTPases in growth cone guidance. *Curr Opin Neurobiol* 11, 103-110.

Ellis, R. E., Jacobson, D. M., and Horvitz, H. R. (1991). Genes required for the engulfment of cell corpses during programmed cell death in *Caenorhabditis elegans. Genetics* 129, 79-94.

Fambrough, D., Pan, D., Rubin, G. M., and Goodman, C. S. (1996). The cell surface metalloprotease/disintegrin Kuzbanian is required for axonal extension in Drosophila. *Proc Natl Acad Sci U S A* 93, 13233-13238.

Galko, M. J., and Tessier-Lavigne, M. (2000). Function of an axonal chemoattractant modulated by metalloprotease activity. *Science* 289, 1365-1367.

Garrity, P. A., Rao, Y., Salecker, I., McGlade, J., Pawson, T., and Zipursky, S. L. (1996). Drosophila photoreceptor axon guidance and targeting requires the dreadlocks SH2/SH3 adapter protein. *Cell* 85, 639-650.

George, S. E., Simokat, K., Hardin, J., and Chisholm, A. D. (1998). The VAB-1 Eph receptor tyrosine kinase functions in neural and epithelial morphogenesis in *C. elegans. Cell* 92, 633-643.

Gertler, F. B., Comer, A. R., Juang, J. L., Ahern, S. M., Clark, M. J., Liebl, E. C., and Hoffmann, F. M. (1995). *enabled*, a dosage-sensitive suppressor of mutations in the *Drosophila* Abl tyrosine kinase, encodes an Abl substrate with SH3 domain-binding properties. *Genes and Development* 9, 521-533.

Goshima, Y., Nakamura, F., Strittmatter, P., and Strittmatter, S. M. (1995). Collapsin-induced growth cone collapse mediated by an intracellular protein related to UNC-33. *Nature* 376, 509-514.

Gumienny, T. L., Brugnera, E., Tosello-Trampont, A. C., Kinchen, J. M., Haney, L. B., Nishiwaki, K., Walk, S. F., Nemergut, M. E., Macara, I. G., Francis, R., *et al.* (2001). Ced-12/elmo, a novel member of the crkii/dock180/rac pathway, is required for phagocytosis and cell migration. *Cell* 107, 27-41.

Hall, A., and Nobes, C. D. (2000). Rho GTPases: molecular switches that control the organization and dynamics of the actin cytoskeleton. *Philos Trans R Soc Lond B Biol Sci* 355, 965-970.

Hao, J. C., Yu, T. W., Fujisawa, K., Culotti, J. G., Gengyo-Ando, K., Mitani, S., Moulder, G., Barstead, R., Tessier-Lavigne, M., and Bargmann, C. I. (2001). *C. elegans* Slit Acts in Midline, Dorsal-Ventral, and Anterior-Posterior Guidance via the SAX-3/Robo Receptor. *Neuron* 32, 25-38.

Hattori, M., Osterfield, M., and Flanagan, J. G. (2000). Regulated cleavage of a contact-mediated axon repellent. *Science* 289, 1360-1365.

Hedgecock, E. M., Culotti, J. G., and Hall, D. H. (1990). The *unc-5*, *unc-6*, and *unc-40* genes guide circumferential migrations of pioneer axons and mesodermal cells on the epidermis in *C. elegans*. *Neuron* 4, 61-85.

Hing, H., Xiao, J., Harden, N., Lim, L., and Zipursky, S. L. (1999). Pak functions downstream of Dock to regulate photoreceptor axon guidance in Drosophila. *Cell* 97, 853-863.

Kidd, T., Bland, K. S., and Goodman, C. S. (1999). Slit is the midline repellent for the robo receptor in *Drosophila*. *Cell* 96, 785-794.

Li, W., Herman, R. K., and Shaw, J. E. (1992). Analysis of the *Caenorhabditis elegans* axonal guidance and outgrowth gene unc-33. *Genetics* 132, 675-689.

Liu, Q. A., and Hengartner, M. O. (1998). Candidate adaptor protein CED-6 promotes the engulfment of apoptotic cells in *C. elegans*. *Cell* 93, 961-972.

Lundquist, E. A., Herman, R. K., Shaw, J. E., and Bargmann, C. I. (1998). UNC-115, a conserved protein with predicted LIM and actin-binding domains, mediates axon guidance in *C. elegans*. *Neuron* 21, 385-392.

May, R. C., Hall, M. E., Higgs, H. N., Pollard, T. D., Chakraborty, T., Wehland, J., Machesky, L. M., and Sechi, A. S. (1999). The Arp2/3 complex is essential for the actin-based motility of *Listeria monocytogenes*. *Curr Biol* 9, 759-762.

Mitchell, K. J., Doyle, J. L., Serafini, T., Kennedy, T. E., Tessier-Lavigne, M., Goodman, C. S., and Dickson, B. J. (1996). Genetic analysis of Netrin genes in Drosophila: Netrins guide CNS commissural axons and peripheral motor axons. *Neuron* 17, 203-215.

Mueller, B. K. (1999). Growth cone guidance: first steps towards a deeper understanding. *Annu Rev Neurosci* 22, 351-388.

Nash, B., Colavita, A., Zheng, H., Roy, P. J., and Culotti, J. G. (2000). The forkhead transcription factor UNC-130 is required for the graded spatial expression of the UNC-129 TGF-beta guidance factor in *C. elegans. Genes Dev* 14, 2486-2500.

Newsome, T. P., Schmidt, S., Dietzl, G., Keleman, K., Asling, B., Debant, A., and Dickson, B. J. (2000). Trio combines with dock to regulate Pak activity during photoreceptor axon pathfinding in Drosophila. *Cell* 101, 283-294.

Nishiwaki, K., Hisamoto, N., and Matsumoto, K. (2000). A metalloprotease disintegrin that controls cell migration in *Caenorhabditis elegans. Science* 288, 2205-2208.

Nobes, C. D., and Hall, A. (1995). Rho, rac, and cdc42 GTPases regulate the assembly of multimolecular focal complexes associated with actin stress fibers, lamellipodia, and filopodia. *Cell* 81, 53-62.

Ogura, K., Shirakawa, M., Barnes, T. M., Hekimi, S., and Ohshima, Y. (1997). The UNC-14 protein required for axonal elongation and guidance in *Caenorhabditis elegans* interacts with the serine/threonine kinase UNC- 51. *Genes Dev* 11, 1801-1811.

Ogura, K., Wicky, C., Magnenat, L., Tobler, H., Mori, I., Muller, F., and Ohshima, Y. (1994). *Caenorhabditis elegans* unc-51 gene required for axonal elongation encodes a novel serine/threonine kinase. *Genes Dev* 8, 2389-2400.

Pan, D., and Rubin, G. M. (1997). Kuzbanian controls proteolytic processing of Notch and mediates lateral inhibition during Drosophila and vertebrate neurogenesis. *Cell* 90, 271-280.

Peschon, J. J., Slack, J. L., Reddy, P., Stocking, K. L., Sunnarborg, S. W., Lee, D. C., Russell, W. E., Castner, B. J., Johnson, R. S., Fitzner, J. N., *et al.* (1998). An essential role for ectodomain shedding in mammalian development. *Science* 282, 1281-1284.

Reddien, P. W., and Horvitz, H. R. (2000). CED-2/CrkII and CED-10/Rac control phagocytosis and cell migration in *Caenorhabditis elegans*. *Nat Cell Biol* 2, 131-136.

Rivero-Lezcano, O. M., Marcilla, A., Sameshima, J. H., and Robbins, K. C. (1995). Wiskott-Aldrich syndrome protein physically associates with Nck through Src homology 3 domains. *Mol Cell Biol* 15, 5725-5731.

Rohatgi, R., Ma, L., Miki, H., Lopez, M., Kirchhausen, T., Takenawa, T., and Kirschner, M. W. (1999). The interaction between N-WASP and the Arp2/3 complex links Cdc42-dependent signals to actin assembly. *Cell* 97, 221-231.

Ruan, W., Pang, P., and Rao, Y. (1999). The SH2/SH3 adaptor protein dock interacts with the Ste20-like kinase misshapen in controlling growth cone motility. *Neuron* 24, 595-605.

Schimmelpfeng, K., Gogel, S., and Klambt, C. (2001). The function of leak and kuzbanian during growth cone and cell migration. *Mech Dev* 106, 25-36.

Serafini, T., Colamarino, S. A., Leonardo, E. D., Wang, H., Beddington, R., Skarnes, W. C., and Tessier-Lavigne, M. (1996). Netrin-1 is required for commissural axon guidance in the developing vertebrate nervous system. *Cell* 87, 1001-1014.

Serafini, T., Kennedy, T. E., Galko, M. J., Mirzayan, C., Jessell, T. M., and Tessier-Lavigne, M. (1994). The netrins define a family of axon outgrowth-promoting proteins homologous to *C. elegans* UNC-6. *Cell* 78, 409-424.

Shamah, S. M., Lin, M. Z., Goldberg, J. L., Estrach, S., Sahin, M., Hu, L., Bazalakova, M., Neve, R. L., Corfas, G., Debant, A., and Greenberg, M. E. (2001). EphA receptors regulate growth cone dynamics through the novel guanine nucleotide exchange factor ephexin. *Cell* 105, 233-244.

Stein, E., and Tessier-Lavigne, M. (2001). Hierarchical organization of guidance receptors: silencing of netrin attraction by slit through a Robo/DCC receptor complex. *Science* 291, 1928-1938.

Steven, R., Kubiseski, T. J., Zheng, H., Kulkarni, S., Mancillas, J., Ruiz Morales, A., Hogue, C. W., Pawson, T., and Culotti, J. (1998). UNC-73 activates the Rac GTPase and is required for cell and growth cone migrations in *C. elegans*. *Cell* 92, 785-795.

Tessier-Lavigne, M., and Goodman, C. S. (1996). The molecular biology of axon guidance. *Science* 274, 1123-1133.

Wadsworth, W. G., Bhatt, H., and Hedgecock, E. M. (1996). Neuroglia and pioneer neurons express UNC-6 to provide global and local netrin cues for guiding migrations in *C. elegans*. *Neuron* 16, 35-46.

Wahl, S., Barth, H., Ciossek, T., Aktories, K., and Mueller, B. K. (2000). Ephrin-A5 induces collapse of growth cones by activating Rho and Rho kinase. *J Cell Biol* 149, 263-270.

Wen, C., Metzstein, M. M., and Greenwald, I. (1997). SUP-17, a *Caenorhabditis elegans* ADAM protein related to Drosophila KUZBANIAN, and its role in LIN-12/NOTCH signalling. *Development* 124, 4759-4767.

White, J. G., Southgate, E., Thomson, J. N., and Brenner, S. (1986). The structure of the nervous system of the nematode *Caenorhabditis elegans*. *Philos Trans R Soc Lond B Biol Sci* 314, 1-340.

Wills, Z., Bateman, J., Korey, C. A., Comer, A., and Van Vactor, D. (1999a). The tyrosine kinase Abl and its substrate enabled collaborate with the receptor phosphatase Dlar to control motor axon guidance. *Neuron* 22, 301-312.

Wills, Z., Marr, L., Zinn, K., Goodman, C. S., and Van Vactor, D. (1999b). Profilin and the Abl tyrosine kinase are required for motor axon outgrowth in the Drosophila embryo. *Neuron* 22, 291-299.

Winberg, M. L., Mitchell, K. J., and Goodman, C. S. (1998). Genetic analysis of the mechanisms controlling target selection: complementary and combinatorial functions of netrins, semaphorins, and IgCAMs. *Cell* 93, 581-591.

Wu, Y. C., and Horvitz, H. R. (1998a). The *C. elegans* cell corpse engulfment gene ced-7 encodes a protein similar to ABC transporters. *Cell* 93, 951-960.

Wu, Y. C., and Horvitz, H. R. (1998b). *C. elegans* phagocytosis and cell-migration protein CED-5 is similar to human DOCK180. *Nature* 392, 501-504.

Zallen, J. A., Yi, B. A., and Bargmann, C. I. (1998). The conserved immunoglobulin superfamily member SAX-3/Robo directs multiple aspects of axon guidance in *C. elegans*. *Cell* 92, 217-227.

Zhou, Z., Hartwieg, E., and Horvitz, H. R. (2001). CED-1 is a transmembrane receptor that mediates cell corpse engulfment in *C. elegans*. *Cell* 104, 43-56.

Zipkin, I. D., Kindt, R. M., and Kenyon, C. J. (1997). Role of a new Rho family member in cell migration and axon guidance in *C. elegans*. *Cell* 90, 883-894.

UC San Francisco LIBRARY
UNIVERSITY OF CALIFORNIA · UNIVERSITY OF CALIFORNIA

For reference

Not to be taken from the room.

7063400

3 1378 00706 3400

San Francisco LIBRARY

UC San Francisco LIBRARY

UNIVERSITY OF CALIFORNIA · UNIVERSITY OF CALIFORNIA